

Technical University of Crete

Department of Electronic and Computer Engineering



"Position and Velocity Estimation of Mobile Station Using Smart Antennas"

by
Papadimitriou Dimitris

A thesis submitted of the requirements of the
Degree of Master of Science in
Department of Electronic and Computer Engineering

Committee:

Professor M. Paterakis (supervisor)
Professor N. Sidiropoulos
Adjunct Asc. Professor I.O. Vardiambasis

This work was supported by the Greek Ministry of National Education and Religious Affairs and the European Union under the ETTEAEK II projects: "Archimedes - Support of Research Groups in TEI of Crete - Smart antenna study & design using techniques of computational electromagnetics and pilot development & operation of a digital audio broadcasting station at Chania (SMART-DAB)" and "Reformation of the Electronics Dept's syllabus".

Chania, August '05

ACKNOWLEDGMENTS

I would like to thank my supervisor, Mr. I.O. Vardiambasis for the invaluable support, guidance and encouragement he has provided me during my thesis. His help was so meaningful. I'd like to thank Mr. M. Paterakis and Mr. N. Sidiropoulos for the time they dedicate to read this thesis. I also appreciate their willingness to take part of the examining committee.

I wish to deeply thank my parents for all their support, guidance and patience over these years. I thank also my lovely sister, Dimitra, for her advises and for putting up with me during difficult times.

I would like to thank Sophia for caring and supporting me throughout my work. As well, I wish to thank my friends Aris, Kostas and Dimitris.

This work was supported by the Greek Ministry of National Education and Religious Affairs and the European Union under the ETTEAEK II projects:

"Archimedes - Support of Research Groups in TEI of Crete - Smart antenna study & design using techniques of computational electromagnetics and pilot development & operation of a digital audio broadcasting station at Chania (SMART-DAB)" and "Reformation of the Electronics Dept's syllabus".

**Aura - Anastasia
Welcome!!!!**

ABSTRACT

The increasing demand for mobile communication services without a corresponding increase in radio frequency (RF) spectrum allocation motivates the need for new techniques to improve spectrum utilization. An approach that shows real spectrum utilization for substantial capacity enhancement is the use of smart antennas. The smart antennas are capable of automatically forming beams in the direction of the desired signal and steering nulls in the directions of the interfering signals. Another approach that satisfies the demand for quality of services in a mobile communication system is the capability of the communication system to estimate and “predict” the location of a mobile user. This kind of estimation helps the network to dynamically optimize its resource assignments consequently, the quality of services provided to the subscribers. In this thesis we provide a system that predicts the position and velocity of a mobile user using smart antennas on the base stations.

Table of Contents

Chapter 1: Introduction

1.1. Motivation.....	1
1.2. Objectives and outline of thesis.....	2

Chapter 2: Multiple Access

2.1. Frequency Division Multiple Access (FDMA)	4
2.2. Time Division Multiple Access (TDMA).....	6
2.3. Code Division Multiple Access (CDMA)	6
2.4. Space Division Multiple Access (SDMA).....	8

Chapter 3: Array and Smart Antennas

3.1. Array antenna theory	10
3.2. Classification of Smart Antenna Systems.....	10
3.2.1. Switched Beam Systems	17
3.2.2. Adaptive Array Systems	19
3.3. Fundamentals of Adaptive Antenna Arrays	20
3.3.1. Uniformly Spaced Linear Array	21
3.3.2. Beamformer Types	26
3.3.3. Beampattern versus Element Spacing.....	29
3.4. Switched beam versus adaptive array systems	32
3.5. Benefits of using Smart Antenna systems	33
3.5.1. Improved Signal Quality.....	34
3.5.2. Extended Coverage	35
3.5.3. Reduced Transmit Power	36

Chapter 4: Performance of Beamforming and Adaptive Algorithms

4.1. Criteria for Performance Optimization	37
4.1.1. Minimum Mean Square Error (MMSE)	37
4.1.2. Maximum Signal to Interference plus Noise Ratio (MSINR)	38
4.1.3. Minimum Variance (MV).....	40
4.1.4. Maximum Likelihood (ML).....	41
4.2. Adaptive algorithms.....	42
4.2.1. Least Mean Squares (LMS)	43
4.2.2. Sample Matrix Inversion (SMI).....	44
4.2.3. Normalized Least mean square (N-LMS).....	45
4.2.4. Hybrid algorithm.....	46

4.3. Transmitted signal	48
Chapter 5: Wireless System Configuration	
5.1. Mobile radio environment	50
5.1.1. Fading	50
5.1.2. Doppler spread	51
5.1.3. Delay station spread	52
5.1.4. A Mathematical Model of Fading in Communication Channels	52
5.2. MS positioning in the cellular network	54
5.2.1. Network based positioning	54
5.2.2. Terminal based positioning	57
5.2.3. Problems in location estimation	58
5.3. Position and velocity estimation in cellular systems	59
5.3.1. Antenna signal model	59
5.3.2. Position and velocity (PVE) algorithm	61
5.3.3. Time advance usage in algorithm	63
Chapter 6: Position and Velocity Estimation Using Smart Antenna Systems	
6.1. Handover	65
6.1.1. Handover algorithm in smart antenna systems	66
6.1.2. Triangle method	67
6.2. Position and velocity algorithm using smart antennas	68
6.3. Simulation scenario	71
6.3.1. Flowchart of algorithm	72
Chapter 7: Simulations and Results	
7.1. Study of beamforming	75
7.2. Study of position and velocity algorithm (PVE)	85
7.3. Summary	93
Chapter 8: Conclusions and Future Work	
8.1. Conclusions	94
8.2. Future work	95

Appendices

References

List of Figures

Figure 2.1: Spectrum of FDMA system.....	5
Figure 2.2: Frame and slot structure of TDMA	6
Figure 2.3: Concept of a CDMA system:	7
Figure 2.4: Concept of SDMA with smart antenna systems.....	8
Figure 3.1: Geometry of N-element array antenna of isotropic elements along z-axis	11
Figure 3.2: Broadside antenna	13
Figure 3.3: Endfire antenna.....	13
Figure 3.4: Linear plot of the Array factor plots for 20 elements and $d=\lambda/2$	14
Figure 3.5: Linear plot of the Array factor plots for 20 elements and $d=\lambda/4$	14
Figure 3.6: Linear plot of the Array factor plots for 20 elements and $d=\lambda/2$	15
Figure 3.7: Linear plot of the Array factor plots for 10 elements and $d=\lambda/2$	15
Figure 3.8: Beam configuration for switched beam antenna systems	17
Figure 3.9: Beam configuration for adaptive array antenna systems.....	17
Figure 3.10: Switched beam coverage pattern.....	18
Figure 3.11: Block diagram of switch beam systems	18
Figure 3.12: Steering radiation beam.....	20
Figure 3.13: Illustration of a plane wave incident on a uniformly spaced linear array for direction θ	21
Figure 3.14: Narrowband beamformer	27
Figure 3.15: Wideband beamformer	28
Figure 3.16: Output SINR versus number of antenna elements	34
Figure 3.17: Improvement of area coverage	36
Figure 4.1: Mapping circuit for MSK.....	48
Figure 5.1: Antenna geometry	59
Figure 6.1: Triangle method	68
Figure 6.2: The signal incident upon the antenna structure.....	70
Figure 7.1: Radiation pattern versus azimuth angle of arrival.....	77
Figure 7.2: Radiation pattern versus element spacing	78
Figure 7.3: Study of convergence rate and stability of LMS versus forget factor.....	79
Figure 7.4: Normalized radiation pattern versus SNR.....	80

Figure 7.5: Normalized array factor in direction of interest changing interferer's power.....	81
Figure 7.6: Radiation pattern in channel with Rayleigh noise.....	81
Figure 7.7: Beamforming pattern varying block sample for SMI algorithm.....	82
Figure 7.8: Normalized Array factor in direction of interest versus μ_o	83
Figure 7.9: Comparison of different adaptive algorithms.....	84
Figure 7.10: Position and Velocity estimations for 7 antenna elements using LMS adaptive algorithm	87
Figure 7.11: Position and Velocity estimations for 9 antenna elements using LMS adaptive algorithm	87
Figure 7.12: Position and Velocity estimations for 16 antenna elements using LMS adaptive algorithm	88
Figure 7.13: Position and velocity accuracy versus antenna elements	88
Figure 7.14: Position and velocity error estimation in Rayleigh noise channel for SNR=10dB.....	89
Figure 7.15: Position and velocity accuracy versus SNR for Gaussian and Rayleigh noise channel.....	89
Figure 7.16: Position and velocity errors for PVE algorithm using different adaptive algorithms using 9 antenna elements and SNR=10dB.....	90
Figure 7.17: Handovers of moving mobile station	91

List of Tables

Table 6.1: Parameters of GSM system	72
Table 7.1: Radiation pattern characteristics.....	77
Table 7.2: Speed of mobile station	85
Table 7.3: Parameters of the simulated system.....	86
Table 7.4: Handovers of mobile station.....	91
Table 7.5: Triangle method for estimating the three nearest BSs.....	92

Chapter 1

Introduction

1.1. Motivation

The increasing demand for mobile communication services without a corresponding increase in radio frequency (RF) spectrum allocation motivates the need for new techniques to improve spectrum utilization. An approach that shows real spectrum utilization for substantial capacity enhancement is the use of spatial process with a cell site adaptive antenna array. The adaptive antenna array is capable of automatically forming beams in the direction of the desired signal and steering nulls in the directions of the interfering (undesired) signals. By using the adaptive antenna in a mobile communication, we can reduce the amount of co-channel interference from other users within its own cell and its neighbouring cells and therefore increase the system capacity. In order to make the antenna work adaptively many algorithms may be used, some of which will be discussed in this thesis.

Another approach that satisfies the demand for quality of services in a mobile communication system is the capability of the system to estimate and “predict” the location of a mobile user. In particular, for a GSM network, a reliable estimation of the position and the velocity of mobile station are very useful. This kind of estimation helps the network to dynamically optimize its resource assignments consequently, the quality of services provided to the subscribers. If the positions and the velocities of the mobile stations (MSs) are determined, large cells can be assigned to fast moving MSs and microcells to slow or temporarily static MSs. Thus handovers between cells would be reduced to a minimum number and furthermore the network’s service quality would be wasted by a large number of handovers. The handovers always consume lots of network resources and their failures would lead to drop-calls and data loss. Also by knowing the position of a MS, the subscriber’s registration into far cells instead of nearby cells, is avoided. Such faulty registrations occur due to microwave

reflections cases and usually result in loss of connection between MS and Base Transceiver (BTS).

1.2. Objectives and outline of thesis

The aim of this thesis is twofold. The first aim is to understand different smart antenna approaches, mainly to obtain a thorough understanding of the adaptive algorithms that apply on smart antenna systems. This thesis will be an investigation of various adaptive algorithms that are used to compute the adaptive parameters (called weights) of the system. The investigation includes a study of algorithms such as the Least Mean Squares (LMS), the Normalized - Least Mean Squares (N-LMS) and the Sample Matrix Inversion (SMI). We also propose a hybrid algorithm based on SMI and LMS algorithm. These algorithms are studied to understand various aspects such as the convergence rate, the stability and the adaptation method. Moreover this thesis provides an algorithm of estimating the positions and the velocities of a mobile user. This location algorithm uses adaptive antenna arrays. By using different adaptive algorithms, we can also study the accuracy of the proposed position and velocity estimation (PVE) algorithm.

This thesis is organized as follows. Chapter 2 will provide a discussion on different access techniques and the way these techniques share the available bandwidth in a wireless communication system. In chapter 3 we introduce the basic antenna theory, which is used to linear antenna arrays. We also present the terminology and the basic concepts related to the adaptive beamforming. The classification of smart antennas and the fundamentals of the adaptive antenna array are also provided in this chapter. Chapter 4 overviews four common criteria, which are used to derive the optimum parameters of the adaptive arrays. We also present the principles of the adaptive algorithms that are used in this thesis, including the proposed hybrid adaptive algorithm. Chapter 5 presents the wireless system and the channel effects that are caused by the various environmental conditions. There is also an overview on methods that are developed to estimate the position of a mobile user, in a communication system. In this chapter we present the transmitted signal model of the antenna and we introduce the principles of the PVE algorithm. In chapter 6, the modification of the PVE algorithm using adaptive antennas, is presented. It is also provided the methods we used and concerning the handover function of the

communication system. Finally in chapter 7 we provide the simulations, the results and in chapter 8 we provide the conclusions, of the discussed issues and proposals for future work.

Chapter 2

Multiple Access

Due to the recent development of wireless communication systems, the range of frequencies available for wireless communication technologies can be utilized in various ways/schemes, and this is referred to as multiple access schemes. These techniques are adopted to allow numerous users to share simultaneously a finite amount of signal spectrum.

The distribution of spectrum is required to achieve this high system capacity by simultaneously allocating the available bandwidth (or available amount of channels) to multiple users. This must be accomplished without severe degradation in the performance of the system in order to achieve high quality communications.

Conventionally, there are three major access schemes used to share the available bandwidth in a wireless communication. Nonetheless, they are known as the frequency division multiple access (FDMA), time division multiple access (TDMA), and the code division multiple access (CDMA).

As a result, there is a lot to debate about which schemes is better. However, the answer to this depends on the combined techniques, such as the modulation scheme, anti-fading techniques, forward error correction, and so on, as well as the requirements of services, such as the coverage area, capacity, traffic, and types of information [1].

2.1 Frequency Division Multiple Access (FDMA)

Frequency division multiple access (FDMA) is the most widespread multiple-access scheme for land mobile communication system due to its ability to discriminate channels effortlessly by filters in the frequency domain. In FDMA, every subscriber is allocated to

an individual unique frequency band or channel. Figure 2.1 shows the spectrum of a FDMA system. The allocated system bandwidth is divided into bands with bandwidth of W_{ch} and guard space between adjacent channels to prevent spectrum overlapping that may be resulted from carrier frequency instability. When a user sends a call request, the system will assign one of the available channels to the user, in which, the channel is used exclusively by that user during a call. However, the system will reassign this channel to a different user when the previous call is terminated.

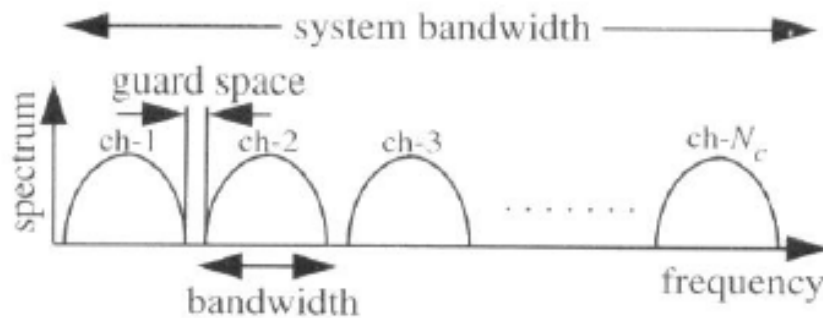


Figure 2.1: Spectrum of FDMA system

One of the most important advantages in FDMA system is there isn't any need for synchronization or timing control and therefore, the hardware is simple. In addition, there is only a need for flat fading consideration as for anti-fading technique because the bandwidth of each channel in the FDMA is sufficiently narrow.

However, there are also various problems associated with FDMA systems and they are:

- Inter-modulation interference increases with the number of carriers.
- Variable rate transmission is difficult because such a terminal has to prepare a lot of modems. For the same reason, composite transmission of voice and non-voice data is also difficult.
- High Q-value for the transmitter and receiver filters is required to guarantee high channel selectivity [1].

2.2 Time Division Multiple Access (TDMA)

In the basic time division multiple access (TDMA) protocol, the transmission time axis is divided into frames of equal duration, and each frame is divided into the same number of time slots having equal duration. Each slot position within a frame is allocated to a different user and this allocation stays the same over the sequence of frames [2]. This means that a particular user may transmit during one particular slot in every frame and thus, it has the entire channel bandwidth at its disposal during this slot. Figure 2.2 illustrated the allocation in a basic TDMA frame with four time slots per frame with the shaded areas representing the guard times in each slot in which transmission is prohibited in this region. It is essential to have the guard times as it prevents transmissions of different (spatially distributed) users from overlapping due to transmission delay differences.

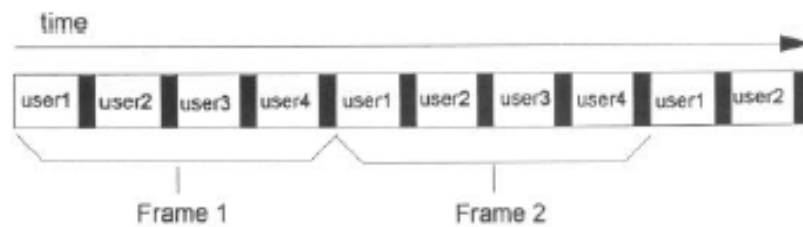
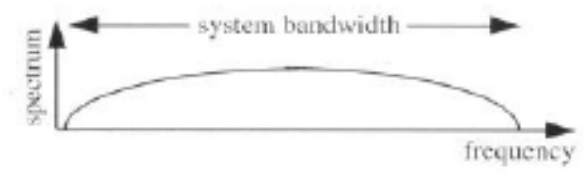


Figure 2.2: Frame and slot structure of TDMA

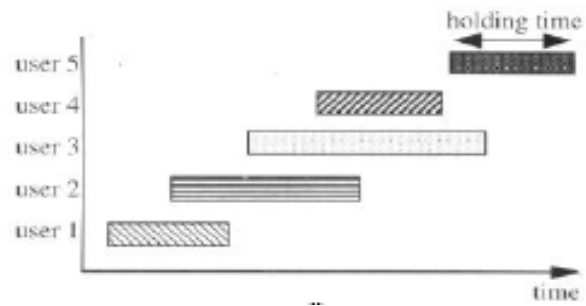
2.3 Code Division Multiple Access (CDMA)

In code division multiple access (CDMA) systems, the signal is multiplied by a very large bandwidth signal called the spreading signal. The spreading signal is a pseudonoise code sequence that as a chip rate which is in orders of magnitudes greater than the data rate of message [19].

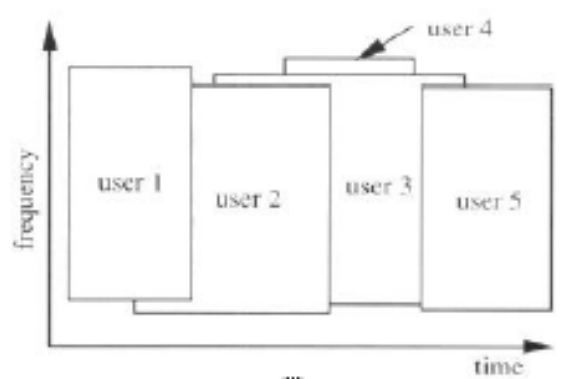
Having its own pseudorandom codeword, all subscribers in a CDMA system use the same carrier frequency and may transmit simultaneously. Figure 2.3(i) displays the spectrum of a CDMA system. The most distinct feature of CDMA system is that all the terminals share the whole bandwidth, and each terminal signal is discriminated by the code.



(i)



(ii)



(iii)

Figure 2.3: Concept of a CDMA system:

- (i) spectrum of a CDMA system**
- (ii) a call initiation and holding model for five-user case**
- (iii) channel allocation to each user**

When each user sends a call request to the base station, the base station assigns one of the spreading codes to the user. When five users initiate and hold the calls as shown in Figure 2.3(ii), time and frequency are occupied as shown in Figure 2.3(iii) [16]. Therefore,

CDMA requires a larger bandwidth as compared to FDMA and TDMA. Furthermore, there is also a need for code synchronization in CDMA system.

2.4 Space Division Multiple Access (SDMA)

In addition to these techniques, smart antennas provide a new method of multiple access to the users, which is known as the space division multiple access (SDMA). The SDMA scheme, which is commonly referred to space diversity, uses smart antenna to provide control of space by providing virtual channels in an angle domain, as seen in Figure 2.4. With the use of this approach, simultaneous calls in various different cells can be established at the same carrier frequency.

The SDMA scheme is based upon the fact that a smart antenna with the capability to form independent beams may be used at the base station. The smart antenna is used to find the location of each mobile, and then beams are formed to cover different mobiles or groups of mobiles. Each beam may be considered as a co-channel cell, and thus may be able to use the same frequency [3].

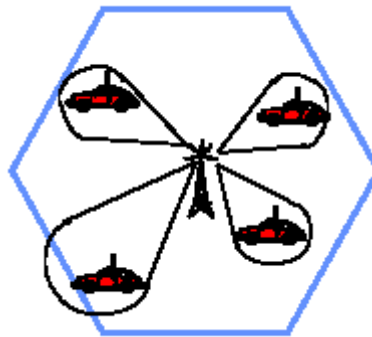


Figure 2.4: Concept of SDMA with smart antenna systems

This technique enables an effective transmission to take place in one cell without affecting the transmission in another cell. Without the use of an array, this can be accomplished by having a separate base station for each cell and keeping cell size permanent, while the use of space diversity enables dynamic changes of cell shapes to reflect the user movement.

Thus, an array of antennas constitutes to an extra dimension in this system by providing dynamic control in space and needless to say, it leads to improved capacity and better system performance.

Chapter 3

Array and Smart Antennas

3.1 Array antenna theory

An antenna array is a configuration of individual radiating elements that are arranged in space and can be used to produce a directional radiation pattern. Single-element antennas have radiation patterns that are broad and hence have a low directivity that is not suitable for long distance communications. A high directivity can be still achieved with single-element antennas by increasing the electrical dimensions (in terms of wavelength) and hence the physical size of the antenna. Antenna arrays come in various geometrical configurations, the most common being; linear arrays (1D). Arrays usually employ identical antenna elements. The radiating pattern of the array depends on the configuration, the distance between the elements, the amplitude and phase excitation of the elements, and also the radiation pattern of individual elements. The radiation pattern of an array is defined by a factor called array factor.

We will analyse a N-element uniform array which consists of equal spaced elements that are fed with current of equal magnitude and can have progressive phase shift along the array. This analysis is helpful to understand the way the AF arises and affects the radiation pattern of an antenna.

The uniform linear array shown in the figure 3.1 consists of N elements equally spaced at distance d along z-axis apart with identical amplitude excitation and has a progressive phase difference of β between the successive elements. Let us assume that the individual radiating elements are point sources with the first element of the array at the origin. The phase of the wave arriving at the origin is set to zero. We assume that the field radiated by these elements is tested in the far field region at point P.

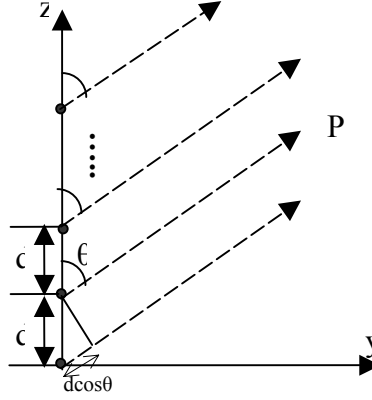


Figure 3.1: Geometry of N-element array antenna of isotropic elements along z-axis

The array factor (AF) of an N -element linear array of isotropic sources is:

$$AF = 1 + e^{j(kd \cos \theta + \beta)} + e^{j2(kd \cos \theta + \beta)} + \dots + e^{j(N-1)(kd \cos \theta + \beta)} \quad (3.1)$$

The equation (3.1) can be re-written as:

$$AF = \sum_{n=1}^N e^{j(n-1)(kd \cos \theta + \beta)} = \sum_{n=1}^N e^{j(n-1)\psi} \quad (3.2)$$

where $\psi = kd \cos \theta + \beta$. Therefore by varying β the array factor of the array can be controlled. The above AF relation can be expressed in a closed form, which is more convenient for pattern analysis, by multiplying last equation with $e^{j\psi}$ and subtracting for $AF = 1 + e^{j(kd \cos \theta + \beta)} + e^{j2(kd \cos \theta + \beta)} + \dots + e^{j(N-1)(kd \cos \theta + \beta)}$:

$$\begin{aligned} AFe^{j\psi} &= \sum_{n=1}^N e^{jn\psi} \Rightarrow \\ \Rightarrow AF(e^{j\psi} - 1) &= e^{j\psi} - 1 \Rightarrow \\ \Rightarrow AF &= \frac{e^{jN\psi} - 1}{e^{j\psi} - 1} = \frac{e^{j\frac{N}{2}\psi} \left(e^{j\frac{N}{2}\psi} - e^{-j\frac{N}{2}\psi} \right)}{e^{j\frac{\psi}{2}} \left(e^{j\frac{\psi}{2}} - e^{-j\frac{\psi}{2}} \right)} \quad (3.3) \\ \Rightarrow AF &= e^{j\frac{N-1}{2}\psi} \frac{\sin \left[\frac{N}{2} \psi \right]}{\sin \left[\frac{\psi}{2} \right]} \end{aligned}$$

In the above analysis the term $e^{j\frac{N-1}{2}\psi}$ is not important (unless one is going to further combine the array output signal with the output from another antenna) [4]. In fact, if the array were centred about the origin, the phase factor would not be present since it represents the phase shift of the array phase centre relative to the origin. Neglecting the phase factor the array factor can be re-written as:

$$AF = \frac{\sin\left[\frac{N}{2}\psi\right]}{\sin\left[\frac{\psi}{2}\right]} \text{ or for small values of } \psi \text{ can be re-written as } AF = \frac{\sin\left[\frac{N}{2}\psi\right]}{\left[\frac{\psi}{2}\right]}$$

this expression is maximum for $\psi = 0$ and has maximum value $AF(\psi = 0) = N$. The normalised form of the array factor can be written as

$$AF_n = \frac{1}{N} \frac{\sin\left[\frac{N}{2}\psi\right]}{\sin\left[\frac{\psi}{2}\right]} \text{ or for small values of } \psi \text{ can be re-written as } AF_n = \frac{1}{N} \frac{\sin\left[\frac{N}{2}\psi\right]}{\left[\frac{\psi}{2}\right]}$$

Nulls and maxima of the array factor

In order to find the nulls of the AF, the AF is set to zero. The analysis to find the angles θ_n at which the nulls occur is as follows:

$$\begin{aligned} \sin\left[\frac{N}{2}\psi\right] = 0 &\Rightarrow \left[\frac{N}{2}\psi\right] = \pm n\pi \Rightarrow \frac{N}{2}(kd \cos \theta_n + \beta) = 0 \Rightarrow \\ \theta_n &= \cos^{-1}\left(\frac{\lambda}{2\pi d}(-\beta \pm 2m\pi)\right), \quad n = 1, 2, \dots \end{aligned} \quad (3.4)$$

There are no existing nulls when $n = N, 2N, \dots$ as the argument of the arccosine exceeds unity.

The angles θ_m at which the maxima occurs can be obtained when

$$\theta_m = \cos^{-1}\left(\frac{\lambda}{2\pi d}(-\beta \pm 2m\pi)\right) \quad (3.5)$$

if d / λ is chosen to be sufficiently small the AF has only one maximum and in occurs

when $m = 0$ in equation (3.5) $\theta_m = \cos^{-1} \left[\frac{\lambda \beta}{2\pi d} \right]$

Half Power Beamwidth (HPBW)

In order to compute the HPBW in addition to the angle of first maximum θ_m , the half-power point θ_h is also required. The half-power point θ_h can be calculated by setting the value of AF_n is equal to 0.707

$$\frac{N}{2} \psi = \frac{N}{2} (kdcod\theta_h + \beta) = \pm 1,391 \Rightarrow \theta_h = \cos^{-1} \left[\frac{\lambda}{2\pi d} \left(-\beta \pm \frac{2.782}{N} \right) \right] \quad (3.6)$$

the HPBW is calculated as $HPBW = 2 | \theta_m - \theta_h |$

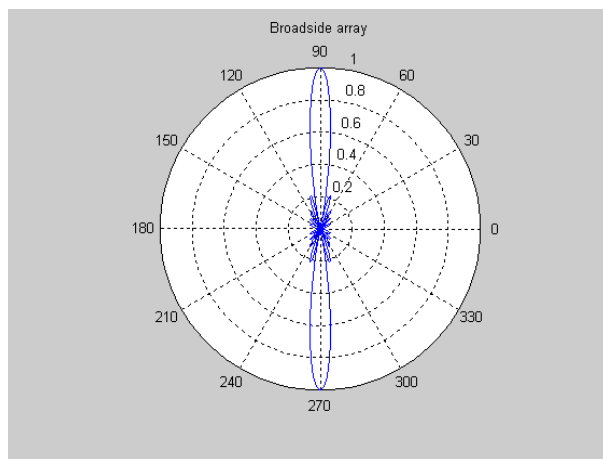


Figure 3.2: Broadside antenna

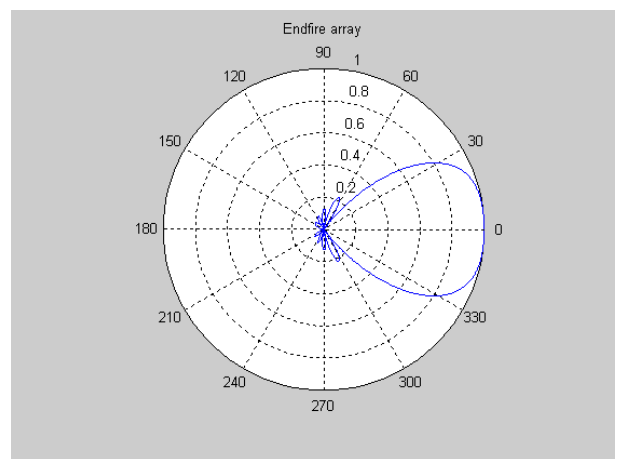


Figure 3.3: Endfire antenna

Broadside array

A broadside antenna is one for which the main beam maximum is in the direction normal to the plane containing the antenna, i.e. when $\theta = 90^0$ (figure 3.2). From equation 3.5 the maximum of the array factor would occur when $\psi = kd \cos \theta + \beta = 0$. If $\theta = 90 \Rightarrow \beta = 0$. There fore a uniform linear array will have maximum radiation in the broadside direction when all the array elements will have the same phase excitation.

End-fire array

An array is referred to as an end-fire array when it has a maximum radiation in the direction along the axis of the array i.e. when $\theta = 0^\circ$ or $\theta = 180^\circ$ (figure 3.3).

$$\begin{aligned} \text{when } \theta = 0 &\Rightarrow \psi = kd \cos \theta + \beta = 0 \Rightarrow \beta = -kd \\ \text{when } \theta = 180 &\Rightarrow \psi = kd \cos \theta + \beta = 0 \Rightarrow \beta = kd \end{aligned} \quad (3.7)$$

Let us now illustrate the dependence of the uniform linear array factor on various parameters including the number of elements and element spacing as a function of wavelength.

The array factor plots shown below indicate that beamwidth inversely proportional to the spacing between the elements for same number of elements. The array factor plot in figures 3.4-3.5 shows that beam width is smaller in the first case when $d = \lambda / 2$ compared to the beamwidth when $d = \lambda / 4$.

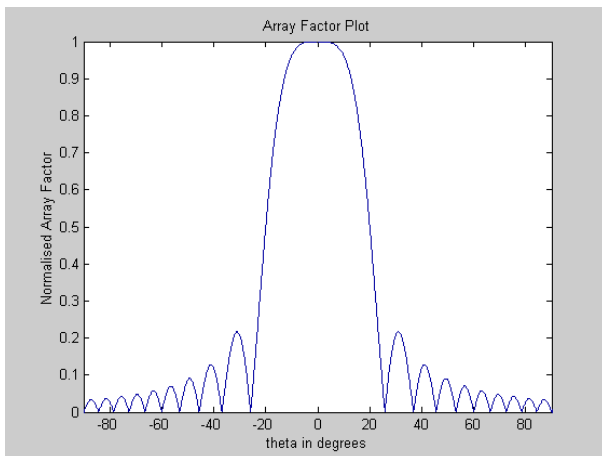


Figure 3.4: Linear plot of the Array factor plots for 20 elements and $d=\lambda/2$

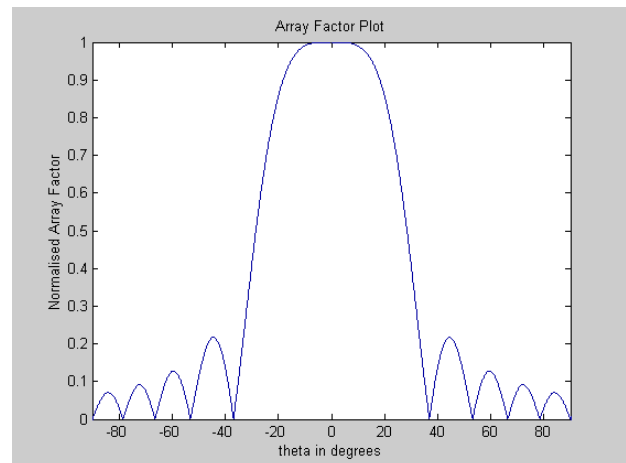


Figure 3.5: Linear plot of the Array factor plots for 20 elements and $d=\lambda/4$

The following array factor plots in figures 3.6-3.7 show that the beamwidth is not only dependent on the element spacing d but also on the number of elements. It is quite evident from the plots that the beamwidth increases as the number of elements in the array increases. Please note that the element spacing is kept constant in both the cases.

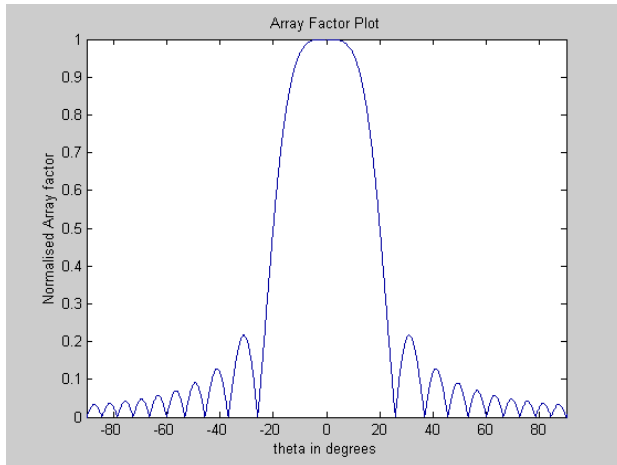


Figure 3.6: Linear plot of the Array factor plots for 20 elements and $d=\lambda/2$

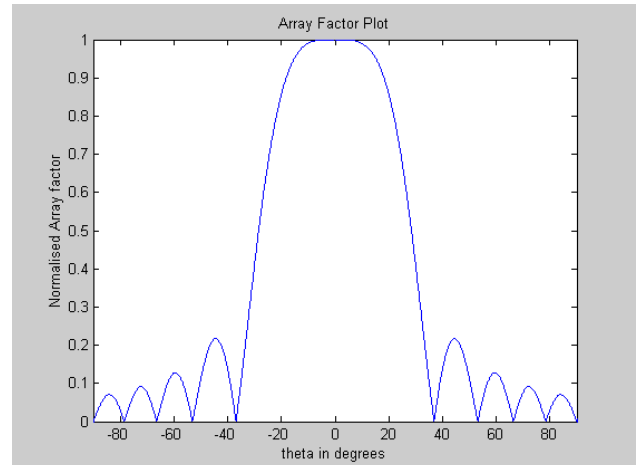


Figure 3.7: Linear plot of the Array factor plots for 10 elements and $d=\lambda/2$

3.2 Classification of Smart Antenna Systems

In mobile communication systems, capacity and performance are usually limited by two major impairments. They are multipath and co-channel interference [5]. Multipath is a condition which arises when a transmitted signal undergoes reflection from various obstacles in the propagation environment. This gives rise to multiple signals arriving from different directions. Since the multipath signals follow different paths, they have different phases when they arrive at the receiver. The result is degradation in signal quality when they are combined at the receiver due to the phase mismatch. Co-channel interference is the interference between two signals that operate at the same frequency. In cellular communication the interference is usually caused by a signal from a different cell occupying the same frequency band.

Smart antenna is one of the most promising technologies that will enable a higher capacity in wireless networks by effectively reducing multipath and co-channel interference [3],[5],[6]. This is achieved by focusing the radiation only in the desired direction and adjusting itself to changing traffic conditions or signal environments. Smart antennas employ a set of radiating elements arranged in the form of an array. The signals from these elements are combined to form a movable or switchable beam pattern that follows the desired user. In a Smart antenna system the arrays by themselves are not smart, it is the digital signal processing that makes them smart. The process of combining the signals and then focusing the radiation in a particular

direction is often referred to as digital beamforming [3], [5]. This term will be extensively used in the following sections.

The early smart antenna systems were designed for use in military applications to suppress interfering or jamming signals from the enemy. Since interference suppression was a feature in this system, this technology was borrowed to apply to personal wireless communications where interference was limiting the number of users that a network could handle. It is a major challenge to apply smart antenna technology to personal wireless communications since the traffic is denser. Also, the time available for complex computations is limited. However, the advent of powerful, low-cost, digital processing components and the development of software-based techniques have made smart antenna systems a practical reality for cellular communications systems.

There are basically two approaches [6],[7],and [8] to implement antennas that dynamically change their antenna pattern to mitigate interference and multipath affects while increasing coverage and range. They are

- Switched beam
- Adaptive Arrays

The switched beam approach is simpler compared to the fully adaptive approach. It provides a considerable increase in network capacity when compared to traditional omnidirectional antenna systems or sector-based systems. In this approach, an antenna array generates overlapping beams that cover the surrounding area as shown in figure 3.8. When an incoming signal is detected, the base station determines the beam that is best aligned in the signal-of-interest direction and then switches to that beam to communicate with the user.

The adaptive array system is the “smarter” of the two approaches. This system tracks the mobile user continuously by steering the main beam towards the user and at the same time forming nulls in the directions of the interfering signal as shown in figure 3.9. Like switched beam systems, they also incorporate arrays. Typically, the received signal from each of the spatially distributed antenna elements is multiplied by a weight. The weights are complex in nature and adjust the amplitude and phase. These

signals are combined to yield the array output. These complex weights are computed by a complicated adaptive algorithm, which is pre-programmed into the digital signal-processing unit that manages the signal radiated by the base station.

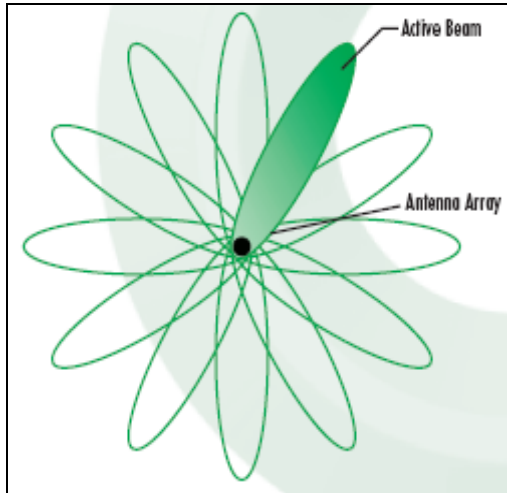


Figure 3.8: Beam configuration for switched beam antenna systems

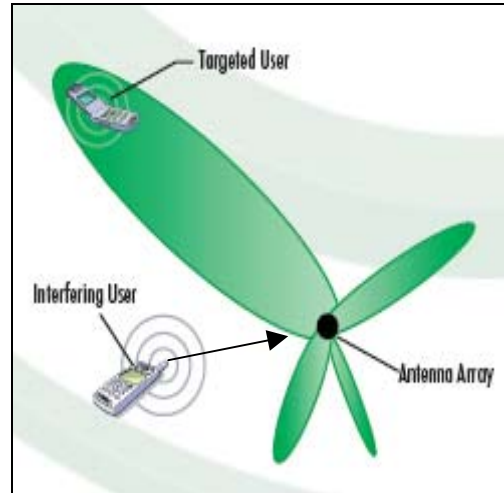


Figure 3.9: Beam configuration for adaptive array antenna systems

3.2.1 Switched Beam Systems

This type of adaptive technique actually does not steer or scan the beam in the direction of the desired signal. Switched beam employs an antenna array which radiates several overlapping fixed beams covering a designated angular area. It subdivides the sector into many narrow beams. Each beam can be treated as an individual sector serving an individual user or a group of users. Consider a traditional cellular area shown in figure 3.10 that is divided into three sectors with 120° angular width, with each sector served by six directional narrow beams. The spatially separated directional beams leads to increase in the possible reuse of a frequency channel by reducing potential interference and also increases the range. These antennas do not have a uniform gain in all directions but when compared to a conventional antenna system they have increased gain in preferred directions. The switched beam antenna has a switching mechanism that enables it to select and then switch the right beam which gives the best reception for a mobile user under consideration. The selection is usually based on maximum received power for that user. Note that same beam can be used both for uplink and downlink communication.

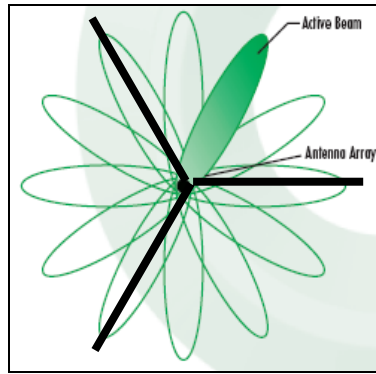


Figure 3.10: Switched beam coverage pattern

A typical switched beam system for a base station would consist of multiple arrays with each array covering a certain sector in the cell. Consider a switched beamforming system shown in figure 3.11. It consists of a phase shifting network, which forms multiple beams looking in certain directions. The RF switch actuates the right beam in the desired direction. The selection of the right beam is made by the control logic. The control logic is governed by an algorithm which scans all the beams and selects the one receiving the strongest signal based on a measurement made by the detector.

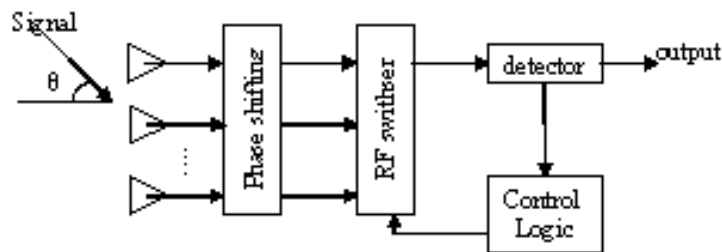


Figure 3.11: Block diagram of switch beam systems

This technique is simple in operation but is not suitable for high interference areas. Let us consider a scenario where a user who is at the side-edge of the beam which is being served by the antenna. If a second user were at the direction of the null then there would be no interference but if the second user moves into the same area of the beam as the first user he could cause interference to the first user. Therefore switched beam systems are best suited for a little or zero-interference environment.

In case of a multipath signal there is a chance that the system would switch the beam to the indirect path signal rather than the direct path signal coming from the user. This leads to the ambiguity in the perception of the direction of the received signal, thus,

switched beam systems are only used for the reception of signals. Since these antennas have a non-uniform gain between the beams the mobile user when moving away from the edge of the beam is likely to suffer from a drop call before he is handed off to the next beam because there is no beam serving that area. Also, these systems lead to frequent handovers when the mobile user is actively moving from the area of one beam to another. Therefore these intra-cell handovers have to be controlled. Switched beam systems cannot reduce multipath interference components with a direction of arrival close to that of the desired signal. Despite of all these disadvantages, the switched beam approach is less complicated (compared to the completely adaptive systems) and provides a significant range extension, increase in capacity, and a considerable interference rejection when the desired user is at the centre of the beam. Also, it is less expensive and can be easily implemented in older systems.

3.2.2 Adaptive Array Systems

From the previous discussion it was quite apparent that switched beam systems offer limited performance enhancement when compared to conventional antenna systems in wireless communication. However, greater performance improvements can be achieved by implementing advanced signal processing techniques to process the information obtained by the antenna arrays. Unlike switched beam systems, the adaptive array systems are really smart because they are able to dynamically react to the changing RF environment. They have a multitude of radiation patterns compared to fixed finite patterns in switched beam systems to adapt to the every changing RF environment. An adaptive array, like a switched beam system uses antenna arrays but it is controlled by signal processing. This signal processing steers the radiation beam towards a desired mobile user, follows the user as he moves, and at the same time minimizes interference arising from other users by introducing nulls in their directions. This is illustrated in a simple diagram shown below in figure 3.12.

The adaptive array systems are really intelligent in the true sense and can actually be referred to as smart antennas. The smartness in these systems comes from the intelligent digital processor that is incorporated in the system. The processing is mainly governed by complex computationally intensive algorithms.

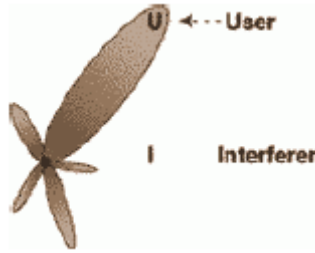


Figure 3.12: Steering radiation beam

3.3 Fundamentals of Adaptive Antenna Arrays

An antenna array consists of a set of antenna elements that are spatially distributed at known locations with reference to a common fixed point [9]. By changing the phase and amplitude of the exciting currents in each of the antenna elements, it is possible to electronically scan the main beam and/or place nulls in any direction.

The antenna elements can be arranged in various geometries, with linear, circular and planar arrays being very common. In the case of a linear array, the centres of the elements of the array are aligned along a straight line. If the spacing between the array elements is equal, it is called a uniformly spaced linear array. A circular array is one in which the centres of the array elements lie on a circle. In the case of a planar array, the centres of the array elements lie on a single plane. Both the linear array and circular array are special cases of the planar array. Arrays whose element locations conform to a given non-planar surface are called conformal arrays.

The radiation pattern of an array is determined by the radiation pattern of the individual elements, their orientation and relative positions in space, and the amplitude and phase of the feeding currents. If each element of the array is an isotropic point source, then the radiation pattern of the array will depend solely on the geometry and feeding current of the array, and the radiation pattern so obtained is called the array factor. If each of the elements of the array is similar but non-isotropic, by the principle of pattern multiplication, the radiation pattern can be computed as a product of the array factor and the individual element pattern [4].

3.3.1 Uniformly Spaced Linear Array

Consider an M -element uniformly spaced linear array which is illustrated in Figure 3.13. In Figure 3.13, the array elements are equally spaced by a distance d , and a plane wave arrives at the array from a direction θ of the array broadside. We assume that the observation point is on the zx -plane ($\varphi=0$), and that it subtends an angle θ with the z -axis. The angle θ is called the direction-of-arrival (DOA) or angle-of-arrival (AOA) of the received signal, and is measured clockwise from the broadside of the array. The received signal at the first element may be expressed as:

$$\tilde{x}_1(t) = u(t) \cos(2\pi f_c t + \gamma(t) + \beta) \quad (3.8)$$

where f_c is the carrier frequency of the modulated signal, $\gamma(t)$ is the information carrying component, $u(t)$ is the amplitude of the signal, and β is a random phase. It is convenient to use the complex envelope representation of $\tilde{x}_1(t)$ which is given by

$$x_1(t) = u(t) \exp\{j(\gamma(t) + \beta)\} \quad (3.9)$$

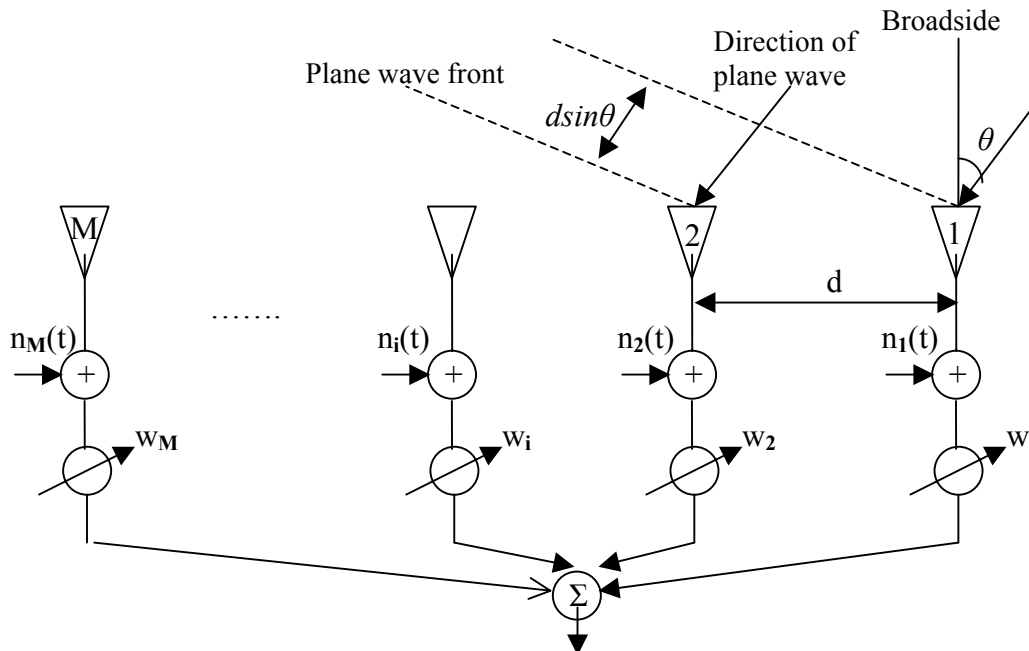


Figure 3.13: Illustration of a plane wave incident on a uniformly spaced linear array for direction θ

The received signal at the first element $\tilde{x}_1(t)$ and its complex envelope $x_1(t)$ may be related by:

$$\tilde{x}_1(t) = \text{Re}[x_1(t) \exp(j(2\pi f_c t))] \quad (3.10)$$

where $\text{Re}[\]$ stands for the real part of $[\]$. Now taking the first element in the array as the reference point, if the signals have originated far away from the array, and these plane waves' advances through a non-dispersive medium that only introduces propagation delays, the output of any other array element can be represented by a time-advanced or time-delayed version of the signal at the first element. From Figure 3.13, we see that the plane wavefront at the first element should propagate through a distance $d \sin(\theta)$ to arrive at the second element. The time delay due to this additional propagation distance is given by: $r = \frac{d \sin(\theta)}{c}$

where c is the velocity of light. Now, the received signal of the second element may be expressed as:

$$\tilde{x}_2(t) = \tilde{x}_1(t-r) = u(t-r) \cos(2\pi f_c(t-r) + \gamma(t-r) + \beta) \quad (3.11)$$

If the carrier frequency f_c is large compared to the bandwidth of the impinging signal, then the modulating signal may be treated as quasi-static during time intervals of order r and in that case equation (3.11) reduces to

$$\tilde{x}_2(t) = u(t) \cos(2\pi f_c t - 2\pi f_c r + \gamma(t) + \beta) \quad (3.12)$$

The complex envelope of $\tilde{x}_2(t)$ is therefore given by

$$x_2(t) = u(t) \exp\{j(-2\pi f_c r + \gamma(t) + \beta)\} = x_1(t) \exp\{-j(2\pi f_c r)\} \quad (3.13)$$

From equation (3.13) we see that the effect of the time delay on the signal can now be represented by a phase shift term $\exp\{-j(2\pi f_c r)\}$. Substituting equation $r = \frac{d \sin(\theta)}{c}$ into (3.13), we have

$$x_2(t) = x_1(t) \exp\{-j(2\pi f_c \frac{d \sin \theta}{c})\} = x_1(t) \exp\{-j(\frac{2\pi}{\lambda} d \sin \theta)\} \quad (3.14)$$

where λ is the wavelength of the carrier. In equation (3.14), we have used the relation between c and f_c , that is, $f_c = \frac{c}{\lambda}$. Similarly, for element i , the complex envelope of the received signal may be expressed as:

$$x_i(t) = x_1(t) \exp\left\{-j\left(\frac{2\pi}{\lambda}(i-1)d \sin \theta\right)\right\} \quad (3.15)$$

Let

$$\mathbf{x}(t) = \begin{bmatrix} x_1(t) \\ x_2(t) \\ \dots\dots\dots \\ x_M(t) \end{bmatrix} \quad (3.16)$$

and

$$\mathbf{a}(\theta) = \begin{bmatrix} 1 \\ e^{-j\frac{2\pi}{\lambda}d \sin(\theta)} \\ \dots\dots\dots \\ e^{-j\frac{2\pi}{\lambda}(M-1)d \sin(\theta)} \end{bmatrix} \quad (3.17)$$

then equation (3.15) may be expressed in vector form as:

$$\mathbf{x}(t) = \mathbf{a}(\theta)x_1(t) \quad (3.18)$$

The vector $\mathbf{x}(t)$ is often referred to as the array input data vector or the illumination vector, and $\mathbf{a}(\theta)$ is called the steering vector. The steering vector is also called direction vector, array vector, array response vector, array manifold vector, DOA vector, or aperture vector. In this case, the steering vector is only a function of the angle-of-arrival. In general, however, the steering vector is also a function of the individual element response, the array geometry, and signal frequency. The collection of steering vectors for all angles and frequencies is referred to as the array manifold.

Though for many simple arrays such as the uniformly spaced linear array discussed above, the array manifold can be computed analytically, in practice, the array manifold is measured as point source responses of the array at various angles and frequencies. This process of obtaining the array manifold is called array calibration.

In the above discussion, the bandwidth of the impinging signal expressed in equation (3.15) is assumed to be much smaller than the reciprocal of the propagation time across the array. Any signal satisfying this condition is referred to as narrowband; otherwise it is referred to as wideband. In most of the discussion that follows, the signal is assumed to be narrowband unless specified otherwise.

We could extend the above simple case to a more general case. Suppose there are q narrowband signals $s_1(t), \dots, s_q(t)$ all centred on a known frequency, say f_c , impinging on the array with a DOA θ_i , $i = 1, 2, \dots, q$. These signals may be uncorrelated, as for the signals coming from different users, or can be fully correlated as happens in multipath propagation, where each path is a scaled and time-delayed version of the original transmitted signal, or can be partially correlated due to the noise corruption. The received signal at the array is a superposition of all the impinging signals and noise. Therefore, the input data vector may be expressed as [34]

$$\mathbf{x}(t) = \sum_{i=1}^q \mathbf{a}(\theta_i) s_i(t) + \mathbf{n}(t) \quad (3.19)$$

where

$$\mathbf{a}(\theta_i) = \begin{bmatrix} 1 \\ e^{-j\frac{2\pi}{\lambda}d \sin(\theta_i)} \\ \dots\dots\dots \\ \dots\dots\dots \\ e^{-j\frac{2\pi}{\lambda}(M-1)d \sin(\theta_i)} \end{bmatrix} \quad (3.20)$$

and $\mathbf{n}(t)$ denotes the $M \times 1$ vector of the noise at the array elements. In matrix notation, equation (3.19) becomes

$$\mathbf{x}(t) = \mathbf{A}(\Theta)\mathbf{s}(t) + \mathbf{n}(t) \quad (3.21)$$

where $\mathbf{A}(\Theta)$ is the $M \times q$ matrix of the steering vectors

$$\mathbf{A}(\Theta) = [\mathbf{a}(\theta_1), \dots, \mathbf{a}(\theta_q)] \quad (3.22)$$

and

$$\mathbf{s}(t) = \begin{bmatrix} s_1(t) \\ \dots \\ s_q(t) \end{bmatrix} \quad (3.23)$$

Equation (3.21) represents the most commonly used narrowband input data model.

Now let's consider a special case. Assume that p users transmit signals from different locations, and each user's signal arrives at the array through multiple paths. Let L_{Mi} denote the number of multipath components of the i -th user. We have $\sum_{i=1}^p L_{Mi} = q$. Let's further assume that all of the multipath components for a particular user arrive within a time window which is much less than the channel symbol period for that user, then the input data vector could be expressed as

$$\mathbf{x}(t) = \sum_{i=1}^p \sum_{k=1}^{L_{Mi}} a_{i,k} \mathbf{a}(\theta_{i,k}) s_i(t) + \mathbf{n}(t) = \sum_{i=1}^p \mathbf{b}_i s_i(t) + \mathbf{n}(t) \quad (3.24)$$

where $\theta_{i,k}$ is the DOA of the k -th multipath component for the i -th user, $\mathbf{a}(\theta_{i,k})$ is the steering vector corresponding to $\theta_{i,k}$. The $a_{i,k}$ is the complex amplitude of the k -th multipath component for the i -th user, and \mathbf{b}_i is the spatial signature for the i -th user and is given by

$$\mathbf{b}_i = \sum_{k=1}^{L_{Mi}} a_{i,k} \mathbf{a}(\theta_{i,k}) \quad (3.25)$$

Similarly, equation (3.24) can be written in matrix form

$$\mathbf{x}(t) = \mathbf{B}\mathbf{s}(t) + \mathbf{n}(t) \quad (3.26)$$

where $\mathbf{B} = [\mathbf{b}_1, \dots, \mathbf{b}_p]$ and $\mathbf{s}(t) = [s_1(t), \dots, s_p(t)]^T$. The matrix \mathbf{B} is called the spatial signature matrix.

In equation (3.21), if the data vector $\mathbf{x}(t)$ is sampled K times, at t_1, \dots, t_k the sampled data may be expressed as

$$\mathbf{X} = \mathbf{A}(\Theta)\mathbf{S} + \mathbf{N} \quad (3.27)$$

where \mathbf{X} and \mathbf{N} are the $M \times K$ matrices containing K snapshots of the input data vector and noise vector, respectively,

$$\mathbf{X} = [\mathbf{x}(t_1), \dots, \mathbf{x}(t_k)] = [\mathbf{x}(1), \dots, \mathbf{x}(K)] \quad (3.28)$$

$$\mathbf{N} = [\mathbf{n}(t_1), \dots, \mathbf{n}(t_k)] = [\mathbf{n}(1), \dots, \mathbf{n}(K)]$$

and \mathbf{S} is the $q \times K$ matrix containing K snapshots of the narrowband signals

$$\mathbf{S} = [\mathbf{s}(t_1), \dots, \mathbf{s}(t_k)] = [\mathbf{s}(1), \dots, \mathbf{s}(K)] \quad (3.29)$$

In equations (3.28) and (3.29), we have replaced the time index t_i with $i, i = 1, \dots, K$ for notational simplicity.

With the data model created above, most array processing problems may be categorized as follows [35]. Given the sampled data \mathbf{X} in a wireless system, determine:

- 1 the number of signals q
- 2 the DOAs $\theta_1, \theta_2, \dots, \theta_q$
- 3 the signal waveforms $\mathbf{s}(1), \mathbf{s}(2), \dots, \mathbf{s}(K)$

We shall refer to (1) as the detection problem, to (2) as the localization problem, and to (3) as the beamforming problem.

3.3.2 Beamformer types

Beamforming is one type of processing used to form beams to simultaneously receive a signal radiating from a specific location and attenuate signals from other locations

[10],[34]. Systems designed to receive spatially propagating signals often encounter the presence of interference signals. If the desired signal and interference occupy the same frequency band, unless the signals are uncorrelated, e. g., CDMA signals, and then temporal filtering often cannot be used to separate signal from interference. However, the desired and interfering signals usually originate from different spatial locations. This spatial separation can be exploited to separate signal from interference using a spatial filter at the receiver. Implementing a temporal filter requires processing of data collected over a temporal aperture. Similarly, implementing a spatial filter requires processing of data collected over a spatial aperture.

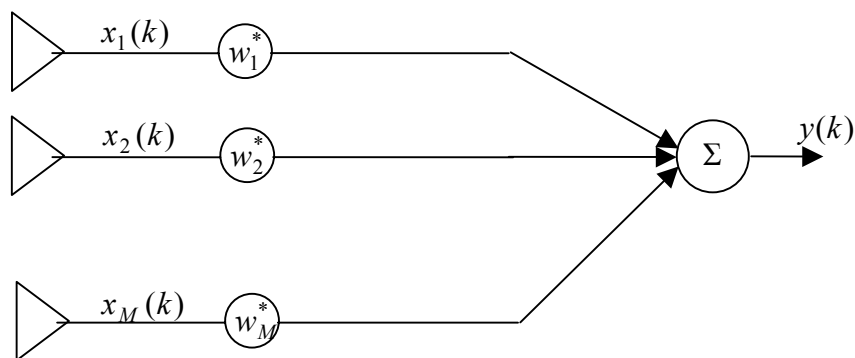


Figure 3.14: Narrowband beamformer

A beamformer is a processor used in conjunction with an array of sensors (e.g., antenna elements in an adaptive array) to provide a versatile form of spatial filtering. The sensor array collects spatial samples of propagating wave fields, which are processed by the beamformer. Typically a beamformer linearly combines the spatially sampled time series from each sensor to obtain a scalar output time series in the same manner that an FIR filter linearly combines temporally sampled data. There are two types of beamformers, narrowband beamformer, and wideband beamformer. A narrowband beamformer is shown in Figure 4.14. In Figure 4.14, the output at time k , $y(k)$, is given by a linear combination of the data at the M sensors at time k :

$$y(k) = \sum_{i=1}^M w_i^* x_i(k) \quad (3.30)$$

where $*$ denotes complex conjugate. Since we are now using the complex envelope representation of the received signal, both $x_i(k)$ and w_i are complex. The weight w_i is

called the complex weight. The beamformer shown in Figure 4.14 is typically used for processing narrowband signals.

Equation (3.30) may also be written in vector form [34] as

$$y(k) = \mathbf{w}^H \mathbf{x}(k) \quad (3.31)$$

where $\mathbf{w} = [w_1 \ w_2 \ \dots \ w_M]^T$ and H denotes the Hermitian (complex conjugate) transpose. The vector \mathbf{w} is called the complex weight vector.

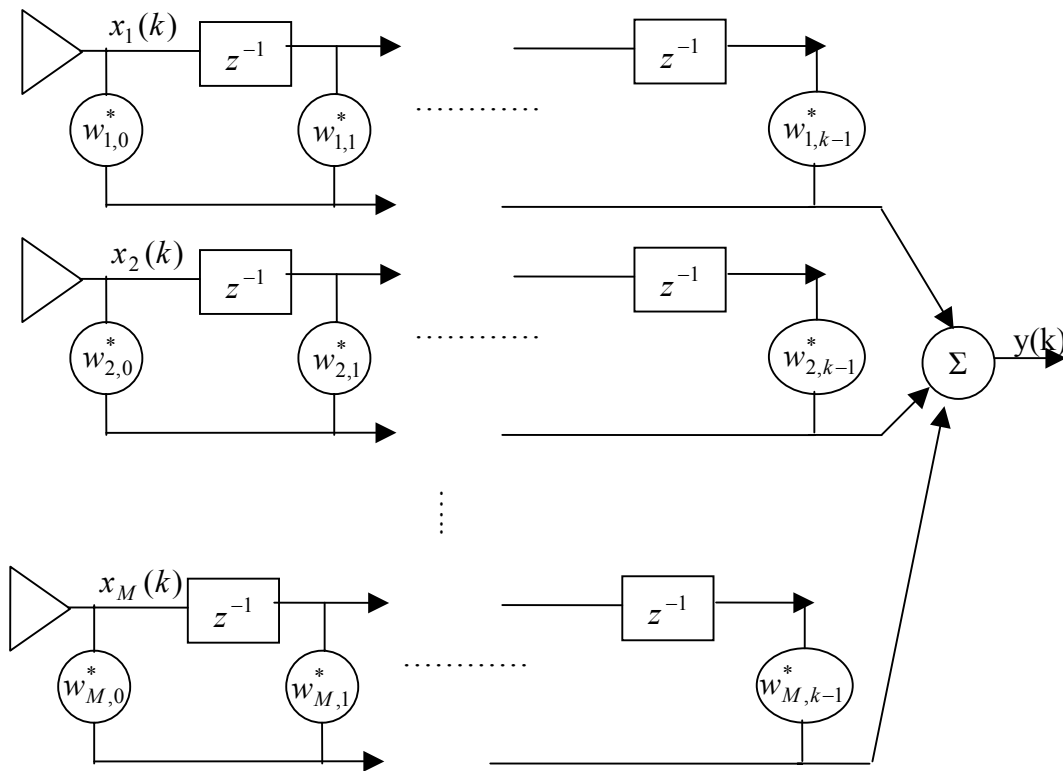


Figure 3.15: Wideband beamformer

Different from a narrowband beamformer, a wideband beamformer samples the propagating wave field in both space and time and is often used when signals of significant frequency extent (broadband) are of interest [10]. A wideband beamformer is shown in Figure 3.15. The output in this case may be expressed as

$$y(k) = \sum_{i=1}^M \sum_{l=0}^{K-1} w_{i,l}^* x_i(k-l) \quad (3.32)$$

where $K - 1$ is the number of delays in each of the M sensor channels. Let

$$\mathbf{w} = [w_{1,0}, \dots, w_{1,K-1}, \dots, w_{M,0}, \dots, w_{M,K-1}]^T \quad (3.33)$$

and

$$\mathbf{x}(k) = [x_1(k), \dots, x_1(k-K-1), \dots, x_M(k), \dots, x_M(k-K+1)]^T \quad (3.34)$$

where T denotes the conventional transpose, equation (3.32) may also be expressed in vector form as in equation (3.31). In this case, both \mathbf{w} and $\mathbf{x}(k)$ are $MK \times 1$ column vectors.

Comparing Figure 3.14 with Figure 3.15, we see that a wideband beamformer is more complex than narrowband beamformer. Since both types of beamformers may share the same data model, we will concentrate on the narrowband beamformer in the following discussion.

3.3.3 Beampattern versus Element Spacing

The beampattern and element spacing of an antenna array may be viewed as the counterpart of the magnitude response of a FIR filter and the sampling period of a discrete time signal in the time domain, respectively. To illustrate this point, we may compare the harmonic retrieval problem in the time domain with the beamforming problem in the space domain [13]. Consider a signal $x(t)$ composed of q complex sinusoids with unknown parameters embedded in additive noise:

$$x(t) = \sum_{i=1}^q a_i \exp\{j(2\pi f_i t + \phi_i)\} + n(t) \quad (3.35)$$

where f_i , a_i , and ϕ_i are the frequency, amplitude, and phase, respectively, of the i -th sinusoid. Suppose that the signal is sampled with a sampling period T_s unrelated to the frequency of the unknown sinusoid, and let $x(l)$ denote the signal at time instant lT_s , we have

$$x(l) = \sum_{i=1}^q a_i \exp\{j(2\pi f_i (lT_s) + \phi_i)\} + n(lT_s) \quad (3.36)$$

Suppose the sampled signal is fed into an FIR filter with $M - 1$ delay units to perform filtering. At time instant lT_s , the filter input and the $M-1$ outputs of the delay units may be expressed as

$$\mathbf{x}(l) = \sum_{i=1}^q \mathbf{a}(f_i) s_i(l) + \mathbf{n}(l) \quad (3.37)$$

where $\mathbf{x}(l) = [x(l), x(l-1), \dots, x(l-M+1)]^T$, $\mathbf{n}(l) = [n(lT_s), \dots, n((l-M+1)T_s)]^T$,

$$\mathbf{a}(f_i) = \begin{bmatrix} 1 \\ e^{-j2\pi T_s f_i} \\ \dots \\ e^{-j2\pi(M-1)T_s f_i} \end{bmatrix} \quad (3.38)$$

and

$$s_i(l) = a_i \exp(j(2\pi f_i(lT_s) + \phi_i)) \quad (3.39)$$

Comparing equation (3.37), (3.38) with equation (3.19), (3.20), we see that for a narrowband uniform linear array (ULA), there is a correspondence between the normalized element spacing, d/λ and the sampling period, T_s , in the FIR filter, also the sine of the DOA θ_i , $\sin(\theta_i)$ can be related to the temporal frequency f_i of the FIR filter input [10].

Since there is a mapping between the ULA and the FIR filter, a theorem applied to the FIR filter in the time domain may also be applied to the uniform linear array in space domain. In time domain, the Nyquist sampling theorem [12] stated that for a band limited signal with highest frequency f , the signal is uniquely determined by its discrete time samples if the sampling rate is equal to or greater than $2f$. If the sampling rate is less than $2f$, aliasing will occur. In the space domain, the sampling rate corresponds to the inverse of the normalized element spacing, and the highest frequency is corresponding to 1 (since $\sin(\theta_i)$ is always less than 1). From the Nyquist sampling theorem, to avoid spatial aliasing, we should have

$$\frac{1}{\frac{d}{\lambda}} \geq 2 \times 1 \Rightarrow d \leq \frac{\lambda}{2} \quad (3.40)$$

Therefore, the element spacing of an array should always be less than or equal to half of the carrier wavelength. However, the element spacing cannot be made arbitrarily small since two closely spaced antenna elements will exhibit mutual coupling effects. It is difficult to generalize these effects since they depend heavily on the type of antenna element and the array geometry. However, the mutual coupling between two elements typically tends to increase as the distance between elements is reduced [4]. Thus the spacing between elements must be large enough to avoid significant mutual coupling. In practical linear arrays, the element spacing is often kept near a half wavelength so that the spatial aliasing is avoided and the mutual coupling effect is minimized.

The frequency response of an FIR filter with tap weights w_i^* , $i = 1, \dots, M$ and a sampling period T_s is given by

$$H(e^{j2\pi f}) = \sum_{i=1}^M w_i^* e^{-j2\pi f T_s (i-1)} \quad (3.41)$$

where $H(e^{j2\pi f})$ represents the response of the filter to a complex sinusoid of frequency f . For the harmonic retrieval problem, if we want to extract the signal with frequency f_i , we need to find a set of complex weights such that the frequency response of the filter has a higher gain at f_i and lower gains (or ideally, nulls) at other frequencies. For the beamforming problem, since f and T_s are corresponding to $\sin \theta$ and $\frac{d}{\lambda}$, respectively, we can replace f and T_s in equation (3.41) with $\sin \theta$ and $\frac{d}{\lambda}$, respectively, to get the beamformer response

$$g(\theta) = \sum_{i=1}^M w_i^* e^{-j\frac{2\pi}{\lambda}(i-1)d \sin \theta} \quad (3.42)$$

where $g(\theta)$ represents the response of the array to a signal with DOA equal to θ . So if there are several signals coming from different directions, and we want to extract the signal with direction θ_i , we need to find a set of weights such that the array response as a higher gain at direction θ_i and lower gains (or ideally, nulls) at other directions. The array response $g(\theta)$ may also be expressed in vector form as:

$$g(\theta) = \mathbf{w}^H \mathbf{a}(\theta) \quad (3.43)$$

where $\mathbf{w} = [w_1 \ w_2 \ \dots \ w_M]^T$ and $\mathbf{a}(\theta)$ is given by equation (3.17). The beamformer response may also be viewed as the ratio of the beamformer output to the signal at the reference element when a single plane wave is incident on the array.

The beam pattern is defined as the magnitude of $g(\theta)$ [10] and is given by $G(\theta) = |g(\theta)|$

Using $G(\theta)$, we may define the normalized beamformer response,

$$g_n(\theta) = \frac{g(\theta)}{\max\{G(\theta)\}} \quad (3.44)$$

where $g_n(\theta)$ is also known as the normalized radiation pattern or array factor of the array.

3.4 Switched beam versus adaptive array systems

Switched beam system

- It uses multiple fixed directional beams with narrow beamwidths.
- The required phase shifts are provided by simple fixed phase shifting networks.
- They do not require complex algorithms; simple algorithms are used for beam selection.
- It requires only moderate interaction between mobile unit and base station as compared to adaptive array system.
- Since low technology is used it has lesser cost and complexity.
- Integration into existing cellular system is easy and cheap.

- It provides significant increase in coverage and capacity compared conventional antenna based systems.
- Since multiple narrow beams are used, frequent intra-cell handovers between beams have to be handled as mobile moves from one beam to another.
- It cannot distinguish between direct signal and interfering and/or multipath signals, this leading to undesired enhancement of the interfering signal more than the desired signal.
- Since there is no null steering involved; switched beam systems offers limited co-channel interference suppression as compared to the adaptive array system.

Adaptive array system

- A complete adaptive system; steers the beam towards desired signal-of-interest and
- Places nulls at the interfering signal directions.
- It requires implementation of DSP technology.
- It requires complicated adaptive algorithms to steer the beam and the nulls.
- It has better interference rejection capability compared to switched beam systems.
- It is not easy to implement in existing systems, i.e. up gradate is difficult and expensive.
- Since continuous steering of the beam is required as the mobile moves; high interaction between mobile unit and base station is required.
- Since the beam continuously follows the user; cell handovers are less.
- It provides better coverage and increased capacity because of improved interference
- Rejection as compared to the switched beam system.
- It can either reject multipath components or add them by correcting the delays to enhance the signal quality.

3.5 Benefits of using Smart Antenna systems

Use of adaptive arrays brings various benefits for mobile communications and has been widely discussed in the literature [6],[8], and [33]. Some of the benefits are summarized below.

3.5.1 Improved Signal Quality

Due to using multiple elements adaptive arrays can provide additional antenna (array) gain, which depends on the number of utilized array elements. This, consequently, leads to improved SINR. Define the input SNR as SNR_{in} than if the number of interferences is smaller than the number of degree of freedom $\text{DoF} = M - 1$ the output SINR in a single propagation environment (without multipath fading) can be found as

$$\text{SINR}_{\text{out}} = M \cdot \text{SNR}_{\text{in}} \quad (3.45)$$

or

$$\text{SINR}_{\text{out}} [dB] = 10 \log_{10} M + \text{SNR}_{\text{in}} [dB] \quad (3.46)$$

where M is the number of array elements.

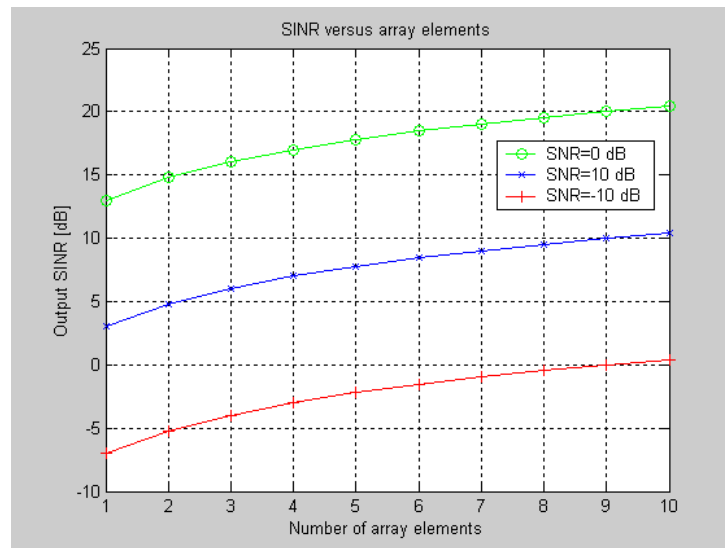


Figure 3.16: Output SINR versus number of antenna elements

In the multipath fading environment, if signal processing is used in both the spatial and temporal domains such as the case of the broadband beamformer more diversity gain could be achieved depending on the fading characteristics. Take a simple case of 2-path model as an example. When the two paths are spatially uncorrelated, for example, the preceding and delayed rays coming from 0^0 and 30^0 , respectively, the output SINR is estimated as

$$\text{SINR}_{\text{out}}[dB] = 10 \log_{10} M + 10 \log_{10}(2) + \text{SNR}_{\text{in}}[dB] \quad (3.47)$$

This means that additional 3dB diversity gain has been obtained in multipath fading environment. The richer the multipath fading environment is, the more diversity gain can be achieved. Figure 3.16 plots the output SINR versus the number of employed array elements.

3.5.2 Extended Coverage

From equation (3.46), it is clear that the array gain achieved by an adaptive array is

$$G = 10 \log_{10} M \quad (3.48)$$

This additional gain allows extending the coverage of the base station. When the angular spread is small and the path loss is modelled with exponent a , the range extension factor (REF) is given by [33]

$$\text{REF} = \frac{r_{\text{array}}}{r_{\text{conv}}} = M^{\frac{1}{a}} \quad (3.49)$$

where r_{conv} and r_{array} are the range covered by the conventional antenna (with single element) and the array antenna (with multiple elements), respectively. The extended area coverage factor (ECF) is [33]

$$\text{ECF} = \left(\frac{r_{\text{array}}}{r_{\text{conv}}} \right)^2 = \text{REF}^2 \quad (3.50)$$

Figure 3.17 shows that with an 6 element array, the coverage area is almost double compared with single antenna case for $a = 5$. Since the inverse of the ECF represents the reduction factor in number of base station required to cover the same area using a single antenna [33], it is clear that using adaptive arrays can significantly reduce the number of base stations. For example, for the above mentioned case with $a = 5$, the number of base station can be reduced to only one half of the original number.

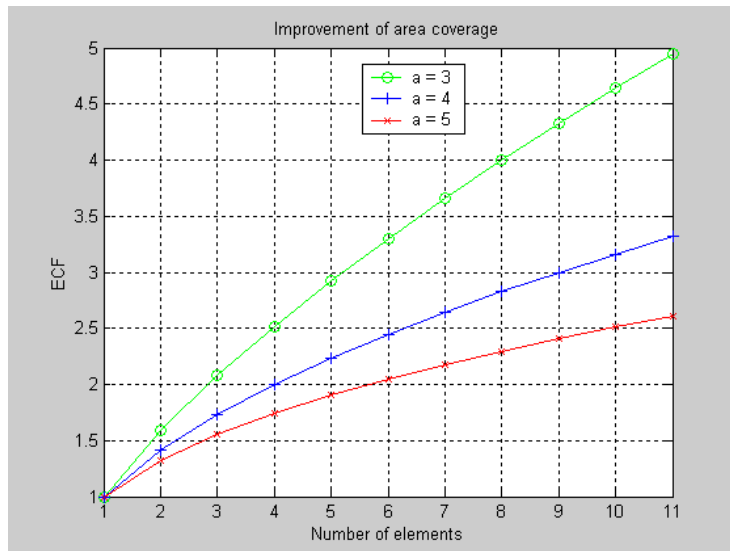


Figure 3.17: Improvement of area coverage

3.5.3 Reduced Transmit Power

We have seen in section 3.5.1 that use of adaptive arrays can provide a large array gain. This gain, consequently leads to the reduction in required transmit power of the base station. If the required reception sensitivity is kept the same, then the power requirement of a base station employed an M -element array is reduced to M^{-1} and correspondingly the required output power of the base station power amplifier can be reduced to M^{-2} [33]. The reduction in the transmit power is beneficial to user's health and implementation cost since high frequency power amplifiers are often very expensive.

Chapter 4

Performance of Beamforming and Adaptive Algorithms

4.1 Criteria for Performance Optimization

As we have mentioned earlier in previous chapter, the adaptive processor controls the beamforming network to optimize the beamforming weights according to a certain criterion. Four common criteria which are often employed to obtain optimum weights for adaptive arrays in mobile communications are Minimum Mean Square Error (MMSE), Maximum Signal to Interference plus Noise ratio (MSINR), Minimum Variance (MV) and Maximum Likelihood (ML). These optimum criteria will be reviewed below.

4.1.1 Minimum Mean Square Error (MMSE)

The MMSE criterion is first considered by Widrow et al. in [13]. The criterion strives to minimize the error between the array output signal $y(t)$ and the desired signal $s(t)$ [34]. In practice, the desired signal $s(t)$ is of course not known. However, using some techniques such as training method or estimation based on the desired signal characteristics one can generate a reference signal $r(t)$ that closely approximates the desired signal to a certain extent. Consider the input signal vector given by

$$\mathbf{x}(t) = s(t)\mathbf{a}(\theta) + \mathbf{u}(t) = \mathbf{s}(t) + \mathbf{u}(t) \quad (4.1)$$

where $\mathbf{a}(\theta)$ is the array response and $\mathbf{u}(t)$ is a vector containing zero mean noise and uncorrelated interferences. For a narrowband adaptive array, the output signal is recalled from equation (3.31) as

$$y(t) = \mathbf{w}^H \mathbf{x}(t) \quad (4.2)$$

The error signal is defined as

$$\varepsilon(t) = r(t) - y(t) = r(t) - \mathbf{w}^H \mathbf{x}(t) \quad (4.3)$$

and the weights are chosen to minimize the mean square error (MSE) of the error signal

$$E\{|\varepsilon(t)|^2\} = E\{|r(t) - \mathbf{w}^H \mathbf{x}(t)|^2\} \quad (4.4)$$

where $E\{\cdot\}$ denotes the expected operation. Expanding equation (4.4) we have

$$\begin{aligned} E\{|\varepsilon(t)|^2\} &= E\{|r(t)|^2\} - \mathbf{w}^T E\{\mathbf{x}^*(t)r(t)\} - \mathbf{w}^H E\{\mathbf{x}(t)r^*(t)\} + \mathbf{w}^H E\{\mathbf{x}(t)\mathbf{x}^H(t)\}\mathbf{w} \\ &= E\{|r(t)|^2\} - \mathbf{w}^T \mathbf{r}_{xr}^* - \mathbf{w}^H \mathbf{r}_{xr} + \mathbf{w}^H \mathbf{R}_{xx} \mathbf{w} \end{aligned} \quad (4.5)$$

where $\mathbf{r}_{xr} = E\{\mathbf{x}(t)r^*(t)\}$ and $\mathbf{R}_{xx} = E\{\mathbf{x}(t)\mathbf{x}^H(t)\}$ are called the correlation vector and the covariance matrix, respectively. Here $(\cdot)^*$ denotes the complex conjugate. The optimum weight vector can be found by setting the gradient of equation (4.5) with respect to \mathbf{w} equal to zero [6]

$$\nabla_{\mathbf{w}} E\{|\varepsilon(t)|^2\} = -2\mathbf{r}_{xr} + 2\mathbf{R}_{xx} \mathbf{w} = 0 \quad (4.6)$$

which gives the solution

$$\mathbf{w}_{MMSE} = \mathbf{w}_{opt} = \mathbf{R}_{xx}^{-1} \mathbf{r}_{xr} \quad (4.7)$$

Equation (4.7) is often referred to as the Wiener-Hopf equation or the optimum Wiener solution [6]. By substituting equation (4.7) into (4.5), we have the optimum MMSE

$$MMSE = E\{|\varepsilon(t)|^2\} = E\{|r(t)|^2\} - \mathbf{r}_{xr}^H \mathbf{R}_{xx}^{-1} \mathbf{r}_{xr} \quad (4.8)$$

4.1.2 Maximum Signal to Interference plus Noise Ratio (MSINR)

The criterion considered in this subsection is the maximum SINR. Recall equation (3.51) and using (4.1), the output of the array can be expressed as

$$\begin{aligned} y(t) &= \mathbf{w}^H \mathbf{x}(t) = \mathbf{w}^H \mathbf{s}(t) + \mathbf{w}^H \mathbf{u}(t) = \\ &= y_s(t) + y_u(t) \end{aligned} \quad (4.9)$$

The average output SINR is given by

$$\text{SINR} = E \left\{ \frac{|y_s(t)|^2}{|y_u(t)|^2} \right\} = E \left\{ \frac{\mathbf{w}^H \mathbf{s}(t) \mathbf{s}^H(t) \mathbf{w}}{\mathbf{w}^H \mathbf{u}(t) \mathbf{u}^H(t) \mathbf{w}} \right\} = \frac{\mathbf{w}^H \mathbf{R}_{ss} \mathbf{w}}{\mathbf{w}^H \mathbf{R}_{uu} \mathbf{w}} \quad (4.10)$$

where $\mathbf{R}_{ss} = E\{\mathbf{s}(t)\mathbf{s}^H(t)\}$ and $\mathbf{R}_{uu} = E\{\mathbf{u}(t)\mathbf{u}^H(t)\}$. Taking the gradient of equation (4.10) with respect to \mathbf{w} gives:

$$\begin{aligned} \nabla_{\mathbf{w}} \text{SINR} &= \frac{\nabla_{\mathbf{w}} (\mathbf{w}^H \mathbf{R}_{ss} \mathbf{w})(\mathbf{w}^H \mathbf{R}_{uu} \mathbf{w}) - (\mathbf{w}^H \mathbf{R}_{ss} \mathbf{w}) \nabla_{\mathbf{w}} (\mathbf{w}^H \mathbf{R}_{uu} \mathbf{w})}{(\mathbf{w}^H \mathbf{R}_{uu} \mathbf{w})^2} \\ &= \frac{2\mathbf{R}_{ss} \mathbf{w} (\mathbf{w}^H \mathbf{R}_{uu} \mathbf{w}) - 2\mathbf{R}_{uu} \mathbf{w} (\mathbf{w}^H \mathbf{R}_{ss} \mathbf{w})}{(\mathbf{w}^H \mathbf{R}_{uu} \mathbf{w})^2} \end{aligned} \quad (4.11)$$

the optimum weight \mathbf{w}_{opt} can be found by setting $\nabla_{\mathbf{w}} \text{SINR} = 0$, which leads to

$$\mathbf{R}_{ss} \mathbf{w} = \frac{\mathbf{w}^H \mathbf{R}_{ss} \mathbf{w}}{\mathbf{w}^H \mathbf{R}_{uu} \mathbf{w}} \mathbf{R}_{uu} \mathbf{w} = \text{SINR} \mathbf{R}_{uu} \mathbf{w} \quad (4.12)$$

If \mathbf{R}_{uu} is invertible, then equation (4.12) can be rewritten as

$$\mathbf{R}_{uu}^{-1} \mathbf{R}_{ss} \mathbf{w} = \text{SINR} \mathbf{w} \quad (4.13)$$

which is the generalized eigen problem. Note that the value on the right hand side of equation (4.11) is bounded by the maximum and minimum eigenvalues of $\mathbf{R}_{uu}^{-1} \mathbf{R}_{ss}$.

The maximum eigenvalue λ_{\max} satisfies the following condition $\mathbf{R}_{uu}^{-1} \mathbf{R}_{ss} \mathbf{w} = \lambda_{\max} \mathbf{w}$.

It is clear that λ_{\max} is the optimum value of SINR. Corresponding to this is λ_{\max} there is only one eigenvector \mathbf{w}_{opt} given by

$$\mathbf{w}_{opt} = \frac{\mathbf{R}_{uu}^{-1} \mathbf{R}_{ss} \mathbf{w}_{opt}}{\text{SINR}} = \frac{\mathbf{R}_{uu}^{-1} E\{s^2(t)\} \mathbf{a}(\theta) \mathbf{a}^H(\theta) \mathbf{w}_{opt}}{\text{SINR}} = \frac{\mathbf{R}_{uu}^{-1} \mathbf{a}(\theta) \mathbf{a}^H(\theta) \mathbf{w}_{opt} E\{|s(t)|^2\}}{\text{SINR}} \quad (4.14)$$

Define

$$\beta = \frac{\mathbf{a}^H(\theta) \mathbf{w}_{opt} E\{|s(t)|^2\}}{\text{SINR}} \quad (4.15)$$

then the optimum weight vector can be expressed in a similar form of the Wiener-Hopf equation as

$$\mathbf{w}_{\text{SINR}} = \mathbf{w}_{\text{opt}} = \beta \mathbf{R}_{uu}^{-1} \mathbf{a}(\theta) \quad (4.16)$$

4.1.3 Minimum Variance (MV)

Minimum variance (ML), also known as linear constrained minimum variance (LCMV), is used when the desired signal and its direction are both known. MV aims to minimize output noise variance. Recall beamformer output from equation (3.31)

$$\begin{aligned} y(t) &= \mathbf{w}^H \mathbf{x}(t) = \mathbf{w}^H \mathbf{s}(t) + \mathbf{w}^H \mathbf{u}(t) \\ &= \mathbf{w}^H \mathbf{a}(\theta) s(t) + \mathbf{w}^H \mathbf{u}(t) \end{aligned} \quad (4.17)$$

In order to obtain the desired signal with a specific gain in a given direction, we can use a constraint [6]

$$\mathbf{w}^H \mathbf{a}(\theta) = g \quad (4.18)$$

Substitute equation (4.18) into equation (4.17), we obtain the array output subject to the constraint as [15]

$$y(t) = gs(t) + \mathbf{w}^H \mathbf{u}(t) \quad (4.19)$$

Since $\mathbf{u}(t)$ is assumed to be uncorrelated and zero mean Gaussian, we have $E\{y(t)\} = gs(t)$. The variance of the array output then is given by

$$\begin{aligned} \text{var}\{y(t)\} &= E\{[y(t) - gs(t)][y(t) - gs(t)]^*\} \\ &= E\{\mathbf{w}^H \mathbf{u}(t) [\mathbf{w}^H \mathbf{u}(t)]^H\} \\ &= \mathbf{w}^H \mathbf{R}_{uu} \mathbf{w} \end{aligned} \quad (4.20)$$

Now using the method of Lagrange, we have

$$\nabla_{\mathbf{w}} \{\mathbf{w}^H \mathbf{R}_{uu} \mathbf{w} - \beta [g - \mathbf{w}^H \mathbf{a}(\theta)]\} = 0 \quad (4.21)$$

or equivalently,

$$\mathbf{R}_{uu} \mathbf{w} - \beta \mathbf{a}(\theta) = 0 \quad (4.22)$$

If \mathbf{R}_{uu}^{-1} is invertible the optimum weight vector using MV criterion can be expressed as

$$\mathbf{w}_{MV} = \beta \mathbf{R}_{uu}^{-1} \mathbf{a}(\theta) \quad (4.23)$$

where [6]

$$\beta = \frac{g}{\mathbf{a}^H \mathbf{R}_{uu}^{-1} \mathbf{a}(\theta)} \quad (4.24)$$

When $g = 1$, the MV beamformer is often referred to as the minimum variance distortionless response (MVDR) beamformer, or the Capon beamformer [6].

4.1.4 Maximum Likelihood (ML)

Recall again the input signal vector from equation (4.1)

$$\mathbf{x}(t) = s(t)\mathbf{a}(\theta) + \mathbf{u}(t) = \mathbf{s}(t) + \mathbf{u}(t) \quad (4.25)$$

and define the probability density function for $\mathbf{s}(t)$ given $\mathbf{x}(t)$ as $p_{x(t)|s(t)}\{\mathbf{x}(t)\}$. Given $\mathbf{x}(t)$, it is desired to maximize $p_{x(t)|s(t)}\{\mathbf{s}(t)\}$.

Since the natural logarithm is a monotone function, increasing $p_{x(t)|s(t)}\{\mathbf{x}(t)\}$ is equivalent with increasing $\ln[p_{x(t)|s(t)}\{\mathbf{x}(t)\}]$. Thus the likelihood function of $\mathbf{x}(t)$ can be defined as

$$L[\mathbf{x}(t)] = -\ln[p_{x(t)|s(t)}\{\mathbf{x}(t)\}] \quad (4.26)$$

Assume that the $\mathbf{u}(t)$ is a stationary zero mean Gaussian vector with a covariance matrix \mathbf{R}_{uu} , and that $\mathbf{x}(t)$ is a Gaussian random vector with mean $s(t)\mathbf{a}(\theta)$. The likelihood function can be expressed as [14]

$$L[\mathbf{x}(t)] = c[\mathbf{x}(t) - \mathbf{a}(\theta)s(t)]^H \mathbf{R}_{uu}^{-1}[\mathbf{x}(t) - \mathbf{a}(\theta)s(t)] \quad (4.27)$$

where c is a scalar constant independent of $\mathbf{x}(t)$ and $s(t)$.

Our objective is to find an estimate $\hat{s}(t)$ of $s(t)$ which minimizes equation (4.27). Setting the partial derivative of $L[x(t)]$ with respect to $s(t)$ to zero [14]

$$\frac{\partial L[\mathbf{x}(t)]}{\partial s(t)} = -2\mathbf{a}^H(\theta)\mathbf{R}_{uu}^{-1}\mathbf{x}(t) + 2\hat{s}(t)\mathbf{a}^H(\theta)\mathbf{R}_{uu}^{-1}\mathbf{a}(\theta) = 0 \quad (4.28)$$

and note that $\mathbf{a}^H(\theta)\mathbf{R}_{uu}^{-1}\mathbf{a}(\theta)$ is a scalar, it follows that

$$\hat{s}(t) = \frac{\mathbf{a}^H(\theta)\mathbf{R}_{uu}^{-1}\mathbf{x}(t)}{\mathbf{a}^H(\theta)\mathbf{R}_{uu}^{-1}\mathbf{a}(\theta)} \quad (4.29)$$

Comparing equation (4.21) with (4.2), it is easy to realize that the optimum weight vector \mathbf{w}_{opt} using ML criterion is given by

$$\mathbf{w}_{ML} = \mathbf{w}_{opt} = \frac{\mathbf{R}_{uu}^{-1}\mathbf{a}(\theta)}{\mathbf{a}^H(\theta)\mathbf{R}_{uu}^{-1}\mathbf{a}(\theta)} \quad (4.30)$$

Define

$$\beta = \frac{1}{\mathbf{a}^H(\theta)\mathbf{R}_{uu}^{-1}\mathbf{a}(\theta)} \quad (4.31)$$

then the optimal weight vector using ML criterion can be expressed in the similar form of the Wiener-Hopf equation as

$$w_{ML} = \beta\mathbf{R}_{uu}^{-1}\mathbf{a}(\theta) \quad (4.32)$$

4.2 Adaptive algorithms

In the preceding section, we have shown that the optimum criteria are closely related to each other. Therefore, the choice of a particular criterion is not critically important in terms of performance. On the other hand, the choice of adaptive algorithms for

deriving the adaptive weights is highly important in that it determines both the speed of convergence and hardware complexity required to implement the algorithm. In this section we will discuss a number of common adaptive techniques. In this section we will express the algorithms in terms of discrete time.

4.2.1 Least Mean Squares (LMS)

The Least Mean Square (LMS) algorithm, introduced by Widrow and Hoff is an adaptive algorithm, which uses a gradient-based method of steepest descent [15], that recursively updates the weight vector. LMS algorithm uses the estimates of the gradient vector from the available data. It is intuitively reasonable that successive corrections to the weight vector in the direction of the negative of the gradient vector should eventually lead to the MSE, at which point the weight vector assumes its optimal value [34].

From the method of steepest descent, the weight vector equation is given by [16],

$$\mathbf{w}(n+1) = \mathbf{w}(n) - \frac{1}{2} \mu \left[-\nabla(E\{\varepsilon^2(n)\}) \right] \quad (4.33)$$

where $\varepsilon(k) = r^*(k) - y(k)$ and μ is the step size which controls the convergence characteristics of $\mathbf{w}(n)$. From equation (4.6) we have

$$\nabla E\{\varepsilon^2(n)\} = -2\mathbf{r}_{xr} + 2\mathbf{R}_{xx}\mathbf{w}(n) \quad (4.34)$$

Replacing (4.34) into (4.33), we have

$$\mathbf{w}(n+1) = \mathbf{w}(n) + \mu[\mathbf{r}_{xr} - \mathbf{R}_{xx}\mathbf{w}(n)] \quad (4.35)$$

In order to update the optimum weight using equation (4.35), it is necessary to know in advance both \mathbf{R}_{xx} and \mathbf{r}_{xr} and it is better to use their instantaneous values

$$\mathbf{R}_{xx}(n) = \mathbf{x}(n)\mathbf{x}^H(n) \quad (4.36)$$

$$\mathbf{r}_{xr}(n) = \mathbf{x}(n)r^*(n) \quad (4.37)$$

Thus equation (4.35) now becomes

$$\begin{aligned}
\mathbf{w}(n+1) &= \mathbf{w}(n) + \mu \mathbf{x}(n)[r^*(n) - \mathbf{x}^H(n)\mathbf{w}(n)] \\
&= \mathbf{w}(n) + \mu \mathbf{x}(n)[r^*(n) - y^*(n)] \\
&= \mathbf{w}(n) + \mu \mathbf{x}(n)[\varepsilon^*(n)]
\end{aligned} \tag{4.38}$$

It is noted that the convergence rate of the LMS algorithm depends on the step size μ and correspondingly on the eigenvalue spread of the covariance matrix \mathbf{R}_{xx} .

The LMS algorithm initiated with some arbitrary value (usually equal to zero) for the weight vector is seen to converge and stay stable for

$$0 < \mu < \frac{2}{\lambda_{\max}} \tag{4.39}$$

where λ_{\max} is the largest eigenvalue of the covariance matrix \mathbf{R}_{xx} . The convergence of the algorithm is inversely proportional to the eigenvalue spread of the covariance matrix \mathbf{R}_{xx} . When the eigenvalues of \mathbf{R}_{xx} are widespread, convergence may be slow. The eigenvalue spread of the covariance matrix is estimated by computing the ratio of the largest eigenvalue to the smallest eigenvalue of the matrix. If μ is chosen to be very small then the algorithm converges very slowly. A large value of μ may lead to a faster convergence but may be less stable around the minimum value.

4.2.2 Sample Matrix Inversion (SMI)

If the desired and reference signals are both known a priori, then the optimal weights could be computed using the direct inversion of the covariance matrix as in (2.22). Since the desired and reference signals are not known in practice it is possible to use their estimates from the input data vector as [6]

$$\mathbf{R}_{xx}(n) = \frac{1}{n} \sum_{i=1}^n \mathbf{x}(i)\mathbf{x}^H(i) \tag{4.40}$$

$$r_{xx}(n) = \frac{1}{n} \sum_{i=1}^n \mathbf{x}(i)r^*(i) \tag{4.41}$$

From equation (4.7), it follows that the estimated weight vector using the SMI algorithm is given by

$$\mathbf{w}(n) = \mathbf{R}_{xx}^{-1}(n)\mathbf{r}_{xr}(n) \quad (4.42)$$

It is noted that the SMI is a block-adaptive algorithm and has been shown to be the fastest algorithm for estimating the optimum weight vector [17][34]. In practice, the signals are not known and the signal environment undergoes frequent changes. Thus, the processor must continually update the weight vector to meet the new requirements imposed by the varying conditions. One of disadvantages of this algorithm is that its stability depends on the ability to invert the large covariance matrix. Another disadvantage that has to be encountered is that even though the algorithm has faster convergence, huge matrix inversions lead to computational complexities that cannot be easily overcome [6].

4.2.3 Normalized Least Mean Square (N-LMS)

In the LMS algorithm the correction $\mu\mathbf{x}(n)[\varepsilon^*(n)]$ applied to vector $\mathbf{w}(n)$ at time $n+1$ is directly proportional to the input $\mathbf{x}(n)$. Therefore when $\mathbf{x}(n)$ is large, the LMS algorithm experiences a gradient noise amplification problem. To overcome this difficulty, we may use the normalized LMS algorithm which is the companion to the ordinary LMS. In particular, the correction applied to the vector $\mathbf{w}(n)$ at time $n+1$ is normalized with respect to the squared Euclidean norm of the vector $\mathbf{x}(n)$ at time n .

We may formulate the normalized LMS algorithm as a natural modification of the ordinary LMS. In order to exercise control over the change in the vector from one iteration to the next without changing its direction, we introduce a positive real scalar factor noted by μ_0 . The desired recursion that computes the weight vector is normalized and is given by:

$$\mathbf{w}(n+1) = \mathbf{w}(n) + \frac{\mu_0}{|\mathbf{x}(n)|^2} \mathbf{x}(n)[\varepsilon^*(n)] \quad (4.43)$$

where μ_0 is a constant, with $0 < \mu_0 < 2$

The principle [11] that normalized LMS satisfies is that in the light of new input data, the parameters of the adaptive system are be disturbed in a minimal fashion.

A problem of normalized LMS is that when the vector $\mathbf{x}(n)$ is small, numerical difficulties may arise because then we have to divide by a small value for the squared norm $|\mathbf{x}(n)|^2$. To overcome this problem, we slightly modify the recursion as follows:

$$\mathbf{w}(n+1) = \mathbf{w}(n) + \frac{\mu_0}{\alpha + |\mathbf{x}(n)|^2} \mathbf{x}(n)[\varepsilon^*(n)] \quad (4.44)$$

with $\alpha > 0$

4.2.4 Hybrid algorithm

The previous discussions on LMS and SMI have provided us with an understanding of their advantages and disadvantages. In the combined algorithm the individual good aspects of both the algorithms are used [34].

SMI algorithm convergences faster than LMS, because uses inversion of matrices. However, this demands extensive computations, especially when the inverted matrix is huge. Moreover SMI requires that the signal environment does not have significant changes when the samples are obtained. The LMS is a very simple and widespread algorithm. In regard with the SMI, LMS can be applied in continuous transmission systems, since it works continuously. The disadvantage is that its convergence speed depends on parameters like μ , and moreover convergence slower than SMI. The demand for an algorithm that has fast convergence, it is simple and has low computation requirements lead us to a propose algorithm called hybrid algorithm. The algorithm that achieves these goals concatenates the SMI and LMS.

The hybrid algorithm that we define in this paragraph uses the advantages of the SMI and LMS algorithm. In order to speed up the convergence rate of the LMS algorithm the initial weight vector is defined using the SMI algorithm. The weight vector is calculated by inversion of the covariance matrix, as illustrated by the following equation:

$$\mathbf{w}_{opt} = \mathbf{R}_{xx}^{-1} \mathbf{r}_{xr} \quad (4.45)$$

where the covariance matrix and the correlation matrix is given by $\mathbf{R}_{xx} = E[x(n)x^H(n)]$ and $\mathbf{r}_{xr} = E[x(n)r^*(n)]$ respectively.

With SMI algorithm we calculate the weight vector using a small block of samples-data. Therefore the initial weight vector can be re-written as $\mathbf{w}_{ini} = \mathbf{R}_b^{-1} \mathbf{r}_b$, where the covariance matrix and the correlation matrix is given by

$$\mathbf{R}_b = \frac{1}{b} \sum_{i=1}^b \mathbf{x}(i)\mathbf{x}^H(i) \text{ and } r_b = \frac{1}{b} \sum_{i=1}^b \mathbf{x}(i)r^*(i).$$

b is the block size. The block size is taken to be small enough so as to ensure that the effect due to changes of signal environment, does not affect the performance of the algorithm. Also, a large block will only mean more matrix inversions making it computationally intensive.

As discussed in paragraph 4.2.1 in LMS algorithm the initial weight vector is taken arbitrarily and for simplicity equal to zero ($\mathbf{w}(0) = 0$). The weight vector is updated using equation 4.38. Since the weight initialization is arbitrary, it may take longer to converge to the final value of weight vector. This happens because the initial vector may not be close to the final value of weight vector

In the hybrid algorithm, the initial weight for the LMS update equation is equal to \mathbf{w}_{ini} , which is obtained using the SMI algorithm. The initial value of the weight vector in LMS algorithm is not arbitrary as usual, but is derived by the SMI algorithm. Using SMI algorithm the initial weight vector's value is close to the final value. Therefore when LMS starts to form the beams of the antenna, the main lobe is already close to direction of the desired signal. With the hybrid algorithm we may encounter the changes of signal environment, since LMS updates the weight vector continuously, using every incoming sample. Therefore hybrid algorithm is better suited for continuous transmission systems compared with SMI algorithm, which is unsuitable for continuous transmission system.

4.3 Transmitted signal

Although estimation algorithms are not inherently dependent upon the modulation scheme we will consider minimum shift keying (MSK) modulation for simulation purposes. We can represent the MSK signal as [18]

$$\begin{aligned} s(t) &= d_I(t) \cos(\pi / 2T_b) \cos(2\pi f_c t) + \dots \\ &+ d_Q(t - T_b / 2) \sin(\pi(t - T_b / 2) / 2T_b) \sin(2\pi f_c (t - T_b / 2)) = \quad (4.46) \\ &= \cos(2\pi f_c + b(t)(\pi / 2)T + \theta(t)) \end{aligned}$$

where $b(t) = -d_I(t)d_Q(t)$ and $\theta(t) = \begin{cases} 0 & d_I(t) = 1 \\ \pi & d_Q(t) = -1 \end{cases}$

The $d_I(t)$ and $d_Q(t)$ are the in phase and quadrature transmission digital sequence which is given in general by the equation:

$$d(t) = \sum_{k=-\infty}^{\infty} d_k g_t(t - kT_b) \quad (4.47)$$

where $g_T(t)$ and T_b are the pulse shape of each transmission digital data and the bit duration, respectively.

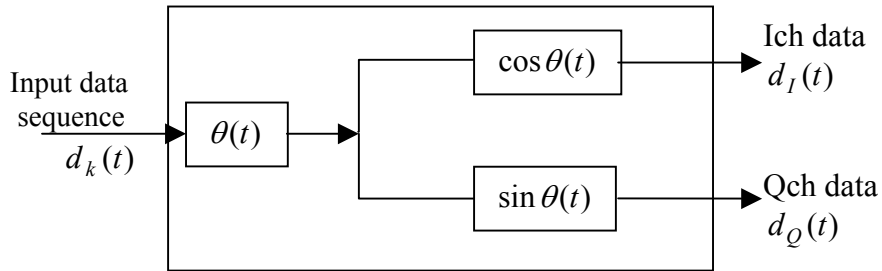


Figure 4.1: Mapping circuit for MSK

In the previous discussion, the MSK configuration based on that of OQPSK. Another approach starts from FSK-based transmission scheme. An MSK signal is regarded as an FSK signal with a continuous phase transition, because the phase locus is smoothly and continuously distributed. The configuration of the configuration of the mapping circuit in this case is shown in figure 4.1. The FSK signal with its continuous phase transition is described as:

$$s(t) = A \cos(2\pi f_c t + \theta(t)) \quad (4.48a)$$

$$\theta(t) = 2\pi\Delta f \int_{-\infty}^t x(\tau) d\tau \quad (4.48b)$$

$$x(t) = \sum_k d_k p(t - kT_b) \quad (4.48c)$$

where $p(t)$ is a rectangular pulse

$$p(t) = \begin{cases} 1 & 0 < t \leq T_b \\ 0 & \text{otherwise} \end{cases} \quad (4.49)$$

the integer d_k : k is a data sequence with ± 1 data and the power spectrum density of the signal MSK is given by:

$$S_{MSK}(f) = \frac{16T_b}{\pi^2} \left(\frac{\cos(2\pi f T_b^2)}{1 - 16f^2 T_b^2} \right) \quad (4.50)$$

For the generation of MSK signal we follow the procedure:

- Using input d_k we calculate $\theta(t)$ which is given by equation (4.48b)

$$\begin{aligned} \theta(kT_b) - \theta((k-1)T_b) &= 2\pi\Delta f \int_{(k-1)T_b}^{kT_b} x(\tau) d\tau \Rightarrow \\ \theta(kT_b) &= \theta((k-1)T_b) + 2\pi\Delta f \int_{(k-1)T_b}^{kT_b} x(\tau) d\tau = \\ &= \theta((k-1)T_b) + 2\pi\Delta f T_b d_k = \\ &= \theta((k-1)T_b) + \frac{\pi}{2} d_k \end{aligned} \quad (4.51)$$

because $\theta(kT_b)$ is continuously connected with $\theta((k-1)T_b)$ in the area $(k-1)T < t \leq kT$, follows that

$$\theta(t) = \theta((k-1)T_b) + \frac{\pi}{2} d_k \frac{t - (k-1)T_b}{T_b} \quad (4.52)$$

- The calculated $\theta(t)$ is input to equation (4.46) to obtain MSK.

Chapter 5

Wireless System Configuration

5.1 Mobile radio environment

Objects surrounding the Base Station (BS) and Mobile Station (MS) severely affect the propagation characteristics of the uplink and downlink channels of cellular systems. This propagation path loss, including reflection and shadowing, tends to degrade system capacity. The height of the MS antenna (e.g. 2 m) is normally much lower than that of the surrounding buildings and natural features. Furthermore, the carrier frequency wavelength is also much less than the size of surrounding structures. Due to this, a MS will experience significant changes of its received signal strength as it moves. The mobile receiver is characterized by “multipath reception”. Its received signal contains a number of electromagnetic waves from the same source (transmitter) arriving at the receiver antenna along different paths. Even when line-of-sight is available, the additional electromagnetic waves beside the direct wave result from the reflection, refraction, scattering and diffraction of the transmitted signal off objects along the propagation path. These extra waves arrived at the receiving antenna displaced with respect to each other in time and space. Due to this phenomenon, the resultant received signal that appears at the receiver amplifier could be much weaker or stronger than the direct wave.

Fading due to multipath and shadowing, Doppler spread (due to the motion of one of the antenna) and delay spread are some of the main channel effects that arise from these phenomena.

5.1.1 Fading

When a mobile station moves over small distances of a fraction of a wavelength, the instantaneous field strength at the receiver antenna may rapidly fluctuate as much as four or five orders of magnitude. This is known as signal fading, or small-scale fading. There are two approximately separate effects known as fast and slow fading. Fast fading is characterized by deep fades that occur within fractions of a wavelength

and is caused by multipath scattering of the signal off objects in the vicinity of mobile. It is most severe in heavily built-up areas where the number of waves arriving from different directions with different amplitudes and phases cause the signal amplitude to follow a Rayleigh distribution. However, fast (Rayleigh) fading also occurs to a certain extent in suburban areas. Finally slow fading is the result of buildings and trees that stand between MS and BS. Slow fading exhibits log-normal distribution.

5.1.2 Doppler spread

In a wireless channel with multipath Rayleigh fading signals, let the n -th reflected wave arrive from an angle θ_n relative to the direction of the motion of the MS antenna. Due to the motion of the antenna the frequency of the received signal will go through a shift. The change in the received signal frequency of this Rayleigh fading is known as Doppler shift. It can be represented by the formula

$$\Delta f_n = \frac{v}{\lambda} \cos \theta_n \quad (5.1)$$

Where v is the speed of the mobile antenna and λ is the wavelength.

Hence motion of the MS antenna that results in the Doppler shift produces phase shifts of each reflected wave. When the waves arrive at the antenna, since they all have different phase shifts, the amplitude of the resulting composite signal will be modified by the Doppler shift, and hence the velocity vector of the MS.

A measure of the time rate of change of the channel due to motion is the Doppler frequency spectrum, which provides statistical information about the variation of the frequency of a tone received by a mobile travelling at velocity v . It is assumed that the received signal at the mobile station came from all directions and was uniformly distributed. The Doppler power spectrum is given by [19]

$$S(f) = \begin{cases} \frac{3}{2\pi f_m \sqrt{1 - \left(\frac{f - f_c}{f_m}\right)^2}} & |f - f_c| < f_m \\ 0 & elsewhere \end{cases} \quad (5.2)$$

where f_m is the maximum Doppler shift given by v/λ and f_c is the working frequency.

Doppler spread causes time-selective fading since it directly impinges on the phase of the signals. Thus the instantaneous received signal amplitude varies with time. The signal amplitude in the presence of Doppler fading is characterized by and inversely proportional to the coherence time. We define the coherence time as the time separation over which the channel impulse response at the two time instants remains strongly correlated

5.1.3 Delay station spread

Delay spread is a well-known phenomenon at high frequency electromagnetic. In wired systems we get delay spread due to the high frequency portion of a signal (e.g. a rectangular pulse) travelling much faster than the lower frequency portion of the signal. Hence at the line termination the signal looks spread out in the time domain, since the lower frequency energy arrives later than the high frequency energy. In wireless systems, time spread occurs due to multipath, in other words due to reflection and differences in the distance traveled by each reflected signal. When the distances are different, although the signals travel at the velocity of light, their arrival times will be different and proportional to the distance traveled. Hence multipath effects create time dispersion and a spreading of the signal. Urban delay spreads of around $3\mu\text{s}$ are commonplace. Delay spread results in frequency –selective fading, that is, it is dependent on the frequency. If the variation of the delay is comparable with the symbol period, delay signals from earlier symbol may interfere either the next symbol, causing intersymbol interference (ISI). It can be characterized by the coherence bandwidth, which is inversely proportional to the delay spread. Coherence bandwidth is defined as the maximum frequency difference for which two frequency-shifted signals are still strongly correlated in terms of either amplitudes or phases.

5.1.4 A Mathematical Model of Fading in Communication Channels

Consider a transmitted signal $s(t) = A\cos(2\pi f_c t + \theta)$ through a fading channel. The received signal can be expressed as (ignoring the effects of noise):

$$y(t) = A \sum_{i=1}^N a_i \cos(2\pi f_c t + \theta_i) \quad (5.3)$$

Where, a_i is the attenuation of the i -th multipath component and θ_i is the phase-shift of the i -th multipath component. The a_i and θ_i are random variables. The above expression can be rewritten as:

$$y(t) = A \left\{ \left(\sum_{i=1}^N a_i \cos(\theta_i) \right) \cos(2\pi f_c t) - \left(\sum_{i=1}^N a_i \sin(\theta_i) \right) \sin(2\pi f_c t) \right\} \quad (5.4)$$

We introduce two random variables X_1 and X_2 , such that the above equation becomes:

$$y(t) = A \{ X_1(t) \cos(2\pi f_c t) - X_2(t) \sin(2\pi f_c t) \} \quad (5.5)$$

If there are large number of scattered waves present, then by Central Limit theorem, we can approximate X_1 and X_2 to be Gaussian random variables with zero mean and variance σ^2 . The above expression can be rewritten as:

$$y(t) = AR(t) \cos(2\pi f_c t + \theta(t)) \quad (5.6)$$

Where, the amplitude of the received waveform R is given by:

$$R = \sqrt{(X_1)^2 + (X_2)^2} \quad (5.7)$$

It can be shown that R has a Rayleigh distribution[20] with a probability density function (pdf) given by:

$$f_R(r) = \frac{r}{2\sigma^2} e^{-\frac{r^2}{2\sigma^2}} \quad r > 0 \quad (5.8)$$

The phase of the received waveform is given by:

$$\theta(t) = \tan^{-1} \left(\frac{X_2(t)}{X_1(t)} \right) \quad (5.9)$$

It can be shown that the $\theta(t)$ has a Uniform Distribution function with a probability density function (pdf) given by:

$$f_{\theta}(\theta) = \frac{1}{2\pi}, \quad -\pi \leq \theta \leq \pi \quad (5.10)$$

The distortion in the phase can be easily overcome if differential modulation is employed. It is the amplitude distortion $R(t)$ that severely degrades performance of digital communication systems over fading channels. It is usually reasonable to assume that the fading stays essentially constant for at least one signalling interval.

Since Rayleigh-fading is a multiplicative process, its simulation involves generating the Rayleigh fading process and multiplying it with the transmitted signal. The generation part directly follows from the fact that the envelope of a complex Gaussian random process (with independent real and imaginary parts) has a Rayleigh distribution. Once the Rayleigh fading signal is generated, it can be multiplied with the transmitted signal to simulate the Rayleigh fading channel.

5.2 MS positioning in the cellular network

The different positioning methods can be divided into two groups: network based solutions and terminal based solutions, depending on if the position estimate computations take place in the fixed Base Transceiver (BTS) network or in the mobile unit. The BTS network can offer more computer power, but a mobile unit would increase personal identity security and decrease the network load. We will not consider this question in this short survey over different positioning methods [21].

A lot of simulations and measurements have been done to compare the different positioning methods, but they often give contradictory results. This is expected since the signal propagation is sensitive to the surrounding environment. However, excluding GPS (Global Positioning System), the methods based on signal propagation time are today the most reliable methods

5.2.1 Network based positioning

In smart antenna technology, BS has played a critical role in making it possible to install large array antennas to achieve adaptive, steerable beamforming where the

multiple beams keep track of the MS. In order to generate these smart beams, the position of each MS should be located.

A satellite system having about 24 satellites is used in GPS system. A GPS receiver installed at the MS provides the position estimate of the MS using a group of satellites. Using an accurate clock for precise timing, the GPS receiver measures the time delay between the signals leaving, four satellites in the sight of the MS and arriving at the MS receiver. This allows calculation of the exact distance between MS and each satellite. Thus the MS position can be computed using triangular method, providing coordinates in latitude, longitude and altitude. The global position system (GPS) is commonly used for navigation purposes today, but the GSM system can give additional information to the GPS receivers to obtain better coverage and accuracy. These methods are very accurate and positioning can be done within metres precision depending on the type of GPS and the surrounding environment. The interest has yet been quite low in this kind of solution from the mobile community since the GPS receivers are relative expensive, require line of sight (LOS) conditions and can not penetrate buildings well enough for indoor positioning. The power consumption in the mobile will also increase which requires more powerful batteries. This might be a problem since there is a trend of almost ever decreasing sizes of the mobile phones.

Mobile position estimation, using signals strength [22]-[23] measurements, is one of the most well known methods using the path loss attenuation with distance information. Its primary source of error is multipath fading and shadowing. Variations in the signal strength can be greater for a distance of the order of half a wavelength. Signal strength averaging can help, but low-mobility MSs may not be able to average out the effects of multipath fading, and there will still be adverse effects due to shadow fading. The errors due to shadow fading may be handled by using pre-measured signal strength contours centred at the BSs. However this approach requires that the contours be mapped out for each BS and a data bank is available for use.

Triangulation using received signal strength requires either a very good fading model or empirical data of the signal strength sampled from all interesting positions in the area. Both approaches are difficult, but there are benefits using a signal strength analysis compared with other methods; the signal strength information can be very useful for the system operator. Empirical models have been derived by Hata [24], but

these models are of global character and do not describe the local fading in a urban area well enough for position location purposes. Since the signal model is only calculated once it is not a time critical step in the algorithms.

The angle of arrival (AOA) methods [25] are sometime also referred to as direction of arrival (DOA) methods. By measuring the angle of arrival of the transmitted signal at two or more different BTS, it is possible to find the position of the mobile by triangulation. The AOAs of the signal from the MS are calculated as the BS by using adaptive phased arrays at the BS. The main beam of the antenna array is electronically steered until it locks on the signal arriving at the MS. Two closely spaced antenna arrays are used to scan horizontally to get the exact direction of the peak strength of the incoming MS signal. Since the antenna elements are closely placed, the time delay between the two elements seen by a signal as it propagates across the array may be modelled by a phase shift. This is the basic arrangement for most AOA estimation algorithms. Accurate AOA is estimated when the signal coming in from the MS is a direct line-of sight (LOS) signal. If the antenna array beam should lock on to a reflected signal the AOA estimate will obviously be wrong. Furthermore, lock on to a reflected signal the AOA estimate will obviously be wrong. Furthermore, the AOA estimator performance degrades as the distance between the MS and the BS increases.

The time-of-arrival (TOA) based estimation [26]-[27] of position is also possible. In free space the time taken for an electromagnetic wave to travel over a distance is proportional to d , since the velocity of the wave is equal to the constant speed of light. Hence the BS may determine the distance d by first indirectly determining the time that the signal takes to travel from the source to the receiver on the forward on the reverse link. This TOA may be obtained by measuring the time in which the MS responds to an inquiry or an instruction transmitted to the MS from the BS. The total time elapsed from the instant the command is transmitted to the instant the MS responds may be stored, and this time is equal to the sum of the round trip signal delay and any processing and response delay within the MS unit. If the MS microprocessor processing delay for the desired response is known with sufficient accuracy, it can be subtracted from total measured time. The resultant time would give the total round trip delay. Half of the round trip delay would be an estimate of the signal delay in one direction. If we multiply this with the velocity of light, we will get

the distance between the BS and the MS. If the MS signal can be detected at a minimum of the three BSs, then the MS position can be computed by the triangulation method.

There are certain problems with the TOA method. The estimate of the microprocessor processing time and response delay of the MS electronics within the MS may be difficult to determine in practice. Indeed different manufacturers of MS phones will use different electronics and circuitry, giving rise to quite different microprocessor-discrete electronics response time. Furthermore, LOS between the BS and the MS is not available and severe timing errors could occur. The problem will be difficult to handle when there are many multipath signals arriving at the BS.

Another popular method seems to be Time Difference of Arrival (TDOA). The method measures the relative arrival time from one mobile at three BTS at the same time (or vice versa). This requires exact synchronisation between the BTS. The position estimate will be given by the intersection of two hyperboloids and the solution to the equation system thus has to be found by some kind of iterative method.

5.2.2 Terminal based positioning

This method requires the MS to use signals from several BSs to calculate its position. It is a self-positioning system, where the MS estimates its own position. Again the signal strength (this time from BS to MS) or the TOA information may be used. However, modification to the existing MS software will be necessary since the position computation will be performed as the MS. The control microprocessor must carry the position-estimation software in order to store and process information from four or more BSs.

The MS receiver must be capable of simultaneously processing information from at least four BS frequency channels, either for signal strength or time delay information. Data from three BSs are required for the position estimation; while the fourth is needed to cycle through all available signals to ensure the best three BS signals are being used for the position estimation. In practical implementation, it is necessary for the network to maintain a BS location database and transfer information to the MS whenever it is requested.

5.2.3 Problems in location estimation

Location estimating using the mobile network is very convenient since it takes advantage of the existing cellular network structure and only requires the signal as input. Unfortunately it also inherits the disadvantages imposed by the design of the network.

In most of the techniques presented above two or more non-serving BTS are involved in the location procedure which might cause problems due to low received signal strength at a remote BTS; especially when the mobile is close to the serving BTS and thus might automatically be forced to transceive at a lower power level. This is called the hearability problem. The fast decay of the signal power is due to the non line of sight (NLOS) conditions and is something that is highly appreciated for interference reduction making the channel reuse distance smaller, but it makes triangulation harder.

Another important problem with NLOS conditions is that signals in urban areas tend to propagate along the streets and timing, signal strength and angle of arrival will differ from what can be expected from a LOS model. The received signal also consists of several copies of the signal but with different time delays, magnitude and phase. This phenomenon, when the signal interferes with itself, is called multi-path propagation and is important to include in a signal propagation model. TDOA reduces this problem since it measures the time of arrival difference between different BTS and the errors are then hoped to cancel, but for more accurate results this effect must be included in the models. For the signal strength this will result in fast fading, which can be described as the rapid changes of the signal strength due to interference. The signal strength also heavily depends on how the user directs the antenna and the very local surroundings. These two phenomena reduces the applicability of the signal strength analysis.

The geographical positions of the BTS can also be important, especially in rural areas or along highways where the BTS tend to be aligned which will reduce the accuracy of the triangulation.

5.3 Position and velocity estimation in cellular systems

Information about the position and velocity of mobile stations can be obtained using the signal strengths of the MS at different BSs and the corresponding propagation time [28]. However both quantities are subject to strong fluctuations caused by short – term fading, shadowing and reflections, which make them useless unless a sophisticated method is used to counter this problem and translate the quantities into required information.

A method of estimating the position and velocity of a MS in a cellular system, based on an electric-field strength model, is presented in this paragraph. The algorithm uses the principle of maximum likelihood estimation.

5.3.1 Antenna signal model

In this paragraph we will present a model for electromagnetic field radiated by an infinitesimal element carrying current of any geometrical shape. The geometry is defined in figure 5.1.

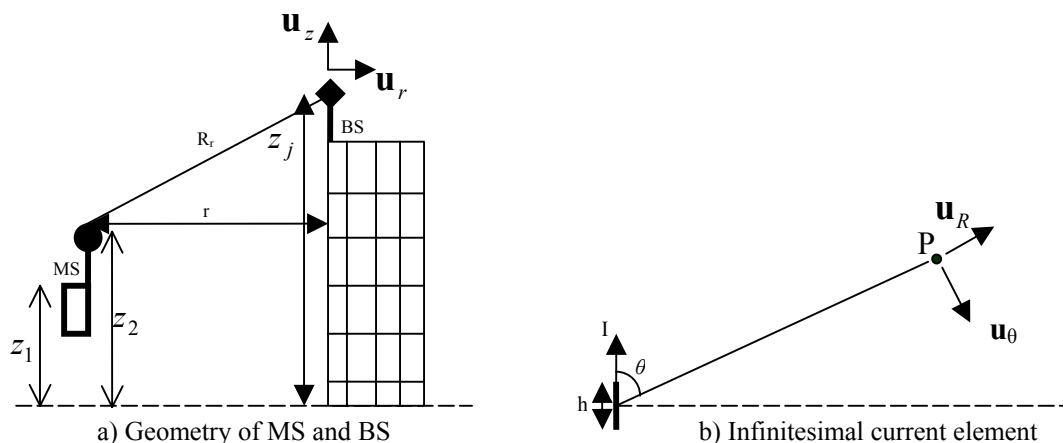


Figure 5.1: Antenna geometry

The radiated electric field from a finite-sized wire antenna is given by [see Appendix A]:

$$\mathbf{E}(R,t) = \mathbf{u}_R \frac{h \cos \theta}{4\pi} \left[\left(\frac{\mu_0}{\varepsilon_0} \right)^{1/2} \frac{2[I]}{R^2} + \frac{2[Q]}{\varepsilon_0 R^3} \right] + \mathbf{u}_\theta \left[\frac{h \sin \theta \mu_0}{4\pi R} \frac{d[I]}{dt} + \left(\frac{\mu_0 [I]}{\varepsilon_0 R^2} \right)^{1/2} + \frac{[Q]}{\varepsilon_0 R^3} \right] \quad (5.11)$$

In cylindrical coordinates, using cylindrical coordinate unit vectors \mathbf{u}_r and \mathbf{u}_z previous equation may be written as [36]

$$\begin{aligned} \mathbf{E}(r,z,t) = & \mathbf{u}_r \left[\frac{3h}{4\pi} \left(\frac{\mu_0}{\varepsilon_0} \right)^{1/2} \frac{rz}{(r^2+z^2)^2} [I] + \frac{\mu_0 h}{4\pi} \frac{rz}{(r^2+z^2)^{2.5}} \frac{d[I]}{dt} + \frac{3h}{4\pi \varepsilon_0} \frac{rz}{(r^2+z^2)^{2.5}} [Q] \right] \\ & + \mathbf{u}_z \left[\frac{h}{4\pi} \left(\frac{\mu_0}{\varepsilon_0} \right)^{1/2} \left(\frac{2z^2}{(r^2+z^2)^2} - \frac{r^2}{(r^2+z^2)^2} \right) [I] - \frac{\mu_0 h}{4\pi} \frac{r^2}{(r^2+z^2)^2} \frac{d[I]}{dt} \dots \right. \\ & \left. + \frac{h}{4\pi \varepsilon_0} \left(\frac{z^2}{(r^2+z^2)^{2.5}} - \frac{r^2}{(r^2+z^2)^{2.5}} \right) [Q] \right] \end{aligned} \quad (5.12)$$

It can be further simplified as the receiving antenna will only pick up the vertical polarized signal, \mathbf{E}_z . Therefore, by ignoring \mathbf{E}_r and assuming that $[Q] = 0$,

$$\mathbf{E}'(r,z,t) = \mathbf{u}_z \left[\frac{h}{4\pi} \left(\frac{\mu_0}{\varepsilon_0} \right)^{1/2} \left(\frac{2z^2}{(r^2+z^2)^2} - \frac{r^2}{(r^2+z^2)^2} \right) [I] - \frac{\mu_0 h}{4\pi} \frac{r^2}{(r^2+z^2)^2} \frac{d[I]}{dt} \right] \quad (5.13)$$

By setting $h = dz$, $h = z_j - z$, $dz = -dz$ and integrating equation (5.13), and considering only far field regions, the electric field strength radiated by a linear dipole antenna of finite length $(z_2 - z_1)$ is of the form [36]

$$E(r,z,t) = \frac{\mu_0}{4\pi} \left[\frac{z_j - z_1}{\sqrt{r^2 + (z_j - z_1)^2}} - \frac{z_j - z_2}{\sqrt{r^2 + (z_j - z_2)^2}} \right] \frac{d[I]}{dt} \quad (5.14)$$

$$[I] = \text{Re} \left(I_0 e^{j\omega(t-R/c)} \right) \quad (5.15)$$

Where I_0 is the amplitude, ω is the angular frequency of the current flowing through the transmitter antenna and μ_0 is magneto-conductance of vacuum. Thus

$$\frac{d[I]}{dt} = j\omega I_0 e^{j\omega(t-R/c)} \quad (5.16)$$

The signal processor operates only in the magnitude of the measured electric field strength. Hence equation (5.16) is reduced to $\left| \frac{d[I]}{dt} \right| = \omega I_0$

Therefore, equation (5.14) can be expressed as [36]

$$E(r, z) = A_0 \left[\frac{z_j - z_1}{\sqrt{r^2 + (z_j - z_1)^2}} - \frac{z_j - z_2}{\sqrt{r^2 + (z_j - z_2)^2}} \right] \quad (5.17)$$

Where $A_0 = \frac{\mu_0 \omega I_0}{4\pi} = 10^{-7} \omega I_0$ and $I_0 = \sqrt{\frac{P_r}{R_r}}$

P_r is the power radiated and R_r is the radiation resistance of the transmitter antenna. The advantage of using this model is that it provides a more realistic picture of a MS-BS communication link as it takes in to account the distance r between the BS and MS as well as their respective heights (z_1 , z_2 and z_j) with respect to the ground

5.3.2 Position and velocity (PVE) algorithm

To determine the two dimensional position and velocity of a MS, the field strengths from the MS received by a minimum of three BSs are required. The theoretical electric field strengths received by the three BSs are $\mathbf{E} = [E_1 \ E_2 \ E_3]$. The measured electric field strengths received at BTSs for a single MS are $\mathbf{E}_m = [E_{m1} \ E_{m2} \ E_{m3}] = \mathbf{E} + \mathbf{n}$ where the subscript m stands for measurements, \mathbf{n} is white Gaussian noise [20]. The problem is to obtain the position of MS, called as $\mathbf{PM}(x,y)$. The first step is to get the distance between the MS and the BSs: $\mathbf{r} = [r_1 \ r_2 \ r_3]$.

The method to get \mathbf{r} is based in non linear mean square method [29][30][31]. The electric field strength \mathbf{E} is a non-linear function of \mathbf{r} and is given by [36]

$$\mathbf{E}(r) = \mathbf{E}(r_o) + \frac{\partial \mathbf{E}}{\partial \mathbf{r}} \Delta \mathbf{r} + \frac{1}{2!} \frac{\partial^2 \left(\frac{\partial \mathbf{E}}{\partial \mathbf{r}} \right)}{\partial \mathbf{r}} \Delta \mathbf{r}^2 + \dots \quad (5.18)$$

We can ignore higher order terms since $\Delta \mathbf{r}$ is very small compared with \mathbf{r} and we can use the Jacobian matrix that follows

$$\mathbf{Jr}_0 = \begin{bmatrix} \frac{\partial E_1}{\partial r_1} & 0 & 0 \\ 0 & \frac{\partial E_2}{\partial r_2} & 0 \\ 0 & 0 & \frac{\partial E_3}{\partial r_3} \end{bmatrix} \quad (5.19)$$

From equation (5.17) we have

$$\frac{\partial E}{\partial r} = -A_0 \left[\frac{z_j - z_1}{[r^2 + (z_j - z_1)^2]^{3/2}} - \frac{z_j - z_2}{[r^2 - (z_j - z_1)^2]^{3/2}} \right] r \quad (5.20)$$

The error between measurement and theoretical value for the field strength is given by

$$\boldsymbol{\varepsilon} = \mathbf{E}_m - \mathbf{E}(\mathbf{r}) = (\mathbf{E}_m - \mathbf{E}_0) - \mathbf{J}_0 \Delta \mathbf{r} \quad (5.21)$$

We assume $\mathbf{u} = \boldsymbol{\varepsilon}^T \boldsymbol{\varepsilon}$ we need to minimize \mathbf{u} by setting $\frac{\partial \mathbf{u}}{\partial \mathbf{r}} = 0$

For equation (5.21) and using $\frac{\partial \mathbf{u}}{\partial \mathbf{r}} = 0$ the main iteration equation for \mathbf{r} is obtained as

$$\mathbf{r}_{n+1} = \mathbf{r}_n + (\mathbf{Jr}_n^T \mathbf{Jr}_n)^{-1} \mathbf{Jr}_n^T (\mathbf{E}_m - \mathbf{E}_n) \quad (5.22)$$

The distance from MS to each of the BSs is obtained from equation 5.22. However, the goal is not to get \mathbf{r} , but the position of MS i.e. PM. Using the estimated vector r , which gives the distances between the BS's positions and the MS, an estimated position of the MS can be obtained. However, sin the radii of the circles taken from the r estimates unlikely to arrive at an exact cross intersection; further processing is necessary to reach a closer estimate of the actual position of MS. The main iteration equation to get PM from \mathbf{r} resembles equation (5.22) and is given by:

$$\mathbf{PM}_{k+1} = \mathbf{PM}_k + (\mathbf{Jp}_k^T \mathbf{Jp}_k)^{-1} \mathbf{Jp}_k^T (0 - \text{errp}_k) \quad (5.23)$$

where $\mathbf{errp}_k = |\mathbf{PM} - \mathbf{PB}| - r$ with $\mathbf{PB} = [PB_1, PB_2, PB_3]$ representing the position of the three BS that uses the MS. These three BS change as MS is moving.

\mathbf{Jp}_k is redefined as

$$\mathbf{Jp}_k = \begin{bmatrix} \frac{\partial \mathbf{errp}_1}{\partial x} & \frac{\partial \mathbf{errp}_1}{\partial y} \\ \frac{\partial \mathbf{errp}_2}{\partial x} & \frac{\partial \mathbf{errp}_2}{\partial y} \\ \frac{\partial \mathbf{errp}_3}{\partial x} & \frac{\partial \mathbf{errp}_3}{\partial y} \end{bmatrix} \quad (5.24)$$

Finally the velocity of the MS can be obtained from sequential position of the MS and is estimated as

$$V_m = \frac{(PM_m - PM_{m-1})}{T}. \quad (5.25)$$

Where “T” is the time interval between two discrete positions of the MS.

5.3.3 Time advance usage in algorithm

The position and velocity algorithm requires an initial set of r values (distance from MS to each of the selected BSs) to proceed. These values can be obtained by making use of timing information provided by the cellular network. It is found that with the help of this timing information to generate the required initial values, the algorithm is able to produce quite accurate results.

In GSM systems, useful timing information called time advance (TA) measurement is provided that gives a round trip propagation time for the microwave signals to travel between a MS and a particular BS. Time advance measurement is a technique used in GSM to inform a MS how much time in advance of the reference signal it should transmit in order to synchronize correctly at the BS. The usage of time advance is significant since the bursts from MS using adjacent time slots could overlap, resulting in a poor transmission quality or even in a loss of communication.

The time advance is coded with eight bits allowing for 63 steps, where one step is a bit period (BP). Bit period is the fundamental unit of a frame and is equal

to $\frac{48}{13} \mu s = 3.69 \mu s$. The distance corresponding to duration of a bit period

is $T_b = \frac{2r}{c} \Rightarrow r = \frac{cT_b}{2} = 554m$. This is twice the distance between MS and a BS as the

uplink is timed relative to the frame structure in the downlink. By using respective time advance measurements, the distance between a MS and BSs (meaning r values) can be coarsely estimated. Although these values are not accurate enough to be used for the estimation of the MS's position, they are useful as the initial values of r .

In CDMA systems, similar timing information is also available, known as pilot strength measurement. This information is available and constantly updated as the MS. During each conversation, the MS continuously search for new pilots, as well as the strengths of the pilots associated with the forward traffic channels. MS reports each pilot's strength and arrival time (or phase) to the control base station whenever required. The pilot arrival time is the time of occurrence, as measured at the MS antenna, of the earliest arriving usable multipath component of the pilot. Thus the reported pilot phase can be used to estimate the round trip delay to the Bs from which the pilot is transmitted. The time delay information can then be used to compute a set of initial r values. The only time this information is used to provide the initial r values is when handover occurred. In such cases, the strongest signal strength received by the MS is assumed to come from the closest BS. Hence handover is based on some signal strength based handover algorithms. When MS travels within a cell the previous position of the MS is used instead to compute the initial r values.

Chapter 6

Position and Velocity Estimation Using Smart Antenna Systems

In previous chapter we presented three types of MS position estimators, known as network based positioning, terminal based position and global position satellite (GPS). In this chapter we consider network based positioning of the MS and we will present the parameters of this task. With MS positioning we manage to enhance system capacity, for beamforming and to help in monitoring the call management between cells. The general techniques used for MS positioning make use of the signal strengths, the angles-of-arrival (AOA), the time-of-arrival (TOA) or the combination of them, measured at several base stations.

With the use of smart antenna systems the conventional MS position algorithm that presented in the previous chapter has to be modified since it involves the array factor of the antenna radiation pattern. The array factor introduces more complications into MS position and velocity estimation.

6.1 Handover

When a call is in progress the mobility of the user may induce the need to change the serving BS, in particular when transmission quality drops below a given threshold. If the system had large cells the probability of changing the serving cell would be small and the loss of call may be acceptable. The achievement of high capacities requires the reduction of cell size and maintains the call despite user mobility becomes an essential requirement to avoid drop calls. The process of automatically transferring a call in progress from one cell (BS) to another to adverse effects of user movements is called handover [32]. This process requires first some means of detecting the need to change BS and second to manage this switching ideally in a way not noticeable by the users.

At first sight, the aim of handover is to avoid losing a call in progress when the MS leaves the radio coverage area of the cell (BS) in charge. Such cut-offs are very badly perceived by the users and have an important weight in the overall perception of the quality of service by the subscribers. This type of handover is called rescue handover, where a high probability exists that the call will be lost if the cell is not changed. In other cases, it may be of interest to change the serving cell of a given MS even if the transmission quality is still adequate. This may happen when the global interference level would be significantly improved if the MS would be in contact with another cell. A handover triggered with the goal to optimise the interference level and not for the sake of the outgoing communication referred as confinement handover. A third kind of handover is referred to as the traffic handover and may happen that a cell is congested whereas neighbour cells are not. Such a situation happens typically when specific events lead to a very local geographical peak. This kind of handover must be handled with great intention, since it is obviously in conflict with confinement criteria.

6.1.1 Handover algorithm in smart antenna systems

As we mentioned one crucial consideration in a call management is the transfer of a call from one BS to another when a mobile moves into the coverage area of a nearby BS. Conventional handover algorithms use signal strengths to decide if handover is necessary and which BS to hand over. However, the signal strength based algorithms become more complicated in smart antenna systems, since the signal strengths received will be a function of the radiated pattern of the BS antenna. Indeed a handover could be avoided by forming a new beam to the MS, so as to increase the uplink and the downlink signal strengths. In addition, a non-control BS (NCBS) will receive weak signal strength from a nearby MS because that signal is considered as interference by the NCBS and hence a null will be put in the direction of arrival of the MS. This also complicates the handover algorithm for smart antennas. BS to MS distance is adopted as handover criteria since distance is the most direct parameter in deciding the control BS. It is understood that in areas where there is heavily shadowing, some form of signal strength criteria should be used with the nearest distance criteria.

Received signal strengths at three nearest BSs and the respective beam patterns formed at these BSs are used to find the position of the MS, with the control BS having the strongest received signal strength. The distance of the mobile from these three BSs is compared from time to time and if the distance corresponding to the control BS is smaller than the distance between the MS and any of the other two BSs by a threshold of say, 10 meters, handover will take place. Such a threshold is necessary to avoid extensive handover due to the fluctuations in the MS position as the edge of the cellular cell. Furthermore a triangle method is used to select the three nearest BSs from the MS by referring to the previous three nearest BSs.

6.1.2 Triangle method

The GSM system measures six signal strengths as any one time to decide the control base station. Once the transmission is being handed over to a new control base station, another set of six adjacent base stations will be chosen. Hence, from time to time, measurements from all the base stations within the same base station controller (BSC) coverage area will be compared. This procedure can be resource consuming since the number of BSs controlled by a BSC can be huge.

The estimated position derived from the position – velocity estimator is used to determine the three nearest BSs. Since any set of the three adjacent BSs forms a triangle, a new triangle will be formed when the user moves out of the current triangle. However only the third BS will be changed when a new triangle is formed. As shown in figure 6.1b BSs BS1 and BS3 will remain the same while BS BS2 will be replaced by BS BS4 when a new triangle is formed.

Hence, our objective is to find the new third adjacent BS when the MS-user moves out of the current triangle. In order to do that, we compute and compare three angles formed by the mobile user and the three adjacent BSs to check if the MS-user is out of the recently occupied triangle.

As shown in figure 6.1a if the mobile user is inside the control triangle (\angle BS1, BS2, BS3) any two of the three angles shown must be larger than 90^0 . When any two of the angles are smaller than 90^0 , it is very likely that the MS is out of the control triangle

(position named MS_{new}). In addition, the further the mobile user is out of the triangle, the more likely that any two of the three angles will be smaller than 90°.

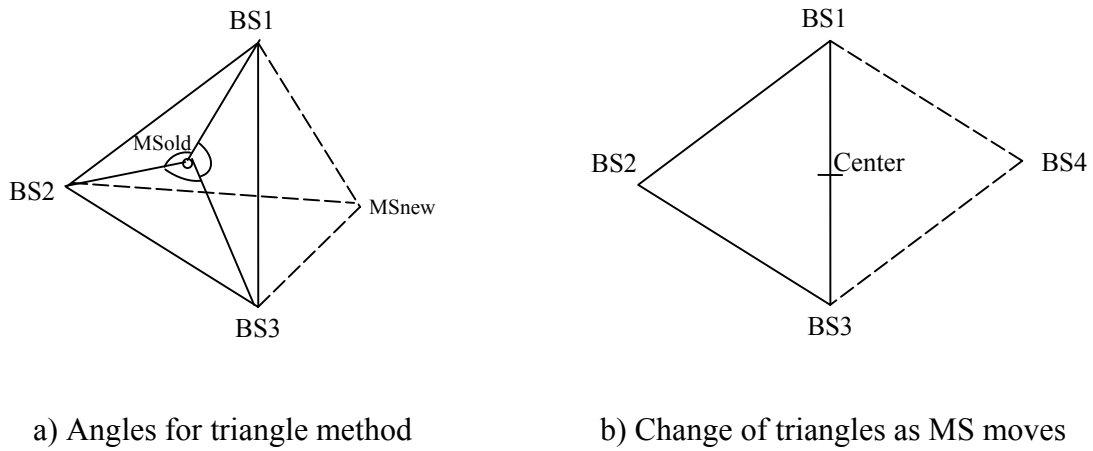


Figure 6.1: Triangle method

Once the MS is out of the control triangle, the following formula, with reference to figure 6.1b is used to calculate the rough position of the new third adjacent BS:

$$\begin{aligned}
 \text{Center} &= 0.5 (\text{BS1} + \text{BS3}) \\
 \text{BS4} &= \text{BS2} + 2 (\text{Center} - \text{BS2}) = \\
 &= \text{BS2} + (\text{BS1} + \text{BS3} - \text{BS2}) = \\
 &= \text{BS1} + \text{BS3} - \text{BS2}
 \end{aligned}$$

However, not all the BSs will have exactly the same separation. Hence, the calculated position of the new third adjacent BS is compared with all the existing BSs tied to a particular base station controller or a mobile switching center, and the nearest BS will be chosen as the exact new third adjacent BS. Through this method, we only use the pre-determined positions of the existing BSs instead of getting time-varying information from all the BSs within the area of a particular MSC.

6.2 Position and velocity algorithm using smart antennas

As mentioned later, an accurate MS positioning method is crucial for accurate beamforming. Besides, the information of the MS position is essential for the monitoring of the handover between base stations

For our simulation purpose, we adopt the method which presented in chapter 5. As mentioned we know that the radiated electric field strength from a finite length antenna element may be written in the form [37]:

$$E_n = E_0 \left[\frac{z_j - z_1}{\sqrt{r_n^2 + (z_j - z_1)^2}} - \frac{z_j - z_2}{\sqrt{r_n^2 + (z_j - z_2)^2}} \right] AF_n \quad (6.1)$$

where E_n is the electric field signal strength received at the BS and is given by

$$E_0 = 10^{-7} \omega \sqrt{\frac{P_r}{R_r}}, \quad \omega = \text{carrier frequency in rads/sec}, \quad P_r = \text{power radiated}, \quad R_r =$$

radiation resistance of the transmitter antenna, z_2 =height of the MS antenna top, z_1 =height of the MS antenna bottom, z_j =height of the BS antenna center, r_n =distance of MS from BTS and AF_n =array factor.

The distance r of MS and the surrounding BSs can be estimated using

$$\mathbf{r}_{n+1} = \mathbf{r}_n + (\mathbf{J}\mathbf{r}_n^T \mathbf{J}\mathbf{r}_n)^{-1} \mathbf{J}\mathbf{r}_n^T (\mathbf{E}_m - \mathbf{E}_n) \quad (6.2)$$

where $\mathbf{J}\mathbf{r}_n$ is the Jacobian matrix of the electric field strengths and \mathbf{E}_m is the column vector representing the measured electric fields strengths at the BSs.

We suppose that smart antenna consists of M elements. The incoming signals are obliquely incident upon the antenna structure with elevation angle Θ and azimuth angle Φ . The array factor for the smart antennas is given by:

$$AF_n = \text{conj}(W_{opt}) \begin{bmatrix} 1 \\ e^{-j\Phi_r} \\ \dots \\ e^{-jM\Phi_r} \end{bmatrix} \quad (6.3)$$

where W_{opt} is the weight vector coming from an adaptive algorithm used for beamforming, $\Phi_r = \frac{2\pi d}{\lambda} \cos \Phi \sin \Theta$

with Φ and $\Theta = \pi - \Theta' = \pi - \tan^{-1} \frac{r}{z_1 + (\lambda/4) - z_j}$ representing the azimuth and the supplementary elevation angle, respectively, that impinges to BS the signal of the MS (Figure 6.2).

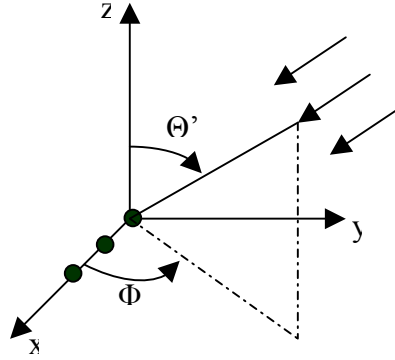


Figure 6.2: The signal incident upon the antenna structure

Using the $Jr_n = \frac{\partial E_n}{\partial r_n}$ we have that

$$Jr_n = J_1 + J_2 \quad (6.4)$$

with

$$J_1 = -E_0 \left[\frac{z_2 - z_j}{\{r_n^2 + (z_2 - z_j)^2\}^{3/2}} - \frac{z_1 - z_j}{\{r_n^2 + (z_1 - z_j)^2\}^{3/2}} \right] r_n \cdot AF_n \quad (6.5)$$

$$J_2 = E_0 \left[\frac{z_2 - z_j}{\sqrt{r_n^2 + (z_2 - z_j)^2}} - \frac{z_1 - z_j}{\sqrt{r_n^2 + (z_1 - z_j)^2}} \right] \cdot \frac{\partial AF_n}{\partial r_n} \quad (6.6)$$

where

$$\frac{\partial AF_n}{\partial r_n} = \left| -j \frac{\partial \Phi_r}{\partial r} W_{opt2} e^{-j\Phi_r} - \dots - j(M-1) \frac{\partial \Phi_r}{\partial r} W_{optM} e^{-j(M-1)\Phi_r} \right| \quad (6.7)$$

and

$$\frac{\partial \theta}{\partial r} = -\frac{z_j - (z_1 + (\lambda/4))}{r^2 + (z_1 + (\lambda/4) - z_j)^2} \quad (6.8)$$

$$\frac{\partial \Phi_r}{\partial r} = \frac{2\pi d}{\lambda} \cos \Phi \cos \Theta \frac{\partial \Theta}{\partial r} = \frac{2\pi d}{\lambda} \cos \Phi \frac{(z_1 + (\lambda/4) - z_j)^2}{\{r^2 + (z_1 + (\lambda/4) - z_j)^2\}^{3/2}} \quad (6.9)$$

$$\text{since } \cos \Theta = -\frac{z_1 + (\lambda/4) - z_j}{\{r^2 + (z_1 + (\lambda/4) - z_j)^2\}^{3/2}}$$

The equation (6.7) become using equations (6.8) and (6.9)

$$\begin{aligned} \frac{\partial AF_n}{\partial r_n} = & \frac{2\pi d}{\lambda} \cos \Phi \frac{(z_1 + (\lambda/4) - z_j)^2}{\{r^2 + (z_1 + (\lambda/4) - z_j)^2\}^{3/2}} \\ & \cdot \left| jW_{opt2} e^{-j\Phi_r} + \dots + j(M-1) \frac{\partial \Phi_r}{\partial r} W_{optM} e^{-j(M-1)\Phi_r} \right| \end{aligned} \quad (6.10)$$

after getting the value of distance r , the MS's position can be estimated using the formula given by equation (5.23) $\mathbf{PM}_{k+1} = \mathbf{PM}_k + (\mathbf{Jp}_k^T \mathbf{Jp}_k)^{-1} \mathbf{Jp}_k^T (0 - \mathbf{errp}_k)$

Where $\mathbf{errp}_k = |\mathbf{PM} - \mathbf{PB}| - r$ and the velocity of the MS can be obtained from sequential position of the MS and is estimated as $V_m = \frac{(PM_m - PM_{m-1})}{T}$ Where T is

the time interval between two discrete positions of the MS.

6.3 Simulation scenario

The position and velocity algorithm is tested by running simulation in MATLAB. The area of interest is a region of about 6500x6500 meters that contains 16 cells, each with a cell radius of about 1500m. A BS is located at the center of each cell The mobile user travels along a route in the region that BSs cover. The mobile user is changing its velocity during his movement in the region specified. Forty sampling are taken along the route.

The basic characteristics of the GSM system that used in the simulation are given in the table below:

Parameters	Description
$f = 1800\text{MHz}$	Carrier frequency
z_1	Height of the lower part of the MS antenna
$z_2 = z_1 + \lambda / 2$	Height of the upper part of the MS antenna
$\lambda = c / f$	
$z_j = 60\text{ m}$	Height of the BS antenna
$R=73\ \Omega$	Radiation resistance of the MS antenna
$P=2\text{ W}$	Radiation power of the MS antenna

Table 6.1: Parameters of GSM system

6.3.1 Flowchart of algorithm

The steps of the PVE algorithm are summarized as follow.

- A) Initialization
- B) Choose Control BS and BS(1:3)
 1. Get estimation of distances r (r : absolute distances between MS and BSs) using time advance (TA) measurement. This value is used as initial for the estimator
 2. Choose Control BS by referring to the $estimate_r$ ($estimate_r$ is the calculated distances of MS of the three serving BSs). BS(1:3) refers to the three BS with the smallest $estimate_r$.
 3. Generating the first set of Θ and Φ (elevation and azimuth angles of the impinging signals) using exact parameters.
 4. Generate parameters for the random beam patterns for all the BSs ($rand_ \Theta$, $rand_ \Phi$, $rand_ interf$: angles of impinging signals). We assume two interferers.
 5. Generate array factors of all the BSs with the respect to the signal of interest-MS, using parameters in step B.2 and B.4. In this step we use the beamforming algorithm.
 6. Generate E -fields (electric fields) received by all the BS (without noise)
 7. Calculate E_m -fields (electric fields) with noise

8. Choose as Control BS, this with the smallest distance of the MS. In case there are more than one BS (within the three nearest BS) with the smallest $estimate_r$ (noting that the is an estimation error of TA), CBS is chosen to be the BS with the strongest received E_m .

C) Sampling loop (kk: sampling point)

1. If $kk=1$ go to step C.6
2. If $kk>1$
3. Generate Θ and Φ using exast parameters
4. Generate array factors of the three nearest BS with respect to SOI
5. Calculate E_m -fields (electric fields) of the three nearest BS (Em_used)
6. Iteration procedure for ddr (iterated value of distances of the three serving BSs)
 - i. Set initial value of ddr as the $estimated_r$
 - ii. Generate Θ_{update} using the updated distances of MS and BSs (we assume that Φ is known to the system)
 - iii. Generate respective array factor (AF) and weight vector ($Wopt$) using the updated parameters
 - iv. Generate $estimate_E$ (EE) and Jacobian matrrix (J) of $estimate_E$
 - v. Update value ddr using $ddr = |ddr + (J^T J)^{-1} J^T (Em_used - EE)$
 - vi. Go back to (ii)

7. Iteration procedure for pp (iterated value of MS position)

- i. Set initial value of pp at the center of the three nearest BSs
- ii. Evaluate the position error $errp = |PB - pp| - ddr$. (PB is the location of the serving BSs)
- iii. Evaluation of new position of the mobile user (ppx is pp in x -direction and ppy is pp in y -direction)

$$ppx_{new} = ppx_{old} + (Jp_x^T Jp_x)^{-1} Jp_x^T (-errpx) \text{ and}$$

$$ppy_{new} = ppy_{old} + (Jp_y^T Jp_y)^{-1} Jp_y^T (-errpy)$$

- iv. Go back to step ii
8. Get estimated velocity
 9. Prepare parameters for the next sampling point
 - i. Deciding on handover by using ddr handover occurs when the distance between MS and the old control BS is bigger by 10 meters of distance between MS and the new control BS. A tolerance of 10 meters is created to avoid excessive handovers while MS fluctuates between two cells.
 - ii. Decide whether or not to change BS smart antenna beam by simulating a beamformed scenario and compare E-field received by the CBS before and after beamforming: a new beam that is steered towards the MS will be formed when a significant improvement in received E-field is expected
 - iii. Generate the new set of parameters for the random beam patterns for the two adjacent BSs ($rand_ \Theta$, $rand_ \Phi$, $rand_ interf$).
 - iv. Decide on the new set of adjacent BSs using triangle method
 - v. Update all the parameters for the next sampling point and set the ddr as the initial value for the next iteration
 10. $kk=kk+1$; if $kk < \text{number of samples}$ go back to step C.2 else go to D
- D) Estimate average position errors and average velocity errors.
- E) End of simulation

Chapter 7

Simulations and Results

In this chapter we present the results of the simulations that have been executed. The simulations and their results will be separated in two parts. In the first section we study how antenna forms its beams under various assumptions. We also inspect the adaptive algorithm for their convergence rate and their stability. In the second section using the adaptive algorithms, we analyse the accuracy of the proposed position and velocity algorithm.

7.1 Study of beamforming

As mentioned, the purpose of this section is to make an in-depth study of the adaptive algorithms used in smart antennas. Simulations are also provided to understand the aspects of the adaptive algorithms such as the convergence rate and stability.

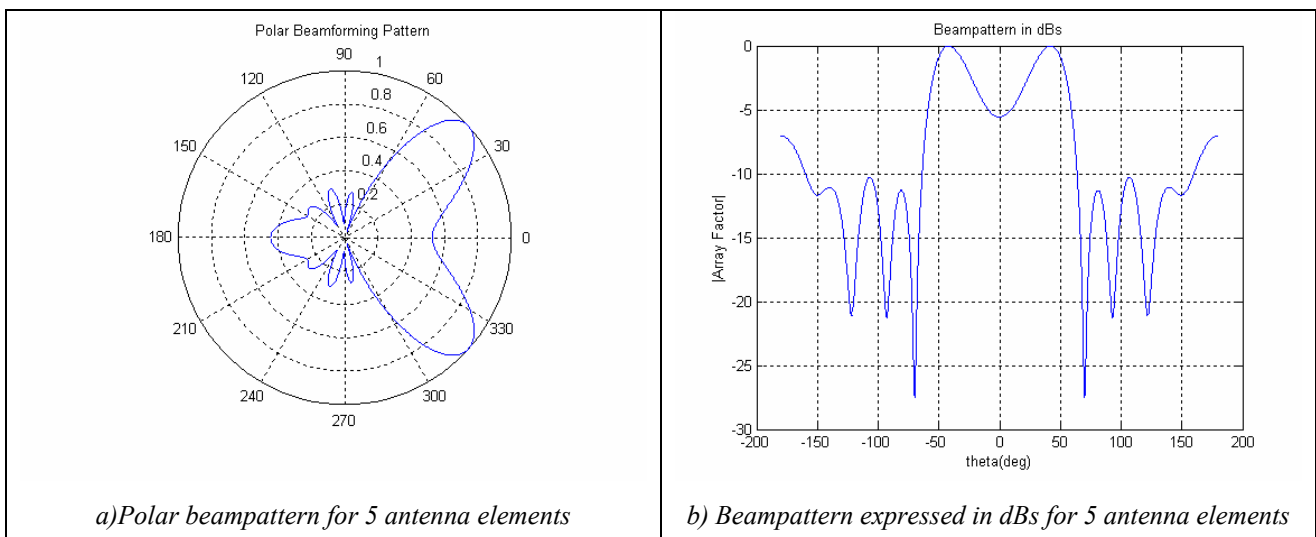
Lets consider that the antenna array consists of M -elements, placed along x -axis, which, abstain distance d , where d is expressed by a fraction of wavelength λ . For testing the beamforming of the array antenna we consider a signal of interest, which obliquely incidents upon the antenna with elevation angle $\theta = 100^\circ$ and azimuth angle $\phi = 40^\circ$. We will call this couple of angles as direction of interest. We also consider, three interferers impinging to the antenna each one, with elevation and azimuth angles equal with $(97^\circ, -10^\circ)$, $(97^\circ, 110^\circ)$, $(97^\circ, -220^\circ)$ respectively. All signals are simulated with random generated bits (± 1) which are modulated by using MSK modulation, as presented in chapter5. We generate 142 bits representing a normal burst [32], of the GSM system. The burst consists of two packets of 58 bits surrounding a training sequence of 26 bits. Three “tail” bits are added on each side for error correction that are omitted. The bits we use are up-sampled by a factor of 8 and consequently, the adaptive algorithms by using 1136 samples-iterations are tested. We assume that signal of interest is affected by Gaussian noise with zero mean value and variance depending on the signal to noise ratio (SNR). The power of the interfering

signals depends on signal to interference ratio (SIR). For simulation purposes we assume SNR=10 dB and SIR= -5dB for all interferers, unless something else is mentioned.

Using Least Mean Squares (LMS) algorithm we investigate the behavior of the adaptive array under various assumptions. After we do the same with the Normalised-LMS, Sample Matrix Inversion (SMI) and hybrid algorithm we proceed in to comparison of these algorithms.

Normalized radiation pattern versus number of elements

Figure 7.1 shows the effect of changing the number of elements on the smart antenna radiation pattern. As expected the main lobe becomes narrower, more directive and better focused on the direction of signal of interest as the number of antenna elements is increased. The results of figure 7.1 show that the interfering signals with directions of arrival ($97^\circ, 110^\circ$) and ($97^\circ, 220^\circ$) will be nulled regardless the number of elements. For the interfering signal that is angularly near to the desired signal the null is not deep enough, even if we increase the number of elements. This is due to the fact that the antenna is unable to null the interferer and point to the desired signal simultaneously, in case two signals are close.



a) Polar beampattern for 5 antenna elements

b) Beampattern expressed in dBs for 5 antenna elements

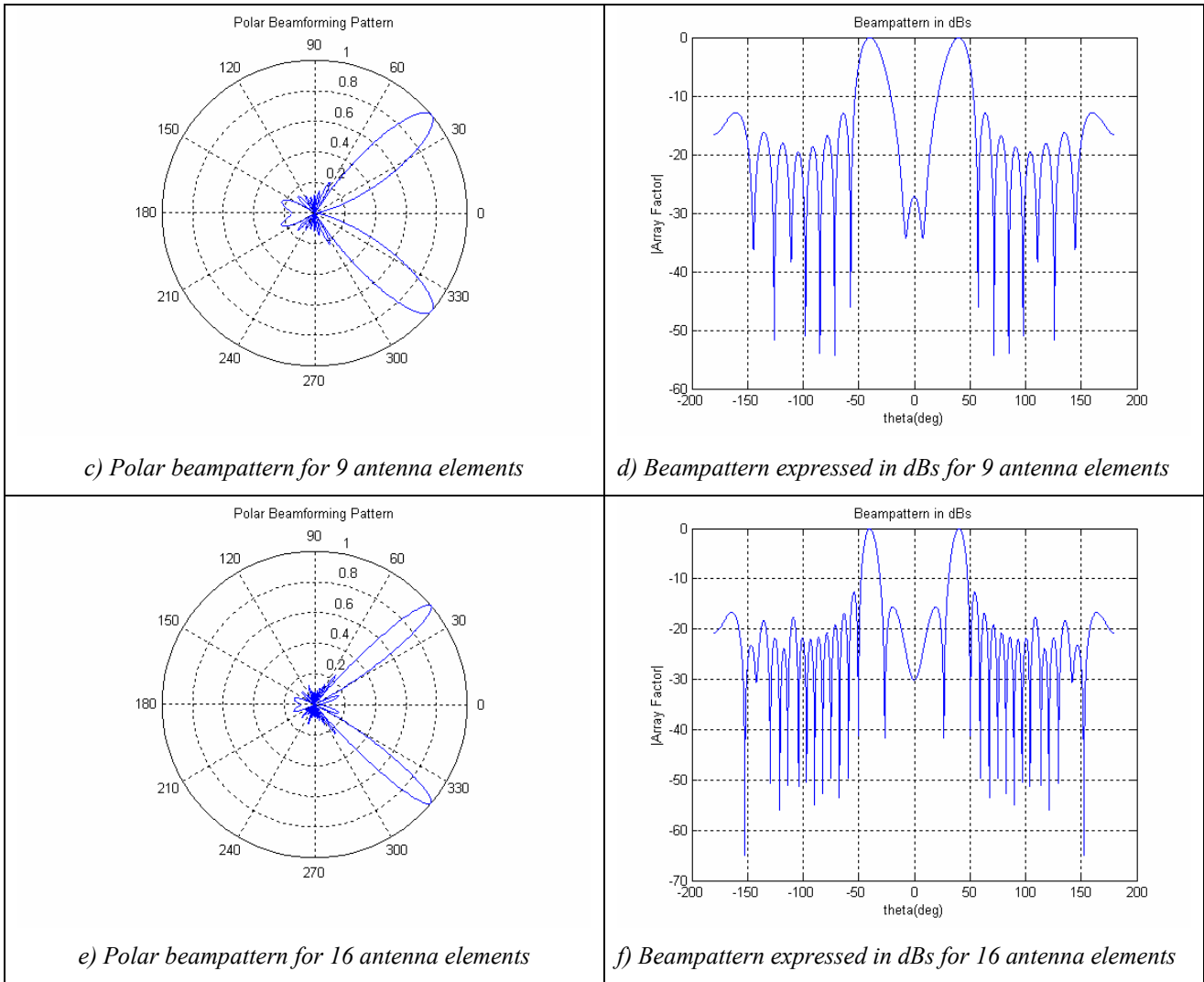


Figure 7.1: Radiation pattern versus azimuth angle of arrival

Canceling interference is one of the objectives in using smart antennas. As the number of elements is increased, the radiation pattern will have more sidelobes. The levels of these sidelobes are much smaller when compared to an antenna array with fewer elements. In table 7.1 we compare the basic characteristics of radiated beam pattern varying the number of antenna elements:

N, number of elements	5 elements	9 elements	16 elements
<i>Array factor in direction of interest</i>	0.8256	0.8675	0.892
<i>Half-power beam width (HPBW)</i>	60°	25°	14°
<i>Sidelobe level (SLL)</i>	0.4220	0.2345	0.2212

Table 7.1: Radiation pattern characteristics

As expected the array factor is greater in direction of interest as elements of the antenna increase and the half-power beam width (HPBW) is getting narrower.

Normalized radiation pattern versus antenna element spacing

Analyzing the effect of elements spacing, we study three cases: i) $d = \frac{\lambda}{4}$, ii) $d = \frac{\lambda}{2}$

(figures 7.1c-7.1d) and iii) $d = \frac{3\lambda}{4}$. We assume that we have 9 antenna elements. As

we notice from figures 7.2a and 7.2b for $d = \frac{\lambda}{4}$ the main beam of the antenna is not

narrow enough in the direction of interest, while the sidelobes are not deep enough.

On the other hand if we determine $d = \frac{3\lambda}{4}$ (figures 7.2c and 7.2d), we notice the phenomenon of spatial aliasing, since sidelobes are almost of equal strength with the main lobe.

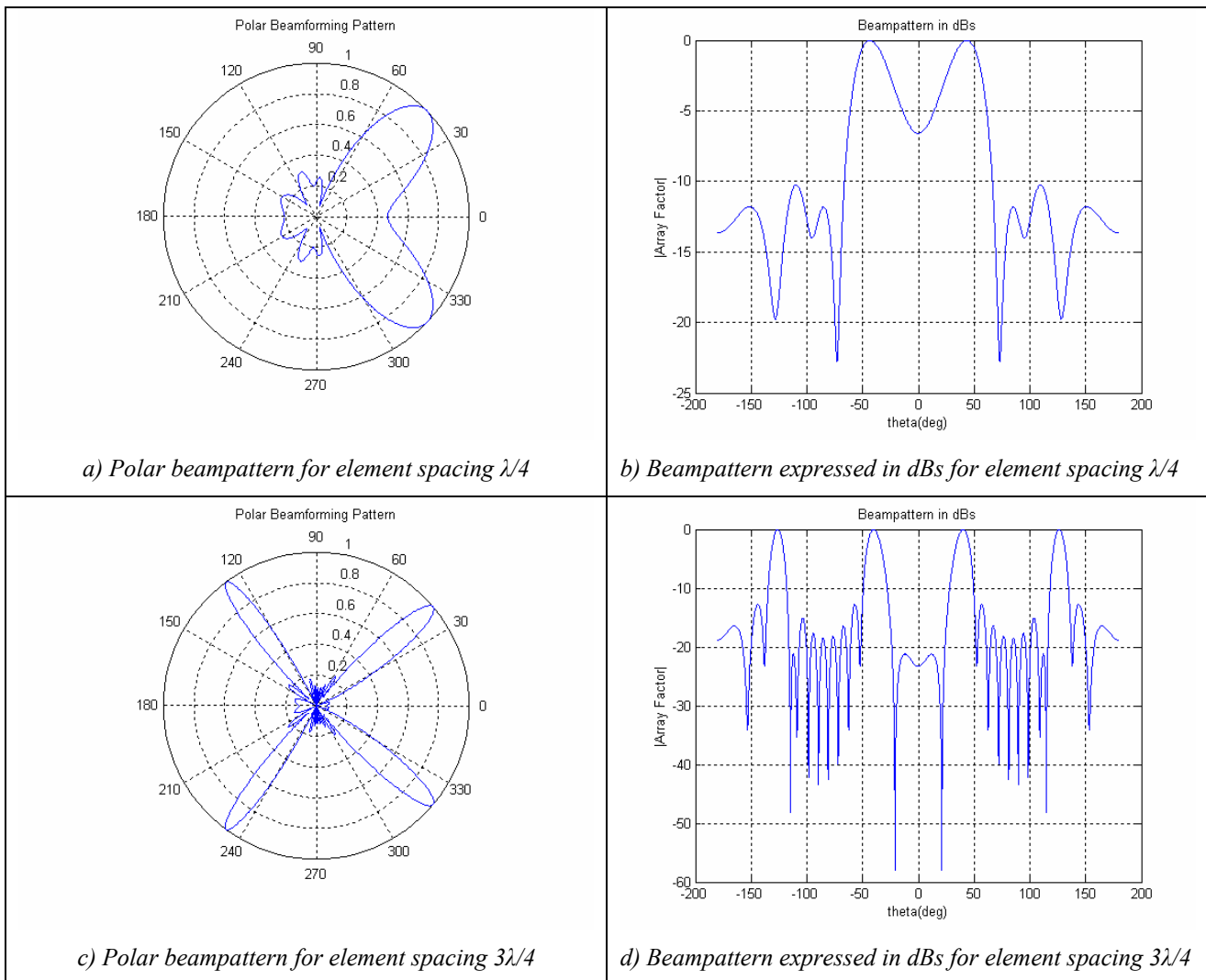


Figure 7.2: Radiation pattern versus element spacing

In practical linear arrays the element spacing must be less or equal to half of the carrier wavelength so that mutual effect is minimized and spatial aliasing is avoided.

Stability LMS versus forget factor μ

As mentioned in chapter 4 the convergence rate and stability of LMS algorithm depends on the value of the forget factor μ . The convergence is tested by using the mean square error (MSE) criterion. The MSE is defined as:

$$MSE = \frac{1}{K} \sum_{k=1}^K |r(k) - y(k)|^2 \quad (7.1)$$

where K is the volume of iterations, $r(k)$ and $y(k)$ the reference and reconstructed signal respectively.

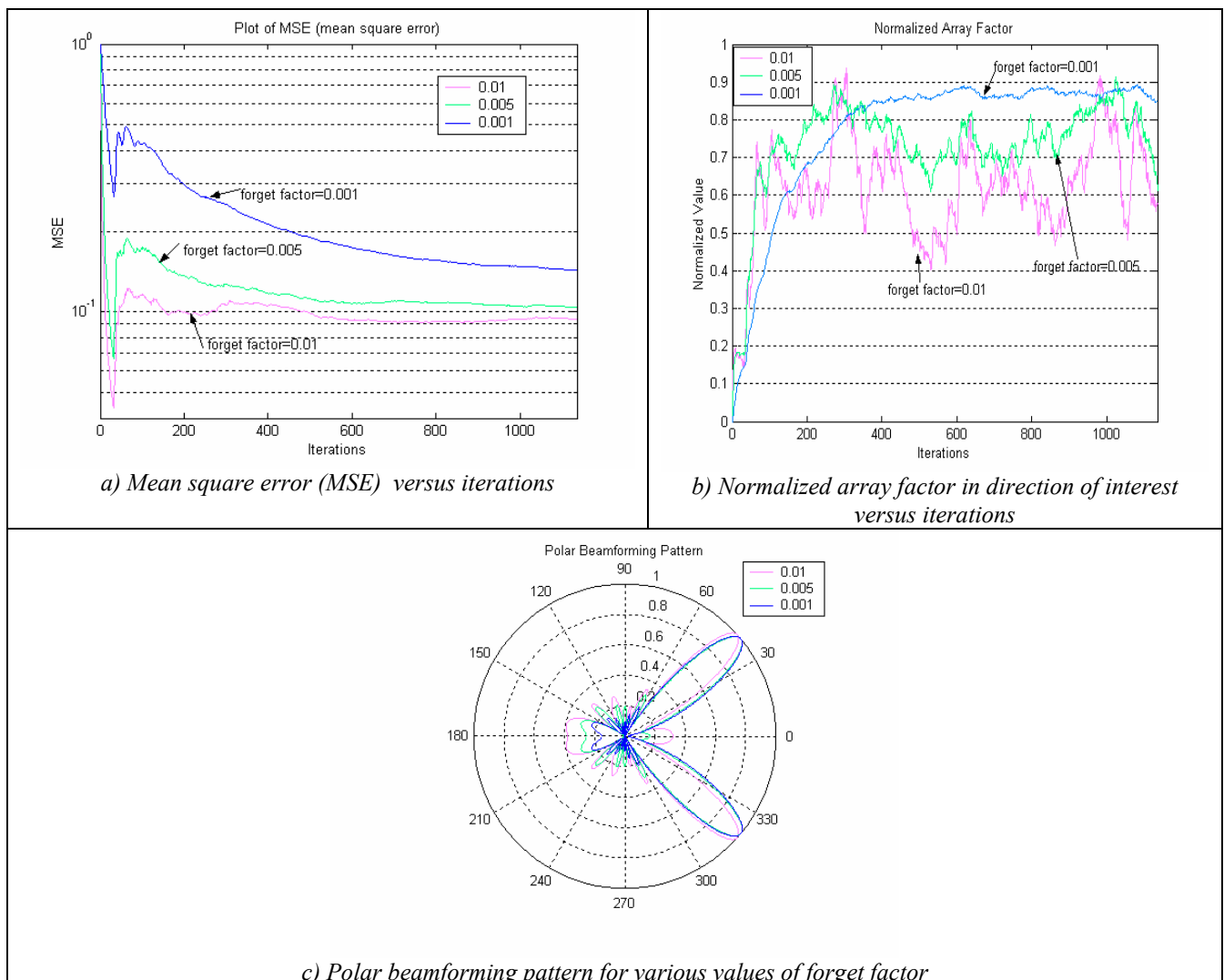


Figure 7.3: Study of convergence rate and stability of LMS versus forget factor

As we notice in figures 7.3a and 7.3b large values of μ (e.g. 0.01) lead to faster convergence, but the system's parameters are less stable around the final value of array factor. On the contrary for small values of μ (e.g. 0.001) the algorithm converges slower, but it is much more stable. Likewise large values of μ produce larger sidelobes, which is undesirable (figure 7.3c). So that we prefer to use small values of μ as long as the samples are adequate.

Normalized radiation pattern versus SNR and SIR

In this part we study the effect of varying the signal to noise ratio, which affects the power of the additive noise in the signal of interest. We can notice from figure 7.4a that as SNR increases the algorithm converges to lower values of MSE. In figure 7.4b we present the normalised array factor in the direction of signal of interest versus SNR. In all cases of number of elements the normalized array factor gets higher value as SNR increases. When SNR is 20 dBs the values of normalized array factor are close.

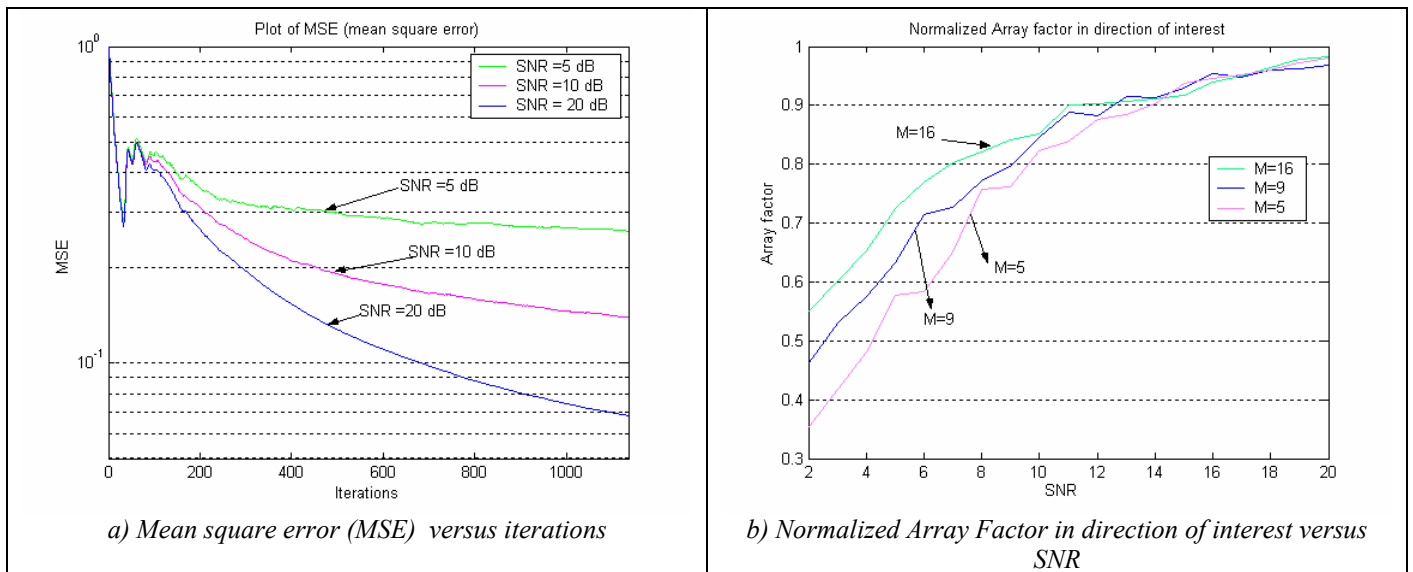


Figure 7.4: Normalized radiation pattern versus SNR

As mentioned earlier the power of the interfering signals depends on the value of SIR. All the interferers in figure 7.1d have SIR= -5dB. If we assume that the interferer for direction of arrival ($100^\circ, 120^\circ$) is stronger, meaning SIR=-15dB, we can see from figure 7.5 that the value of array factor in the direction of the signal of interest is getting smaller. Likewise as all the interferers are getting stronger the radiated power in the direction of interest is reduced.

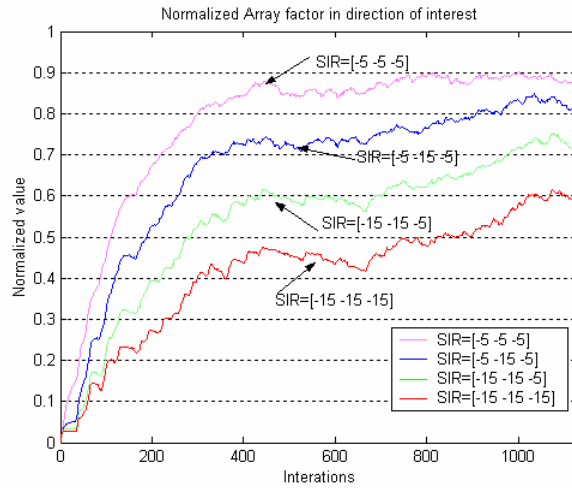


Figure 7.5: Normalized array factor in direction of interest changing interferer's power

Normalized radiation pattern in Rayleigh fading channel

Until now we have tested the adaptive algorithm LMS considering that the signal of interest is affected by additive Gaussian noise. Here we will extend the simulation using the mathematical model for Rayleigh fading channels, described in chapter 5. We use this model to see how radiation pattern in the direction of interest is affected in a multipath condition. As we can see in figure 7.6b the array factor in the direction of interest has lower value than in case that the signal is affected only by Gaussian noise. We can also observe the MSE converges in higher value, using figure 7.6a. These marks are expected since the detection of a signal becomes more complicated when the signal appears with multipath.

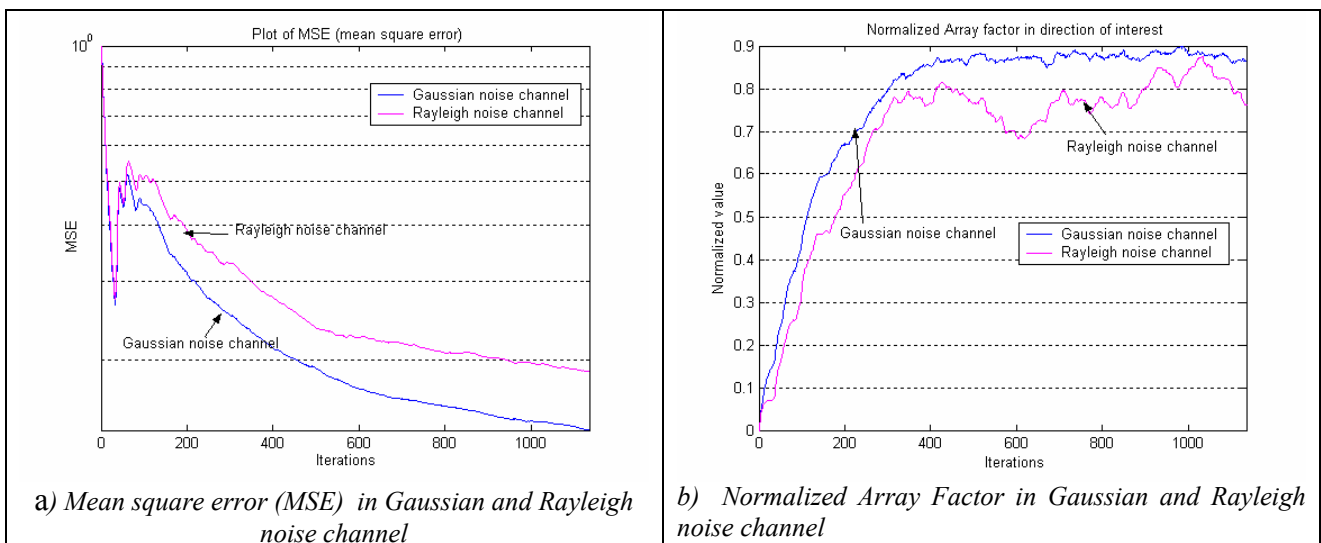


Figure 7.6: Radiation pattern in channel with Rayleigh noise

Analysis of SMI and NLMS algorithm

In this section we discuss the behaviour of SMI and NLMS algorithms. As we have already mentioned the SMI algorithm has a speedy convergence because uses matrix inversion, though it is very computationally intensive. Moreover the SMI uses a block adaptive approach, which requires that the signal environment does not undergo significant changes during the block acquisition. For the simulations we mentioned that we use 1136 samples. In figure 7.7 we notice how array factor in the direction of interest changes, varying the block of samples. When block size of samples is decreased the radiation pattern produces many powerful sidelobes. This conclusion is verified by the value of array factor in direction of interest. In particular for 1136, 142 and 71 samples the value of the array factor is 0.8992, 0.8402 and 0.8250 respectively.

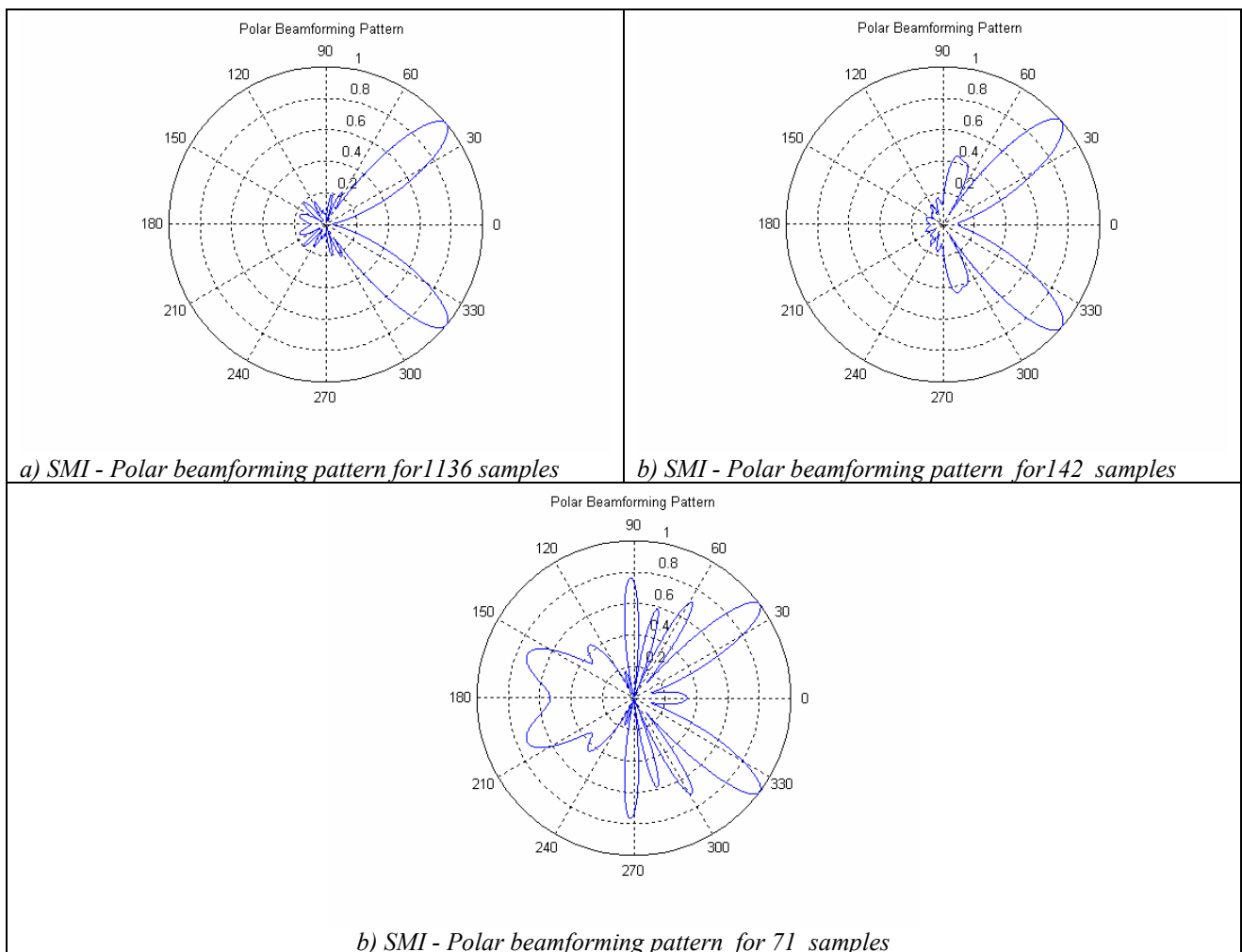


Figure 7.7: Beamforming pattern varying block sample for SMI algorithm

We also test the convergence speed and stability of the NLMS varying the factor μ_o . As mentioned in chapter 4 μ_o vary between zero and two. In figure 7.8 we notice that as the value of μ_o increase, the normalized radiation pattern in the direction of interest presents increasing instability. The instability results the radiation pattern in having stronger sidelobes. Therefore we prefer to use small values for μ_o .

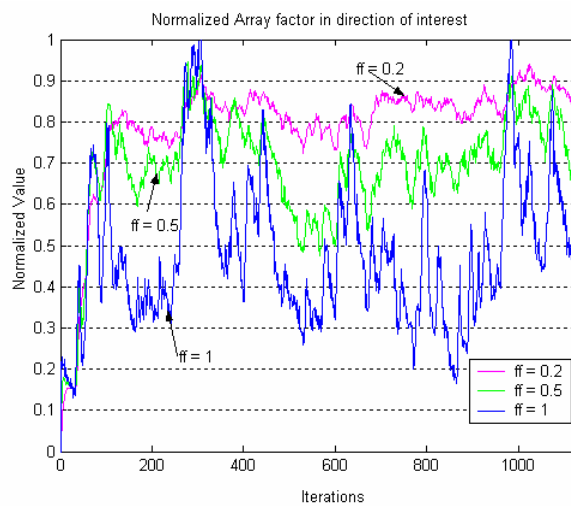


Figure 7.8: Normalized Array factor in direction of interest versus μ_o

Comparison of LMS, NLMS and Hybrid algorithm

This section provides a comparison of the adaptive algorithms we use in simulation. In hybrid algorithm we use a block of 208 samples (corresponding to 26 training bits of GSM burst) in order to estimate the weight vector, which will be used as initial vector to the LMS algorithm that follows. The LMS algorithm will be executed using rest samples. From figure 7.9b we notice that in LMS and hybrid algorithm the normalized array factor in the desired direction converges in higher values than NLMS algorithm. On the other hand in MSE plotting (figure 7.9a) the hybrid algorithm have faster convergence in lower value than rest algorithms. So that, if we do not have enough samples we may use the hybrid or the NLMS algorithm. If figure 7.9b the normalized array factor of the hybrid algorithm has almost immediate convergence while the NLMS seems to converge faster than LMS. However NLMS converges in lower value that LMS's. But if we care about the weight vector we must use the hybrid algorithm. In figures 7.9c-7.9e we notice that all algorithms produce quite satisfactory radiation pattern with small enough sidelobes.

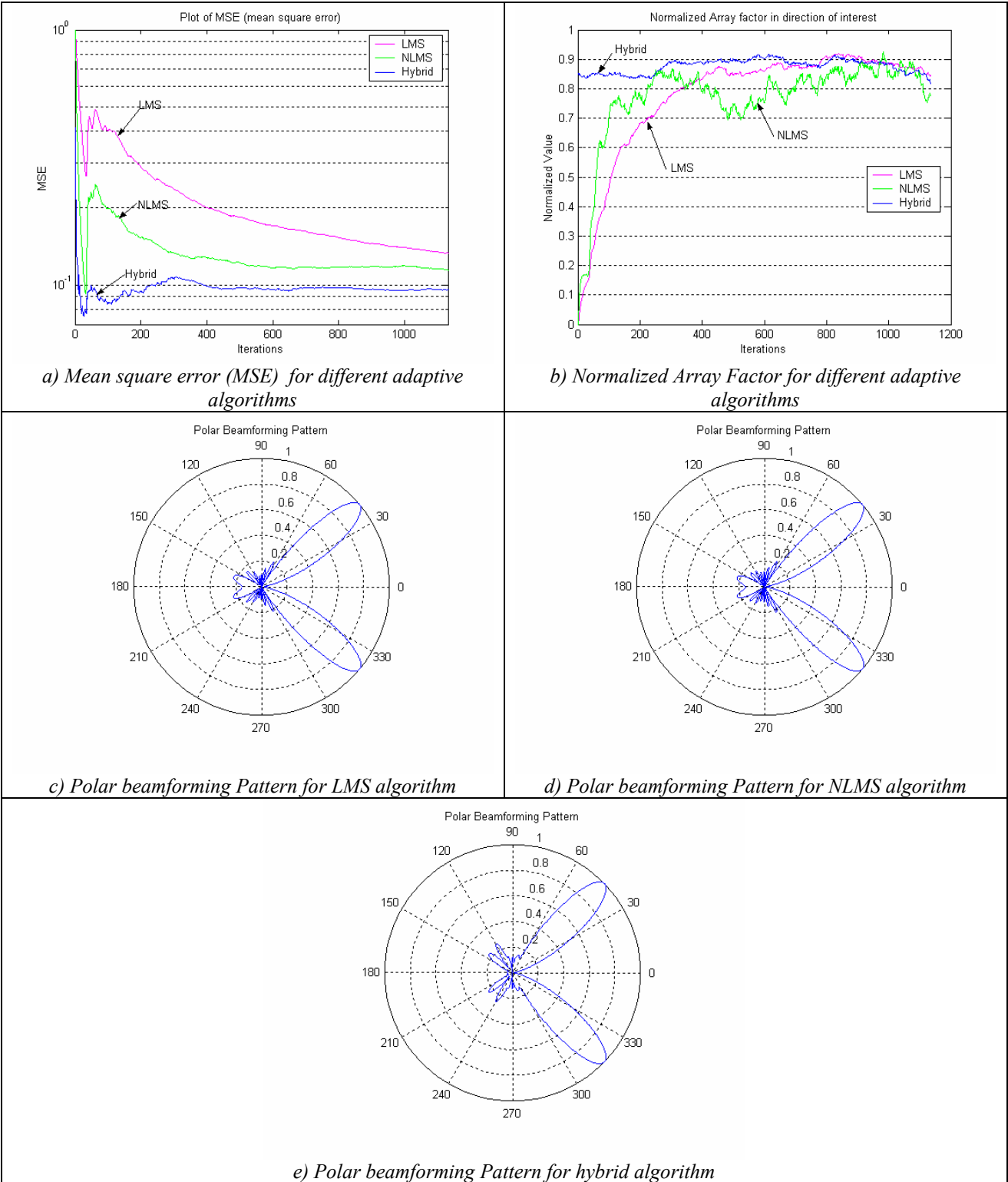


Figure 7.9: Comparison of different adaptive algorithms

7.2 Study of position and velocity algorithm (PVE)

The PVE algorithm is tested by using the adaptive algorithms described in the previous section. The area of interest is as discussed in chapter 6, a region of 6500x6500 meters that contains 16 cells-BS, each with a cell radius of about 1500 meters. In this area we assume that hold the specifications of GSM system. Cells of the used size are called microcells in GSM system. A BS is located in the center of each cell and is indicated by the alphabet “A”. Cells are not an exactly cycle, because in reality they are not also. All BSs we assume that have the same altitude which equals to about 50 meters. The mobile station is moving along a route inside the covered area. The estimated position of the mobile station, after using PVE algorithm is marked with “x”. The velocity of the mobile station changes as shown in table 7.2. The estimated velocity using PVE is also marked with “x”. While mobile station moves we use the procedures that concern handover, triangle method etc. Along the route, forty samples are taken at a time interval of 4.8 secs. This interval is relevant with the fact that the field strength is reported every 0.48 secs, in GSM [32]. For every 10 reports the algorithm estimates the position and velocity of the MS.

Steps	Speed of MS (km/h)	Acceleration of MS (m/sec)
1:8	50	
8:9		3,2
9:16	105	
16:17		-2,03
17:24	70	
24:25		2,3
25:32	110	
32:33		-3,1
33:40	55	

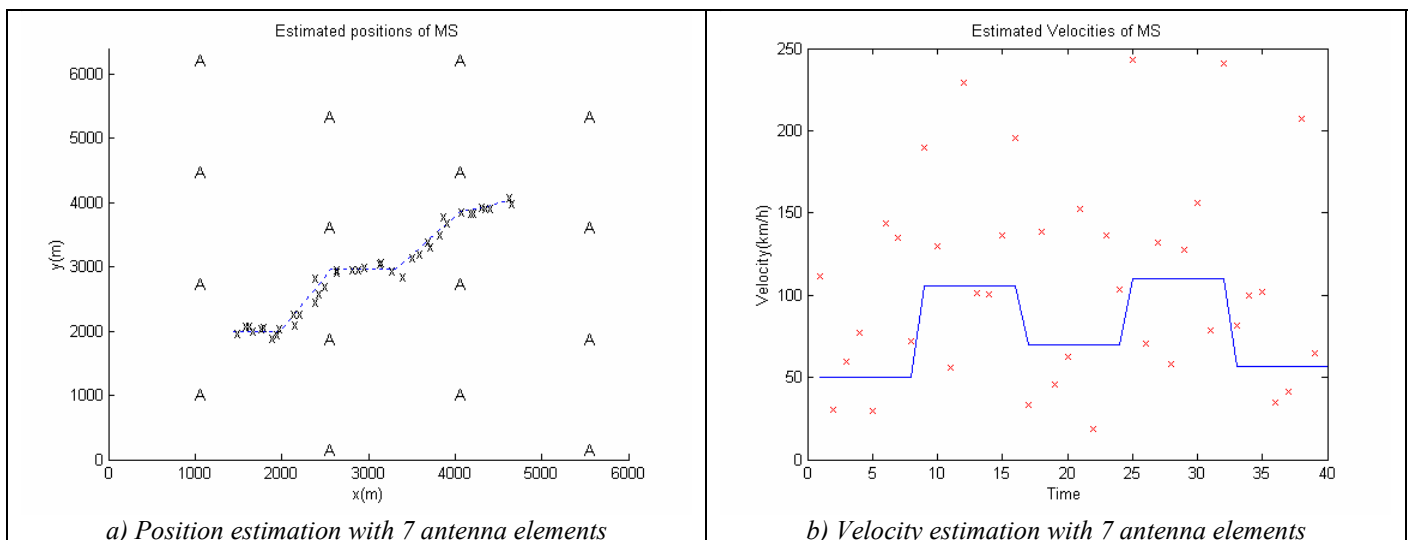
Table 7.2: Speed of mobile station

The lower and the higher part of mobile station is assumed to be $z_1 = 2m$ and $z_2 = z_1 + \frac{\lambda}{2}$ respectively. The mobile station’s radiation resistance is about 75 ohms and the radiated power is between 0.2 and 2 Watts. In table 7.3 we present the basic parameters of simulation.

Parameters	Description
z_1	Height of the lower part of the mobile station's antenna
$z_2 = z_1 + \lambda / 2$	Height of the upper part of the mobile station's antenna
$\lambda = c / f$	Wave length of used system
f	Working frequency in GSM sytem
$P=0.02 \sim 2 \text{ W}$	Radiation power of a mobile station antenna
$R=75\Omega$	Radiation resistance of a mobile station antenna
$\mu_o=4\pi \times 10^{-7}$	Magneto-conductance of vacuum

Table 7.3: Parameters of the simulated system

BSs are using adaptive array antennas and the derived array factors and weight vectors are used to estimate the position and velocity of the mobile station. Figures 7.10 – 7.12 present the position and velocity estimation and also the position and velocity error in each location, for antenna elements $M=7, 9, 16$. We assume that noise is Gaussian, as determined in previous section, and the adaptive algorithm is the LMS. We consider that in every position there are 2 interferers impinging on antenna with random azimuth and elevation angles.



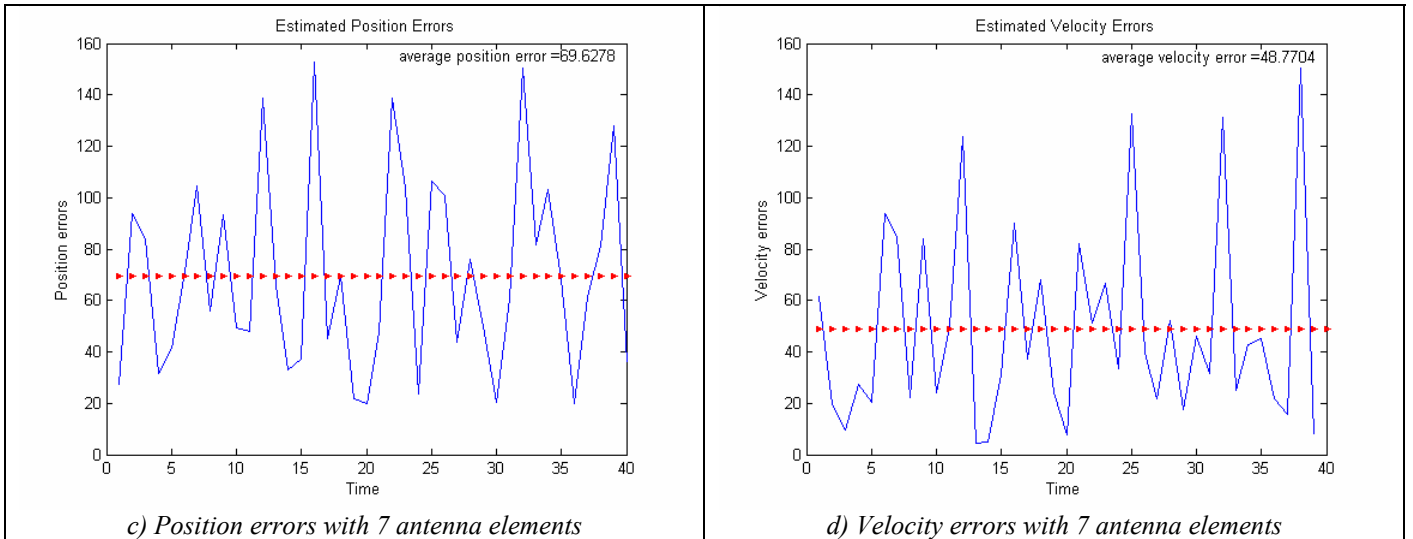


Figure 7.10: Position and Velocity estimations for 7 antenna elements using LMS adaptive algorithm

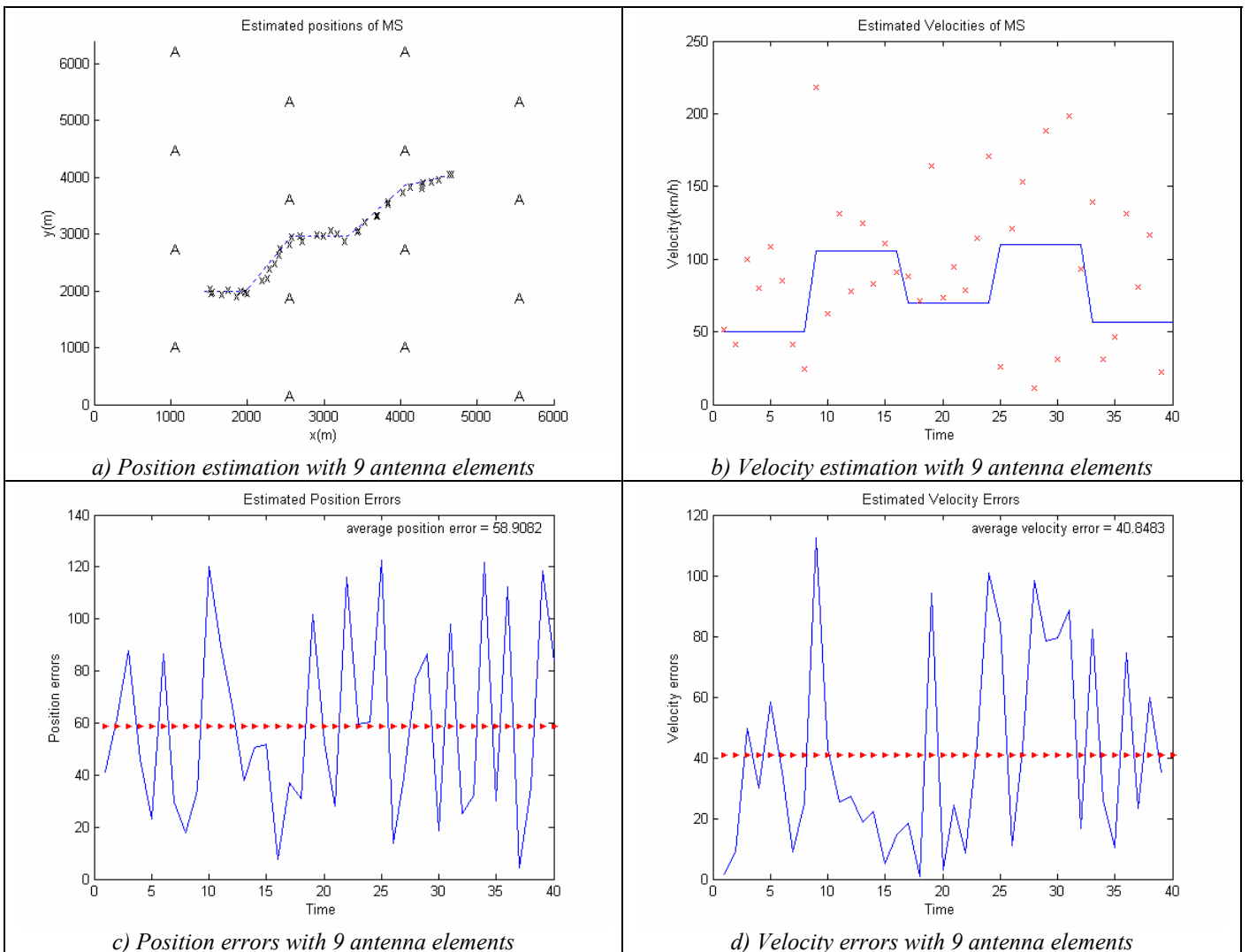


Figure 7.11: Position and Velocity estimations for 9 antenna elements using LMS adaptive algorithm

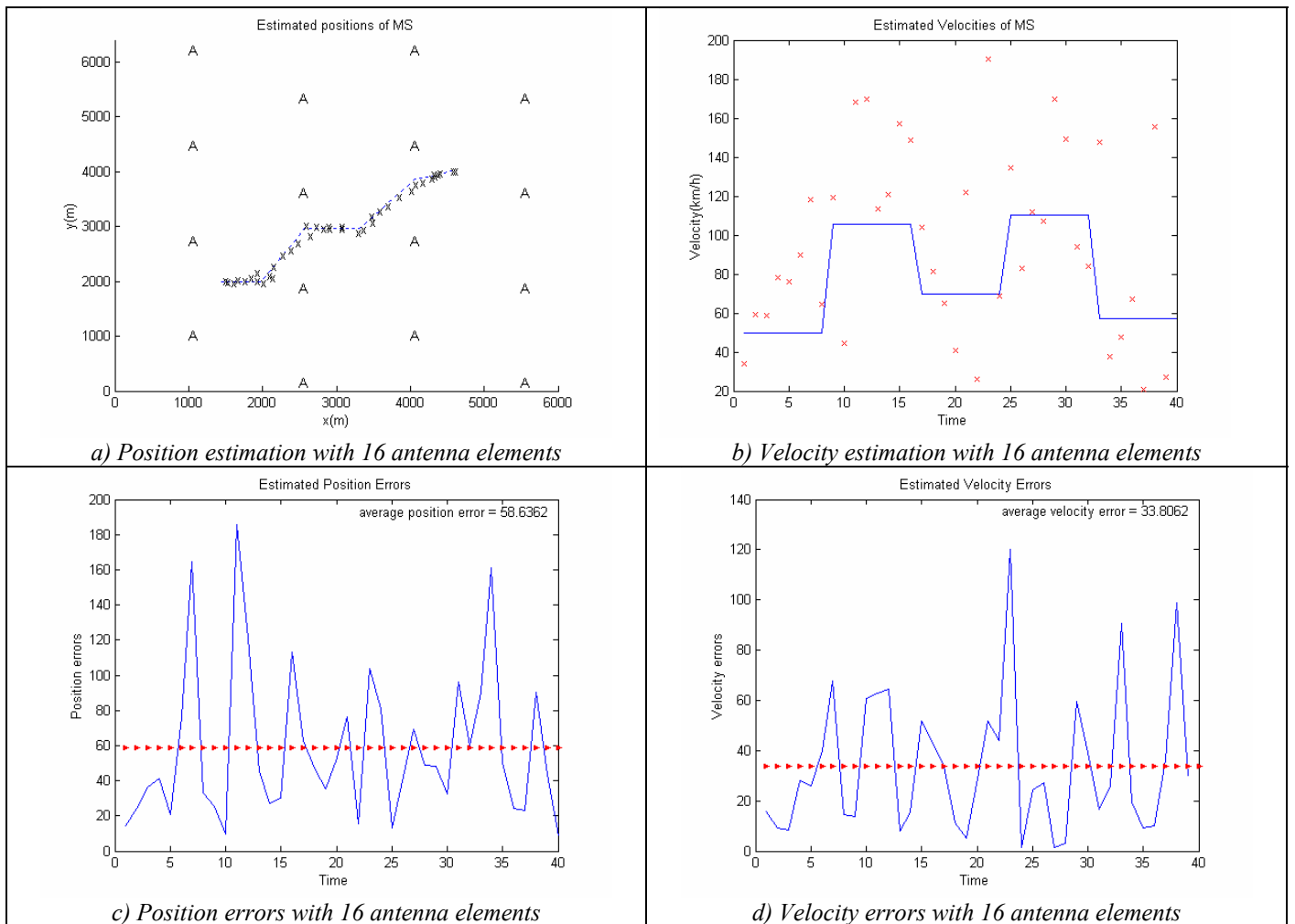


Figure 7.12: Position and Velocity estimations for 16 antenna elements using LMS adaptive algorithm

Figure 7.13 summarizes the relation between position and velocity accuracy versus antenna elements. As expected the accuracy increases rapidly as antenna's elements increase. Moreover for 9 and 16 antenna elements the position accuracy does not have significant changes.

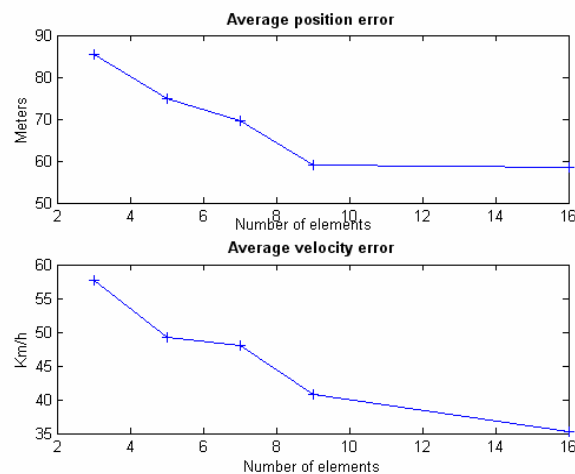


Figure 7.13: Position and velocity accuracy versus antenna elements

In figure 7.14 we simulate the PVE in conditions of Rayleigh noise channel. For SNR=10dB the position error is 70.78 meters and the velocity error 46.44 km/h. Errors have bigger values than in case of using Gaussian noise channel (position error equals with 58.9 meters and velocity error with 40.8 km/h). Assuming again, $M=9$ and LMS adaptive algorithm, we can see in figure 7.15 that for a channel with Gaussian noise the average position and average velocity errors have smaller values than in case of Rayleigh noise channel. In both cases, as SNR increase the average errors decrease.

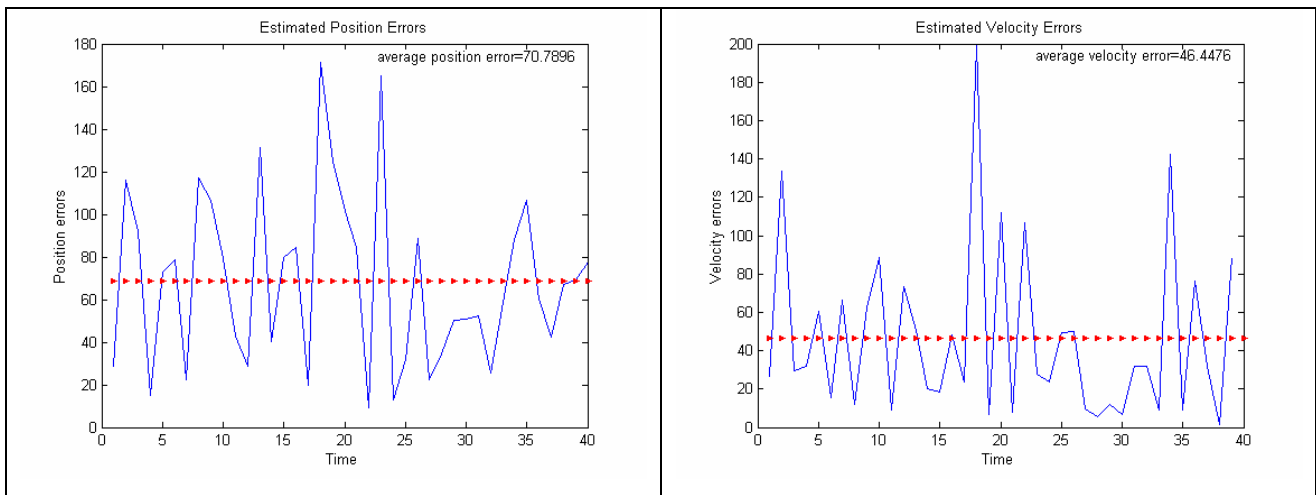


Figure 7.14: Position and velocity error estimation in Rayleigh noise channel for SNR=10dB

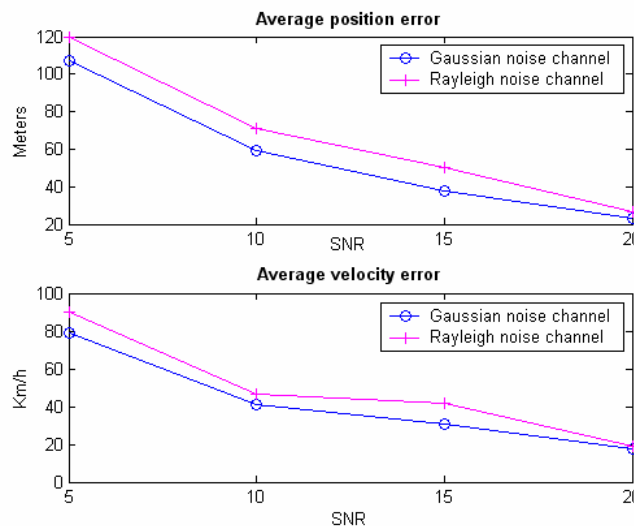


Figure 7.15: Position and velocity accuracy versus SNR for Gaussian and Rayleigh noise channel

We compare the accuracy of PVE algorithm using different adaptive algorithms. We will examine the LMS, N-LMS and hybrid algorithms. As we notice comparing figures 7.11 - 7.16 the N-LMS have the worst performance. This was expected since the radiation pattern in direction of interest of NLMS was smaller than this derived by

rest algorithms. The hybrid algorithm is close to LMS algorithm. Moreover in figure 7.17 we compare the accuracy of the used adaptive algorithms for different number of elements. The N-LMS algorithm performs the worst accuracy compared with LMS and hybrid algorithm. This happens even if the antenna elements become 16. In case of hybrid algorithm, even if we increase the number of elements the accuracy has small improvement. The hybrid algorithm has better performance than LMS when the antenna elements are few. But when we increase the antenna elements LMS is preferred.

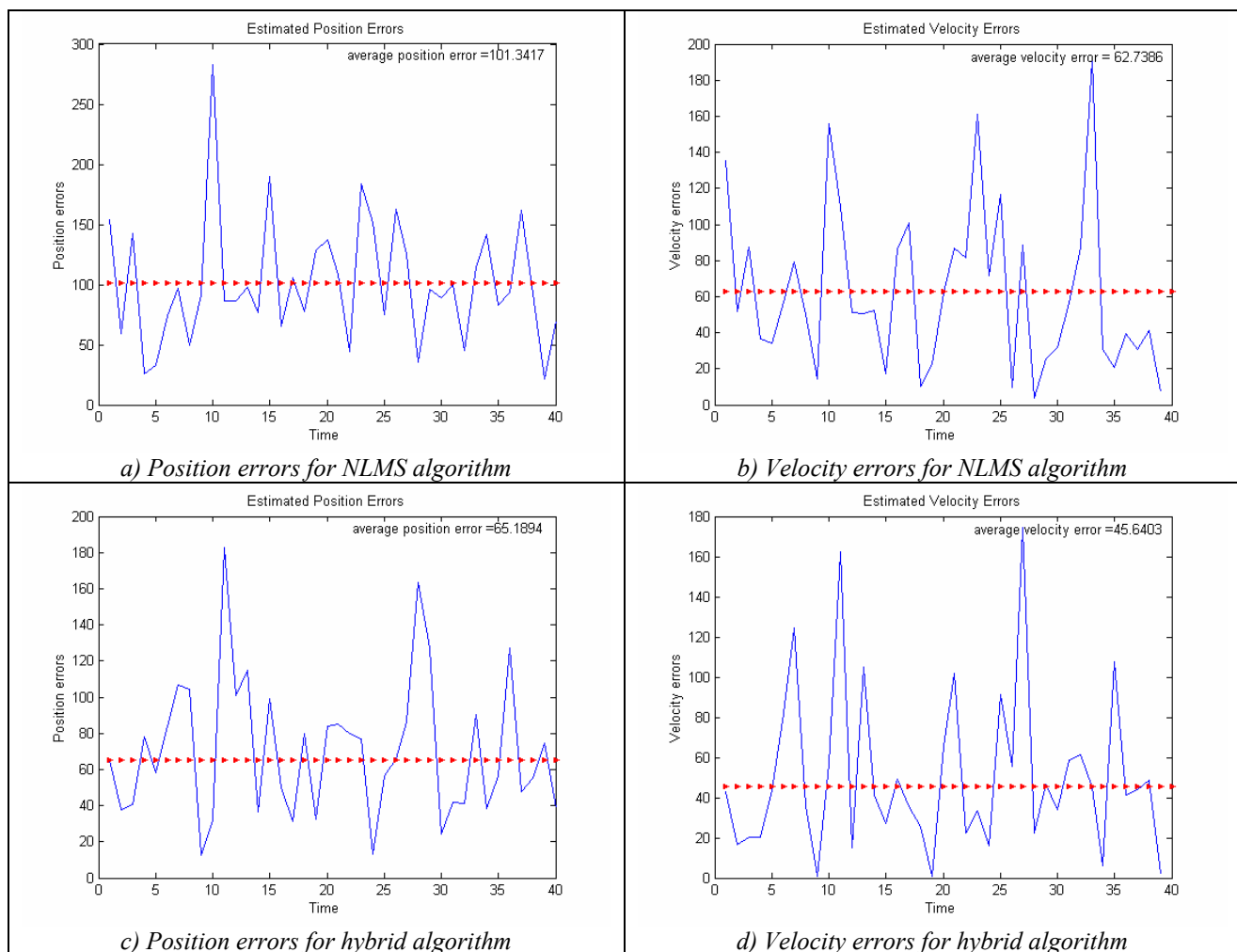


Figure 7.16: Position and velocity errors for PVE algorithm using different adaptive algorithms using 9 antenna elements and SNR=10dB

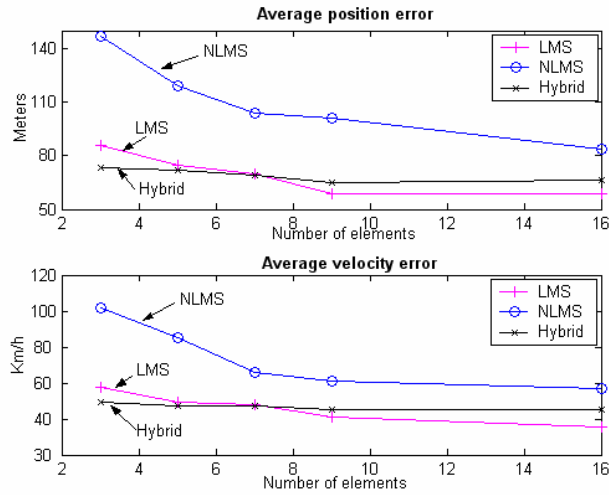


Figure 7.17: Accuracy comparison using LMS, NLMS and hybrid adaptive algorithm

Study of Handovers

In figure 7.16 shows the positions where handover occurred as the mobile station moves through the region of the installed base stations. We use $M=9$, LMS adaptive algorithms and $SNR=10dB$. With number is indicated the control base station and “O” points the position where handover occurred. In table 7.4 we indicate the distances between mobile station and BSs justifying why handover occurred. The underlined distance justify that the control BS must be changed. The control BS is bolded. Tests with different antenna elements, adaptive algorithms and SNR indicated that handovers take place almost at the sampling number – positions.

Position	Old Triple of BS – New Triple of BS	Old distances from BSs - New distances from BSs
3	(2 , 6, 1) (6 , 2, 1)	(952.8, <u>873.6</u> , 1180.8) (852.4 , 889.8, 1137.2)
16	(6 , 2, 7) (7 , 6, 2)	(1008.1, 1392.2, <u>748.5</u>) (661.6 , 1038.1, 1502.4)
23	(7 , 6, 10) (10 , 7, 6)	(915.8, 1353.5, <u>864.6</u>) (808.1 , 964.8, 1229.2)
31	(10 , 11, 15) (11 , 10, 15)	(934.8, <u>860.6</u> , 1716.4) (710.3 , 1056.8, 1533.6)

Table 7.4: Handovers of mobile station

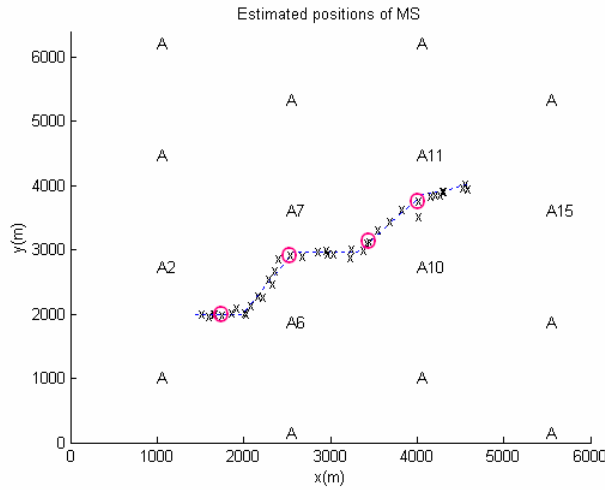


Figure 7.18: Handovers of moving mobile station

Study of triangle method

Table 7.5 shows the location of the three BSs which are nearest to the moving mobile station. The change of the third BS (shown in bold) occurs almost at the same sampling number –position for all tests that were performed under various parameters. It can be seen that a new third nearest BS will be computed if and only if more than one angle between BS1-MS-BS2 is less than 90° . The excluded BS is this we participate in the angles, which are smaller than 90° .

Position	Old Triple of BS	Angles involved in triangle methods	New Triple of BS
11	6 – 2 – 1	(6,2)→ 170° (2,1)→ 62° (6,1)→ 30°	6 – 2 – 7
17	7 – 6 – 2	(7,6)→ 162° (6,2)→ 78° (2,7)→ 82°	7 – 6 – 10
28	10 – 7 – 6	(10,7)→ 125° (7,6)→ 56° (6,10)→ 44°	10 – 7 – 11
30	10 – 7 – 11	(10,7)→ 43° (7,11)→ 48° (11,10)→ 132°	10 – 11 – 15

Table 7.5: Triangle method for estimating the three nearest BSs

7.3 Summary

In this chapter we study the performance of adaptive algorithms and the accuracy of the position and velocity algorithm. Using adaptive algorithms derived that N-LMS has quicker convergence than LMS, but it is more unstable. Moreover using LMS the normalized array factor in direction of interest has bigger value than in case of N-LMS. Both algorithms manage to steer the radiated main lobe in the direction of interest. The hybrid algorithm also steer main lobe successfully in the desired direction. Moreover converge quicker than the other algorithms.

In the position and velocity algorithm if the BSs derived that as the antenna elements increase the system has better performance, regardless of the used adaptive algorithm. The usage of hybrid algorithm is preferred if the BSs use $M=3,5,7$ elements. The LMS algorithm is preferred when the elements are increased. The N-LMS has the worst performance compared with the other two algorithms. Finally, simulations testify that the handover algorithm and triangle method are independent of the applied adaptive algorithm.

Chapter 8

Conclusions and Future Work

8.1 Conclusions

In this thesis we have developed an algorithm to determining the position and the velocity of a mobile station in a region applied the GSM system. This algorithm is based on using smart antennas and particularly adaptive antenna arrays. The adaptive antenna arrays are simulated by using the Least Mean Squares (LMS), the Normalized - Least Mean Squares (N-LMS) the Sample Matrix Inversion (SMI) and a proposed hybrid algorithm. These algorithms were studied to understand aspects such as the convergence speed and the stability. These characteristics were studied to inspect the radiation pattern in a specific direction of interest, the beampattern of the antenna and the mean square error of the beamformer output and a reference signal.

It was derived from simulation results that SMI convergences faster but its stability depends on the ability to invert a large covariance matrix. The LMS algorithm has slower convergence than N-LMS, although it is more stable around a significant value of array factor. This, probably, happens because the adaptation method of N-LMS is based on the incoming signal that suffers from additive noise. Finally the hybrid algorithm has better convergence since the weight vector of the antenna is derived faster than the other algorithms. Hybrid algorithm performs the lower value of mean square error. So that if the samples to be used are not enough the hybrid algorithm is better to be chosen. Moreover the hybrid algorithm encounters the disadvantage of SMI, which requires that the signal's environment does not undergo significant changes. All algorithms manage to steer the main lobe in the direction of interest unless an interferer is close to signal of interest.

Using the adaptive algorithms we developed the PVE algorithm. By the simulations have pointed out that as the elements of the antenna array are increased, the position and velocity accuracy is getting better. The PVE algorithm was also tested, assuming Rayleigh fading channels. The performance of the algorithm is decreased compared to

the simulation under Gaussian noise channel. Comparing the adaptive algorithms that were used in PVE derived that the N-LMS has worst accuracy then hybrid and LMS algorithm. In this point we must note that the position accuracy, for each studied case, has spread of about 7%. Studying the handover procedure we make out that handovers are not affected by the adaptive algorithm. Alike conclusion is derived in case of triangle method that helps to estimate the three nearest to mobile user BSs.

8.2 Future work

Much work has been done in the area of adaptive antenna arrays and position estimation, however there is still more to be done. One of the objectives of this thesis was how adaptive arrays can be mounted on BS to combat interference and multipath signals. We focus on SMI, LMS, N-LMS and on the proposed hybrid algorithm using training sequence. These algorithms are depending on minimum mean square criterion. As we have mentioned in chapter 4 there are three more criteria that could also be applied. Consequently we may examine the adaptive and the PVE algorithm to estimate parameters of antenna by using rest of optimum criteria. In case we are using the reference signal we can, also, use the recursive least square (RLS). All algorithms were tested for linear array. We could extend study using configurations of circular or rectangular arrays.

Instead of using a reference signal, we can compute the weight vector by using “blind” algorithms. These algorithms try to extract the unknown channel response and the unknown transmitted data from the received signal at the antenna elements. Even though “blind” algorithms do not know the actual bits, they use additional knowledge about the structure of the transmitted signal, e.g. finite alphabet or cyclostationarity. However “blind” algorithms require too much computational time to be employed in real time. So that we can combine blind algorithms with training sequence algorithms.

In this thesis we use three BSs to estimate the position of a mobile user. We could use more than three BS for this purpose. This scheme would be used by modifying the triangle method, such as to determined the BSs that serve the mobile user. Another improvement to the proposed algorithm would be the division each cell into three sectors, each covering area of 120° wide.

In our study we preferred to use MSK modulation, which is close to GMSK modulation that is used to GSM system. In future we could test the PVE algorithm using GMSK, BPSK or other modulation schemes, including parameters as the bit rate.

In the tested system the beams of the antenna are formed to a single direction since we are only concerned by one signal of interest – mobile user. We can extend the system forming mainlobes to several directions assuming more than one mobile users are served simultaneously. With this issue we extend even more the capacity of a mobile communication system.

Finally we will investigate the performance of a wireless communication system when smart antennas are applied to BSs and MSs. Although setting smart antennas on a MS may not be practical for current MS handsets, reduction in their antenna size and also the usage of notebook computers in wireless applications may make this issue feasible in the future.

Appendix A

To derive the electric field for the line element, let us consider an infinitesimal element of length h , carrying current as shown in figure A.1. Let $[I]$ be the retarded current carried by the element and $[Q]$ be the retarded electric charge. Both quantities are a function of $(t - R/c)$, where t is time, R are the distance from the point P to the centre of line element and c is the speed of light. $[Q]$ is related to $[I]$ by the

equation: $\frac{d[Q]}{dt} = [I]$

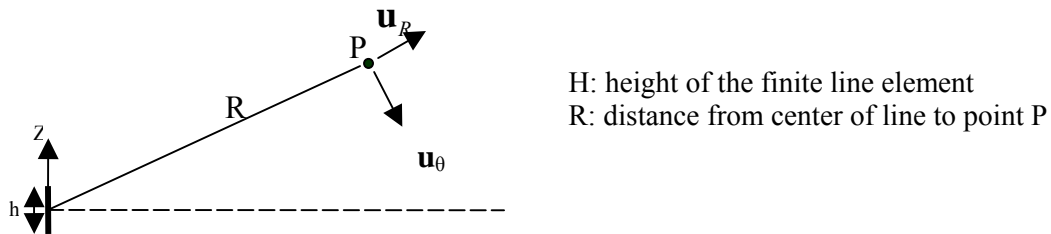


Figure A.1: orientation of an infinitesimal element carrying current

The three equations governing electromagnetic field are:

$$\mathbf{E}(R, t) = -\nabla V(R, t) - \frac{\partial \mathbf{A}(R, t)}{\partial t} \quad (\text{A.1})$$

$$\mathbf{B}(R, t) = \nabla \mathbf{A}(R, t) \quad (\text{A.2})$$

$$\nabla \mathbf{A}(R, t) = \frac{1}{c^2} \frac{\partial \mathbf{V}(R, t)}{\partial t} \quad (\text{A.3})$$

The magnetic potential, \mathbf{A} , is given by:

$$\mathbf{A} = \frac{\mu_o}{4\pi} \int_v \frac{[\mathbf{J}]}{r} dv \quad (\text{A.4})$$

From the geometry of the problem in figure A.1 the equation (A.4) can be expressed:

$$\mathbf{A} = \mathbf{u}_z \frac{\mu_o}{4\pi} \int_{-h/2}^{h/2} \frac{[\mathbf{J}]}{R} dz \quad (\text{A.5})$$

Assuming that $R \gg h$, equation A.5 is approximated to

$$\mathbf{A} = \mathbf{u}_z \frac{\mu_o h}{4\pi R} [I] \quad (\text{A.6})$$

Expressing this in spherical coordinates

$$\mathbf{A} = \mathbf{u}_R \frac{\mu_o [I]}{4\pi R} h \cos \theta - \mathbf{u}_\theta \frac{\mu_o [I]}{4\pi R} h \sin \theta \quad (\text{A.7})$$

Divergence of \mathbf{A} in spherical coordinates is given by

$$\nabla \cdot \mathbf{A} = \frac{1}{R} \frac{\partial}{\partial R} (R^2 A_R) + \frac{1}{R \sin \theta} \frac{\partial}{\partial \theta} (A_\theta \sin \theta) \quad (\text{A.8})$$

The first terms in the divergence \mathbf{A} can be expressed as

$$\frac{\partial}{\partial R} (R^2 A_R) = \frac{\mu_o h \cos \theta}{4\pi} \left(\frac{\partial [I]}{\partial R} R + [I] \right) \quad (\text{A.9})$$

As $[I]=I(\theta)$, where $\theta = t-R/c$,

$$\frac{\partial [I]}{\partial R} = \frac{\partial [I]}{\partial \theta} \frac{d\theta}{dR} = \frac{\partial [I]}{\partial \theta} \frac{dt}{d\theta} \frac{d\theta}{dt} = -\frac{1}{c} \frac{\partial [I]}{\partial t} \quad (\text{A.10})$$

hence,

$$\frac{\partial}{\partial R} (R^2 A_R) = \frac{\mu_o h \cos \theta}{4\pi} \left(-\frac{R}{c} \frac{\partial [I]}{\partial t} + [I] \right) \quad (\text{A.11})$$

Following the same procedure the second term is found to be

$$\frac{\partial}{\partial \theta} (A_\theta \sin \theta) = -\frac{\partial}{\partial \theta} \left(\frac{\mu_o [I]}{4\pi R} h \sin^2 \theta \right) = -\frac{\mu_o [I]}{4\pi R} (2h \sin \theta \cos \theta) \quad (\text{A.12})$$

Hence equation A.8 becomes

$$\nabla \cdot \mathbf{A} = \frac{\mu_o h \cos \theta}{4\pi} \left(-\frac{1}{Rc} \frac{d[I]}{dt} - \frac{[I]}{R^2} \right) \quad (\text{A.13})$$

From equation A.3 we have

$$\frac{\partial \mathbf{V}(R,t)}{\partial t} = -\frac{1}{c^2} \nabla \mathbf{A}(R,t) \quad (\text{A.14})$$

Intergrating both sides with respect to time t ,

$$\mathbf{V}(R,t) = -c^2 \int \nabla \mathbf{A}(R,t) dt \quad (\text{A.15})$$

Assuming that when $t < 0$, the integral is zero, i.e. no potential before $t=0$,

$$\mathbf{V}(R,t) = -c^2 \int_0^t \frac{\mu_o h \cos \theta}{4\pi} \left(-\frac{1}{Rc} \frac{d[I]}{dt} - \frac{[I]}{R^2} \right) dt = \frac{c^2 \mu_o h \cos \theta}{4\pi} \left(\frac{[I]}{Rc} + \frac{1}{R^2} \int_0^t [I] dt \right) \quad (\text{A.16})$$

Now from the relationship of $[I]$ and $[Q]$ in equation $\frac{d[Q]}{dt} = [I]$,

$$\mathbf{V}(R,t) = \frac{c^2 \mu_o h \cos \theta}{4\pi} \left(\frac{[I]}{Rc} + \frac{[Q]}{R^2} \right) \quad (\text{A.17})$$

After finding the $\mathbf{V}(R,t)$ and $\mathbf{A}(R,t)$, the electric field of the line element can be found by substituting these terms in equation A.1. Using

$$\nabla \mathbf{V}(R,t) = u_R \frac{\partial V}{\partial R} + u_\theta \frac{1}{R} \frac{\partial V}{\partial \theta} + u_\phi \frac{1}{R \sin \theta} \frac{\partial V}{\partial \phi} \quad (\text{A.18})$$

and letting $k = -\frac{c^2 \mu_o h}{4\pi}$ we have

$$\begin{aligned}
\frac{\partial V}{\partial R} &= \frac{\partial}{\partial R} \left[k \cos \theta \left(\frac{[I]}{Rc} + \frac{[Q]}{R^2} \right) \right] = k \cos \theta \left(\frac{d[I]}{dR} \frac{1}{Rc} - \frac{[I]}{R^2 c} + \frac{d[Q]}{dR} \frac{1}{R^2} - \frac{2[Q]}{R^3} \right) = \\
&= k \cos \theta \left(\frac{1}{Rc^2} \frac{d[I]}{dt} - \frac{[I]}{R^2 c} + \frac{d[Q]}{dt} \frac{1}{R^2 c} - \frac{2[Q]}{R^3} \right) \quad (\text{A.19}) \\
&= k \cos \theta \left(\frac{1}{Rc^2} \frac{d[I]}{dt} - \frac{2[I]}{R^2 c} - \frac{2[Q]}{R^3} \right)
\end{aligned}$$

$$\frac{\partial V}{\partial \theta} = \frac{\partial}{\partial \theta} \left[k \cos \theta \left(\frac{[I]}{Rc} + \frac{[Q]}{R^2} \right) \right] = -k \sin \theta \left(\frac{[I]}{Rc} + \frac{[Q]}{R^2} \right) \quad (\text{A.20})$$

$$\frac{\partial V}{\partial \phi} = 0 \quad (\text{A.21})$$

Hence,

$$\nabla V(R, t) = u_R \left[k \cos \theta \left(\frac{1}{Rc^2} \frac{d[I]}{dt} - \frac{2[I]}{R^2 c} - \frac{2[Q]}{R^3} \right) \right] + u_\theta \left[-k \sin \theta \left(\frac{[I]}{Rc} + \frac{[Q]}{R^2} \right) \right] \quad (\text{A.22})$$

$$\frac{\partial \mathbf{A}(R, t)}{\partial t} = u_R \frac{\mu_o h \cos \theta}{4\pi R} \frac{d[I]}{dt} - u_\theta \frac{\mu_o h \sin \theta}{4\pi R} \frac{d[I]}{dt} \quad (\text{A.23})$$

Since

$$\mathbf{E}(R, t) = -\nabla V(R, t) - \frac{\partial \mathbf{A}(R, t)}{\partial t}$$

We have

$$\begin{aligned}
\mathbf{E}(R, t) &= \mathbf{u}_R \left[k \cos \theta \left(\frac{1}{Rc^2} \frac{d[I]}{dt} + \frac{2[I]}{R^2 c} + \frac{2[Q]}{R^3} \right) \right] + \mathbf{u}_\theta \left[k \sin \theta \left(\frac{[I]}{Rc} + \frac{[Q]}{R^2} \right) \right] \\
&\quad - \mathbf{u}_R \frac{\mu_o h \cos \theta}{4\pi R} \frac{d[I]}{dt} + \mathbf{u}_\theta \frac{\mu_o h \cos \theta}{4\pi R} \frac{d[I]}{dt} \\
&= \mathbf{u}_R \left[\frac{c^2 \mu_o h \cos \theta}{4\pi R} \left(\frac{1}{Rc^2} \frac{d[I]}{dt} + \frac{2[I]}{R^2 c} + \frac{2[Q]}{R^3} \right) - \frac{\mu_o h \cos \theta}{4\pi R} \frac{d[I]}{dt} \right] \\
&\quad + \mathbf{u}_\theta \left[\frac{c^2 \mu_o h \sin \theta}{4\pi} \left(\frac{[I]}{Rc} + \frac{[Q]}{R^2} \right) + \frac{\mu_o h \sin \theta}{4\pi} \frac{d[I]}{dt} \right]
\end{aligned}$$

$$\mathbf{E}(R,t) = \mathbf{u}_R \frac{h \cos \theta}{4\pi} \left[\left(\frac{\mu_o}{\epsilon_o} \right)^{1/2} \frac{2[I]}{R^2} + \frac{2[Q]}{\epsilon_o R^3} \right] + \mathbf{u}_\theta \frac{h \sin \theta}{4\pi} \left[\left(\frac{\mu_o}{\epsilon_o} \right)^{1/2} \frac{[I]}{R^2} + \frac{[Q]}{\epsilon_o R^3} + \frac{\mu_o [I]}{R} \frac{d[I]}{dt} \right] \quad (\text{A.24})$$

Transforming equation A.24 into cylindrical coordinates, taking into account

$$\text{equations} \quad \cos \theta = \frac{z}{(r^2 + z^2)^{1/2}}, \quad \sin \theta = \frac{r}{(r^2 + z^2)^{1/2}}, \quad R^2 = r^2 + z^2$$

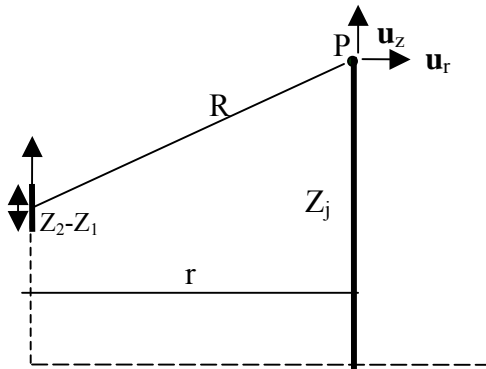
using figure A.2 we have

$$E(r, z, t) = (E_R \cos \theta - E_\theta \sin \theta) \mathbf{u}_z + (E_R \sin \theta - E_\theta \cos \theta) \mathbf{u}_r \quad (\text{A.25})$$

with

$$\mathbf{E}_z = \mathbf{u}_z \frac{h}{4\pi} \left[\left(\frac{\mu_o}{\epsilon_o} \right)^{1/2} \frac{2z^2 - r^2}{(r^2 + z^2)^2} [I] + \frac{1}{\epsilon_o} \frac{2z^2 - r^2}{(r^2 + z^2)^{2.5}} [Q] - \mu_o \frac{r^2}{(r^2 + z^2)^{1.5}} \frac{d[I]}{dt} \right] \quad (\text{A.26})$$

$$\mathbf{E}_r = \mathbf{u}_r \frac{h}{4\pi} \left[\left(\frac{\mu_o}{\epsilon_o} \right)^{1/2} \frac{3rz}{(r^2 + z^2)^2} [I] + \frac{1}{\epsilon_o} \frac{3rz}{(r^2 + z^2)^{2.5}} [Q] + \mu_o \frac{rz}{(r^2 + z^2)^{1.5}} \frac{d[I]}{dt} \right] \quad (\text{A.27})$$



- $z_2 - z_1$: Length of finite line element
- R: distance from center of line to point P
- r: Horizontal projection of R in the direction \mathbf{u}_r
- z: Vertical projection of R in the direction \mathbf{u}_z

Figure A.2: Orientation of a finite line element of length $z_2 - z_1$

Using equations A.26 and A.27, we may derive an expression for the electric field radiated by a finite length of thin current carrying conductor. From figure A.2, it can be seen that the receiving antenna of BTS will only pick up the \mathbf{E}_z , the vertical polarized signal. Ignoring the \mathbf{E}_r and assuming that $[Q] = 0$, we get the

$$\mathbf{E}'(r, z, t) = \mathbf{u}_z \left[\frac{h}{4\pi} \left(\frac{\mu_0}{\varepsilon_0} \right)^{1/2} \frac{2z^2}{(r^2 + z^2)^2} - \frac{r^2}{(r^2 + z^2)^2} [I] - \frac{\mu_0 h}{4\pi} \frac{r^2}{(r^2 + z^2)^2} \frac{d[I]}{dt} \right] \quad (\text{A.28})$$

Setting $h = dz$ and redefining variable z as $z = z_j - z$, $dz = -dz$ in (A.28) we may obtain the electric field radiated by a finite length of thin wire:

$$E(r, z, t) = \frac{\mu_0}{4\pi} \left[\frac{z_j - z_1}{\sqrt{r^2 + (z_j - z_1)^2}} - \frac{z_j - z_2}{\sqrt{r^2 + (z_j - z_2)^2}} \right] \frac{d[I]}{dt} \quad (\text{A.29})$$

Appendix B



**Proceedings of the 4th WSEAS International Conference on:
TELECOMMUNICATIONS and INFORMATICS
(TELE-INFO '05)**

Prague, Czech Republic, March 13-15, 2005

<http://www.wseas.org>

EDITORS:

**Miroslav Husak
(Czech Republic)**

**Nikos Mastorakis
(Greece)**

ASSOCIATE EDITOR:

**Al Falou Ayman
(France)**

ISBN: 960-8457-11-4

Hybrid Algorithms for Adaptive Array Systems

D. PAPADIMITRIOU and I.O. VARDIAMBASIS

Microwave Communications & Electromagnetic Applications Laboratory,
Telecommunications Division, Department of Electronics,
Technological Educational Institute (T.E.I.) of Crete - Chania Branch,
Romanou 3, Chalepa, 73133 Chania, Crete.

GREECE

ivardia@chania.teicrete.gr

Abstract: - In recent years, mobile communications have caused an explosive growth to the number of wireless users. This growth has triggered an enormous demand not only for capacity but also for better coverage and quality of services with priority on interference cancellation. This need lead scientists in using adaptive array antennas. The aim of this paper is to study the adaptive beamforming approaches as part of smart antenna technology. This work's focus is on the investigation of various adaptive algorithms and their ability to automatically respond to an unknown interference environment by steering nulls and reducing side lobe levels in the direction of interference, while keeping desired signal beam characteristics. The investigation covers three well known algorithms [Sample Matrix Inversion (SMI), Least Mean Squares (LMS), Normalized Least Mean Squares (N-LMS)], along with the combination of SMI and LMS and the combination of SMI and N-LMS, which are proposed here.

Keywords: - Smart antennas, Beamforming, Adaptive arrays, Sample Matrix Inversion algorithm, Least Mean Squares algorithm, Mobile communications.

1 Introduction

Rapid growth of the capacity needed by mobile communication systems, leads to increased density of radio sources. Consequently, undesired noise appears in the signal environment, which tends to reduce communication systems' performance. In order to overcome this problem, adaptive arrays are used, because they can discriminate the interference sources in the wireless channel suppressing them automatically. Thus, system's performance is improved, without any knowledge about the location of interference-sources.

Fig. 1a shows an adaptive array system in the form of an adaptive linear combiner, which is the basic building block of almost all adaptive filters, thus having a wide variety of practical applications [1]-[5]. The necessary learning system is generally characterized as signal operator with adjustable parameters by an adaptive algorithm, which adjusts automatically all system's parameters in order to optimise its performance. The adjustable parameters of Fig. 1 are weights (indicated by arrowed circles), while the input signals are stochastic. The adaptive (adjusting weights) algorithm is using information obtained from inputs. Its efficiency depends on minimizing the input information usage and maximizing solution's quality (achieving parameter

adjustments close to optimum). However, input information minimization corresponds to slow adaptive convergence, fact which is the learning systems' trade off.

Adaptive array systems adjust their directional parameters, so as to maximize the signal to noise ratio (SNR), because the desired signal is received by the array along with many interference signals. Then using an adaptive algorithm, the variable system's weights automatically adjust, and the system manages to have a main lobe in the direction of the desired signal and at the same time to reject any interference incident from other directions.

In the following paragraphs, three known adaptive algorithms (SMI, LMS, N-LMS) and two new hybrid algorithms are used in an adaptive array system in order to demonstrate their convergence speed and stability, with respect to noise cancellation. In Section 2 the configuration of an adaptive array system is given and the used adaptive algorithms are introduced. Finally in Section 3, the simulation parameters and results are described along with relative conclusions.

2 Adaptive Beamforming

2.1 Beamforming principles

Consider the adaptive beamforming configuration shown in Fig. 1a, which is a uniform linear array (ULA) with M isotropic elements, placed along x -axis of Fig. 1b. The output $y(t)$ of this array system is the weighted sum of the received signals $s_\ell(t)$ ($\ell=1,2,\dots,q$) and the noise $n(t)$. The weights w_m ($m=1,2,\dots,M$) are computed iteratively based on the array output $y(t)$ and the reference signal $d(t)$, which is approximately the desired transmitted signal. The reference signal is known to the receiver by using training block data, while its format varies and depends upon the implemented system. Also, the correlation between the reference and the desired signals influences the accuracy and the convergence of the selected algorithm.

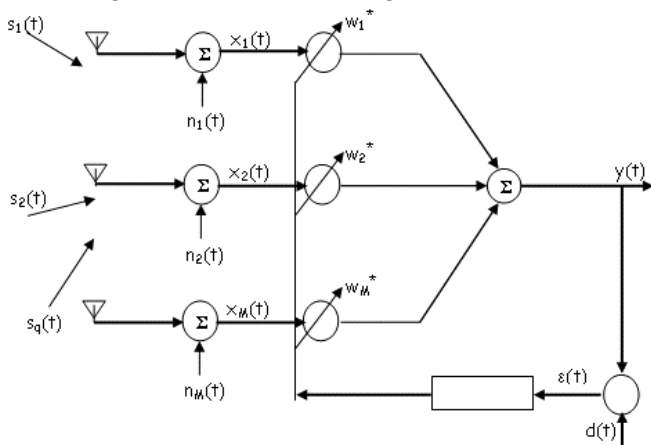


Figure 1 (a): An adaptive array system.

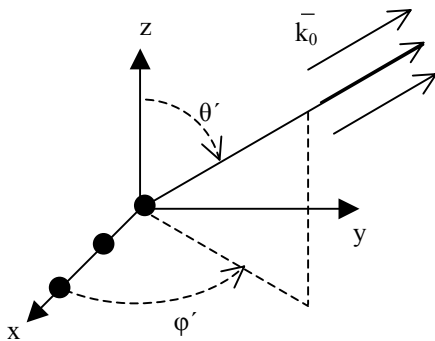


Figure 1 (b): The wave incident upon the structure.

Assuming that $x_M(t)$ is the input data to the M -th antenna element at time t , and w_M is the weight of the M -th element, the array's input data and weight factors can be written in vector form:

$$\bar{x}(t) = [x_1(t) \ x_2(t) \ \dots \ x_M(t)]^T, \quad (1a)$$

$$\bar{w} = [w_1 \ w_2 \ \dots \ w_M]^T, \quad (1b)$$

where superscript T denotes the transpose operation. Using this notation, the array output $y(t)$ is:

$$y(t) = \bar{w}^H \cdot \bar{x}(t), \quad (1c)$$

where superscript H denotes the Hermitian

(complex conjugate) transpose. So, in order to compute the optimum weight vector \bar{w}_{opt} , the input data vector $\bar{x}(t)$ has to be determined.

Considering as $s(t)$ either the desired or the interfering input signal, which is obliquely incident upon the antenna structure with elevation angle $\pi/2 - \theta'$ and azimuth angle ϕ' (as in Fig. 1(b)), the input data vector $\bar{x}(t)$ can be expressed as:

$$\bar{x}(t) = \begin{bmatrix} e^{-j2\pi f_c \cdot \tau_1(\theta', \phi')} \\ e^{-j2\pi f_c \cdot \tau_2(\theta', \phi')} \\ \dots \\ e^{-j2\pi f_c \cdot \tau_M(\theta', \phi')} \end{bmatrix} \cdot s(t) = \bar{a}(\theta', \phi') \cdot s(t), \quad (2)$$

where $\bar{a}(\theta', \phi')$ is termed the array propagation vector or the steering vector for the particular values of (θ', ϕ') , f_c represents the carrier frequency, $\tau_m(\theta', \phi') = d \cdot \sin(\theta') \cdot \cos(\phi') / c$ stands for the time delay due to the distance d between array elements, and c is the velocity of light in free space.

Since there are q narrowband signals $s_\ell(t)$ impinging upon the array with different arrival directions (θ_ℓ, ϕ_ℓ) , the input data vector may be expressed as:

$$\bar{x}(t) = \sum_{\ell=1}^q \bar{\alpha}_\ell(\theta_\ell, \phi_\ell) \cdot s_\ell(t) + \bar{n}(t), \quad (3)$$

where $\bar{n}(t)$ denotes the $M \times 1$ vector of noise at the M array elements. Using matrix notation:

$$\bar{x}(t) = \bar{A}(\theta', \phi') \cdot \bar{S}(t) + \bar{n}(t), \quad (4)$$

where $\bar{A}(\theta', \phi') = [\bar{a}_1(\theta_1, \phi_1) \ \bar{a}_2(\theta_2, \phi_2) \ \dots \ \bar{a}_q(\theta_q, \phi_q)]$ is the $M \times q$ matrix of steering vectors and $\bar{S}(t) = [s_1(t) \ s_2(t) \ \dots \ s_q(t)]^T$ is the $q \times 1$ vector of impinging signals.

If $s_d(t)$ denotes the desired signal arriving from the direction (θ_d, ϕ_d) upon the array and $s_j(t)$ ($j=1, \dots, N_u$) denotes anyone of the $N_u (= q-1)$ undesired interfering signals arriving from (θ_j, ϕ_j) , (3) may be rewritten as follows:

$$\bar{x}(t) = \bar{a}(\theta_d, \phi_d) \cdot s_d(t) + \sum_{j=1}^{N_u} \bar{a}(\theta_j, \phi_j) \cdot s_j(t) + \bar{n}(t) \quad (5)$$

where it should be noted that the directions of arrival are known a priori using a direction of arrival (DOA) algorithm.

Therefore, (5) requires an adaptive algorithm in order to estimate $s_d(t)$ from $\bar{x}(t)$ while minimizing the error between the array output $y(t)$ and the reference signal $d^*(t)$ approximating the desired

signal $s_d(t)$. The signal $d^*(t)$ may be constructed at the receiver during the training period (the complex conjugate expression of the reference signal stands only for mathematical convenience).

If $y(k)$ and $d^*(k)$ denote the sample signals of $y(t)$ and $d^*(t)$ at time instant t_k , the array system's error is given by $\varepsilon(k)=d^*(k)-y(k)$ and the mean square error (MSE) $E[\varepsilon^2(k)]$ is given by:

$$E[\varepsilon^2(k)] = E\left[\left(d^*(k)-y(k)\right)^2\right] = E\left[\left(d^*(k)-\bar{w}^H \cdot \bar{x}(k)\right)^2\right] \Rightarrow \\ \Rightarrow E[\varepsilon^2(k)] = E\left[d^2(k)\right] - 2 \cdot \bar{w}^H \cdot \bar{r} + \bar{w}^H \cdot \bar{R} \cdot \bar{w} \quad (6)$$

where $\bar{r} = E[d^*(k) \cdot \bar{x}(k)]$ is the $M \times 1$ cross-correlation matrix between the desired signal and the input data vector and $\bar{R} = E[\bar{x}(k) \cdot \bar{x}^H(k)]$ is the $M \times M$ covariance matrix of the input data vector. The minimum mean square error can be obtained by setting the gradient vector of (6), with respect to w , equal to zero, i.e.

$$\nabla_w \left(E[\varepsilon^2(k)] \right) = 0 \Rightarrow -2 \cdot \bar{r} + 2 \cdot \bar{R} \cdot \bar{w} = 0. \quad (7)$$

Therefore the optimum solution for the weights is given by:

$$\bar{w}_{\text{opt}} = \bar{R}^{-1} \cdot \bar{r}, \quad (8)$$

which is referred to as the optimum Weiner solution.

2.2 Adaptive algorithms

2.2.1 Least Mean Squares (LMS) algorithm

A common adaptive algorithm that is well known [4] is the least mean squares (LMS) algorithm. It is based on the steepest-descent method, which is an optimization method [6] working recursively to compute and update the weights vector. The optimum value of weights vector means that the system's success to minimize the MSE. The successive corrections of the weights vector are in the direction of the negative of the gradient vector. Using steepest-descent method, the weight vector equation, at time instant t_k , is given [2] by:

$$\bar{w}(k+1) = \bar{w}(k) + \frac{1}{2} \mu \cdot \left[-\nabla \left(E\{\varepsilon^2(k)\} \right) \right], \quad (9)$$

where gain constant μ (step size) controls the convergence characteristics of the algorithm. Using (7), follows that:

$$\bar{w}(k+1) = \bar{w}(k) + \mu \cdot \left[\bar{r} - \bar{R} \cdot \bar{w}(k) \right]. \quad (10)$$

Using the instantaneous estimates (at t_k) of covariance matrices \bar{R} and \bar{r} , instead of their actual values, the weights can then be updated as:

$$\bar{w}(k+1) = \bar{w}(k) + \mu \cdot \bar{x}(k) \cdot \left[d^*(k) - \bar{x}^H(k) \cdot \bar{w}(k) \right] \Rightarrow \\ \Rightarrow \bar{w}(k+1) = \bar{w}(k) + \mu \cdot \bar{x}(k) \cdot \varepsilon^*(k). \quad (11)$$

Note that this is a continuously adaptive approach, where the weights are updated as the data are sampled, so that the resulting weight vector sequence converges to the optimum solution. The LMS algorithm is initiated with the arbitrary value $\bar{w}(0) = 0$. In order the weight vector to have stable convergence, μ must take values in the interval:

$$0 < \mu < \lambda_{\text{max}}^{-1}, \quad (12)$$

where λ_{max} is the largest eigenvalue of the covariance matrix \bar{R} . The convergence of the algorithm is inversely proportional to the eigenvalue spread of the correlation matrix. If μ is chosen to be large, then the algorithm's convergence is faster, but may be less stable around the minimum value. On the contrary a small value of μ leads to slow convergence.

2.2.2 Sample Matrix Inversion (SMI) algorithm

One way to succeed a faster convergence rate is to use the sample matrix inversion algorithm, since it employs direct inversion of the covariance matrix \bar{R} [7]. If a priori the desired and the interfering signal are known, then the optimum weights can be calculated directly using SMI. Supposing that the signals are known and the signal environment undergoes frequent changes, the adaptive system must update the weights vector continually, in order to meet the new requirements. Here it is considered that these changes do not happen during the processing of the block data, although the covariance matrices \bar{R} and \bar{r} arise in a finite observation interval:

$$\hat{\bar{R}} = \sum_{i=N_1}^{N_2} \bar{x}(i) \cdot \bar{x}^H(i), \quad (13a)$$

$$\hat{\bar{r}} = \sum_{i=N_1}^{N_2} d^*(i) \cdot \bar{x}(i), \quad (13b)$$

where N_1 and N_2 are the lower and upper limits of the observation interval, respectively. The weights vector can now be estimated by the equation:

$$\hat{\bar{w}} = \hat{\bar{R}}^{-1} \cdot \hat{\bar{r}}. \quad (14)$$

There is always a residual error in the SMI algorithm (since it is based on estimation):

$$\bar{\varepsilon} = \hat{\bar{R}} \cdot \bar{w}_{\text{opt}} - \hat{\bar{r}}. \quad (15)$$

This error is usually greater when compared to LMS error. One of disadvantages of this algorithm is that its stability depends on the ability to invert the large

covariance matrix. In order to avoid a covariance matrix's singularity, the zero mean noise is added to the array response vector. Another disadvantage that has to be encountered is that even though the algorithm has faster convergence, huge matrix inversions lead to computational complexities that cannot be easily overcome.

2.2.3 Normalized Least Mean Squares (N-LMS) algorithm

Though other algorithms, such as the RLS one, may be more complex, less stable and more difficult to implement, they often converge much faster than the LMS. Improving the convergence speed, but keeping the simplicity of the LMS, has been the major consideration of much algorithmic research, resulting in the normalized least mean squares (N-LMS) algorithm. This algorithm, which has been studied widely and has various applications to mobile communications [8], is a variation of the constant-step-size LMS algorithm, using data-dependent step size at each iteration. For example, at the n -th iteration the step size is given by:

$$\mu(t) = \frac{\mu_0}{\bar{\mathbf{x}}^H(t) \cdot \bar{\mathbf{x}}(t) + a}, \quad (16)$$

where μ_0 is a constant (usually $1/2$) and a is a very small number introduced to prevent division by zero, if the product $\bar{\mathbf{x}}^H(t) \cdot \bar{\mathbf{x}}(t)$ is very small. This algorithm does not need an estimation of the correlation matrix's eigenvalues or trace, in order to select the maximum permissible step size. The N-LMS algorithm normally has better convergence performance and less signal sensitivity compared to the normal LMS algorithm.

2.2.4 Hybrid algorithm

In this work two hybrid algorithms combining the LMS or the N-LMS algorithm with the SMI one are proposed. Because both algorithms are characterized by similar concepts, only the hybrid LMS is introduced here. As mentioned before, LMS is a simple algorithm with possible slow convergence. LMS is a continuous algorithm, so it is well suited for continuous transmission systems. On the other hand, SMI has a very faster convergence speed, as it uses inversion of the correlation matrix, but is requiring a signal environment changing slightly during the process of a data block. Therefore, there is need for an algorithm that: a) is simple to implement, b) has fast convergence and c) is not computational intensive.

In the LMS algorithm, as discussed previously, weights are initialized arbitrarily with $\bar{\mathbf{w}}(0) = 0$ and

then are updated using (11). Due to arbitrary weights initialization, the LMS takes longer to converge. In order to speed up convergence, an initial weights vector, that has been come through the SMI algorithm, is used. So, using only a small block of incoming data derives the weights vector. Therefore the initial weights vector is:

$$\bar{\mathbf{w}}_{in} = \hat{\mathbf{R}}_p \cdot \hat{\mathbf{t}}_p, \quad (17)$$

where the covariance and correlation matrices are:

$$\hat{\mathbf{R}}_p = \sum_{i=1}^p \bar{\mathbf{x}}(i) \cdot \bar{\mathbf{x}}^H(i), \quad (18a)$$

$$\hat{\mathbf{t}}_p = \sum_{i=1}^p d^*(i) \cdot \bar{\mathbf{x}}(i), \quad (18b)$$

where p is the block size, taken to be small in order to encounter the probability of changes in the signal environment. Besides, large block will need large matrix's inversion, resulting in a computationally complex method. After the initial weights vector derivation, the LMS algorithm is implemented. At time instant t_k , the weights vector update is:

$$\bar{\mathbf{w}}(k+1) = \bar{\mathbf{w}}(k) + \mu \bar{\mathbf{x}}(k) \left[d^*(k) - \bar{\mathbf{x}}^H(k) \cdot \bar{\mathbf{w}}(k) \right] \quad (19)$$

with initial weights vector $\bar{\mathbf{w}}(0) = \bar{\mathbf{w}}_{in}$.

When the LMS algorithm begin adaptation, the antenna beam has already steered close to the approximate direction of the desired signal. Therefore LMS algorithm takes less time to converge. After that, even if the signal environment changes, the hybrid algorithm is able to encounter these changes.

3 Simulation and Results

In this section, the performance of the algorithms described in the previous section, is shown and compared. For simulation purposes, a 9-element linear array antenna is used, with its individual elements placed along the x -axis with a half-wave length distance between them. The full wavelength distance $\lambda = c/f_c$ is computed with $f_c = 900$ MHz as the working frequency of the communication system. Fig. 2 shows that increasing the elements of the antenna array, the system manages to steer its main lobe in the direction of the interesting signal and to reject the incident interferences from other propagation directions. So, for the sake of simplicity and cost we use a 9-element linear array antenna.

The desired signal is a simple sinusoidal signal with frequency f_1 . All interfering signals are also sinusoidal signals with frequency f_2 close to f_1 .

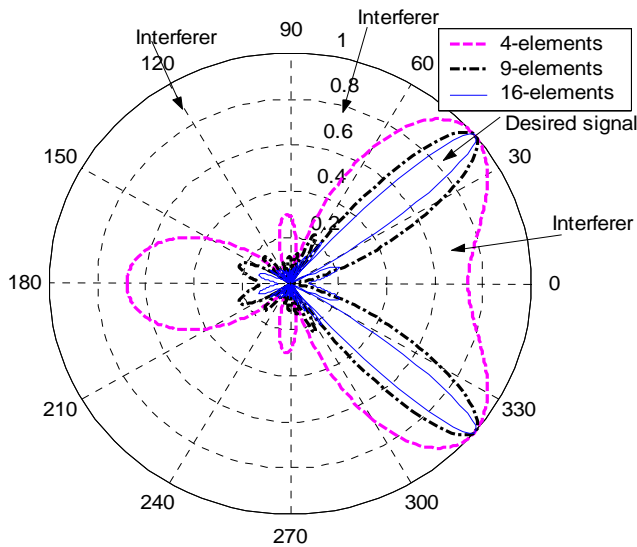


Figure 2. Beam patterns for various antenna elements.

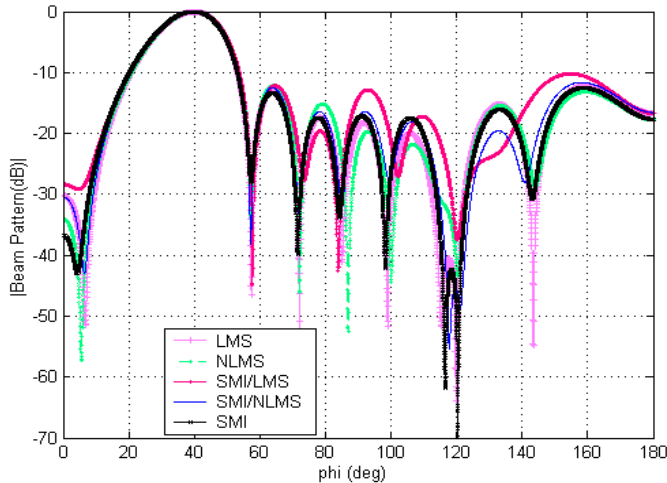


Figure 3. Beam patterns vs. azimuth angle φ for the presented algorithms, when $\theta = \pi/2$.

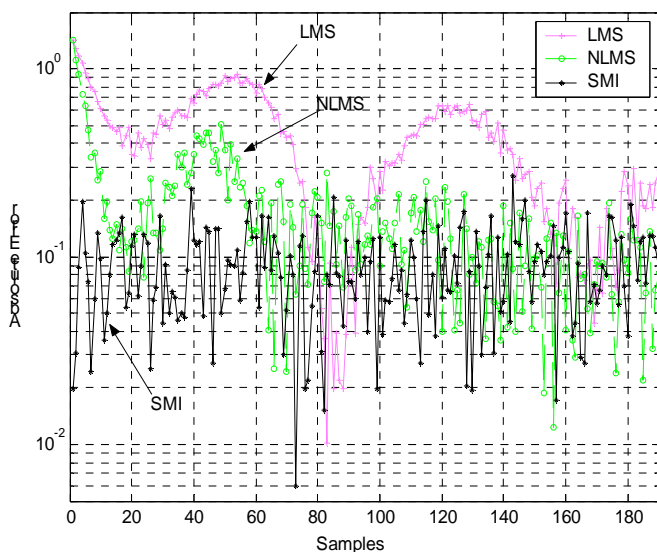


Figure 4. Absolute error of SMI, LMS and N-LMS algorithms vs. the number of samples used.

The SNR is taken to be 10 dB, while the signal to

interference ratio (SIR) is taken to be -5 dB for all interferes. The signal of interest is considered to be impinging to the antenna array from the direction (θ_0, φ_0) , while interference signals are impinging from different directions (θ_i, φ_i) , where elevation (or azimuth) incidence angles θ (or φ) take values in the interval $\pi/2 < \theta < \pi$ (or $0 < \varphi < 2\pi$). In the present simulations we consider 3 interferers and white gaussian noise with zero mean and variance $\sigma^2 = 0.1$. Finally for testing we use a block of 3,000 samples.

Fig. 3 shows the φ -plane of beam patterns in case of the presented algorithms. It is assumed that signal of interest impinges to the antenna array from direction $(100^\circ, 40^\circ)$, while the three interference signals from coming from directions $(97^\circ, 10^\circ)$, $(92^\circ, 80^\circ)$, and $(97^\circ, 120^\circ)$ (all used in radians). As can be seen, all algorithms manage to steer the main lobe in the direction of interest and force nulls to the directions of all interferers.

Fig. 4, which presents the absolute error of the adaptive algorithms, shows that the SMI algorithm converges immediately, even though it remains unstable. The rest four algorithms are more stable than the SMI, while the faster convergent algorithm appears to be the normalized LMS (N-LMS).

The convergence speed is shown in Fig. 5, where the mean square error is plotted. The normalized-LMS convergences faster than LMS. At the same time, the hybrid NLMS excels over the hybrid LMS. At the end the mean square error of NLMS and hybrid NLMS value less than that of LMS and hybrid LMS, respectively.

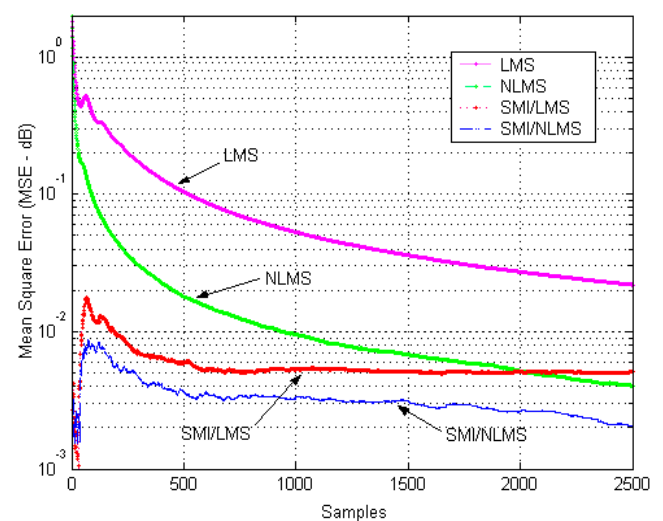


Figure 5. MSE vs. the number of samples, for the proposed algorithms (1st scenario).

In Fig. 6, the mean square error is plotted for the case that the white gaussian noise is added to the

signal, before this impinges to the antenna array (second scenario). The NLMS has faster convergence than LMS, and the same also happens with hybrid NLMS and hybrid LMS. But the mean square error results in higher values than the values of the previous scenario. This, however, was expected because the system cannot significantly determine the transmitted signal, and this is why communication systems use training symbols. As a consequence in Fig. 7 the weight estimation is characterized by instability, especially for the NLMS algorithms, since the weights updating are more dependent on the incoming signal than for the rest algorithms.

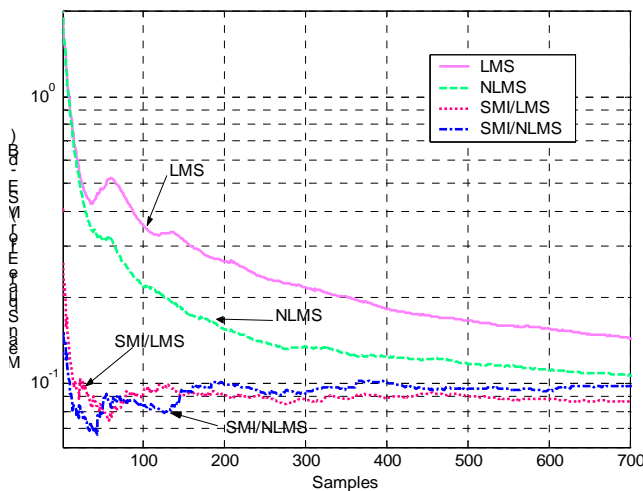


Figure 6: MSE vs. the number of samples, for the proposed algorithms (2nd scenario).

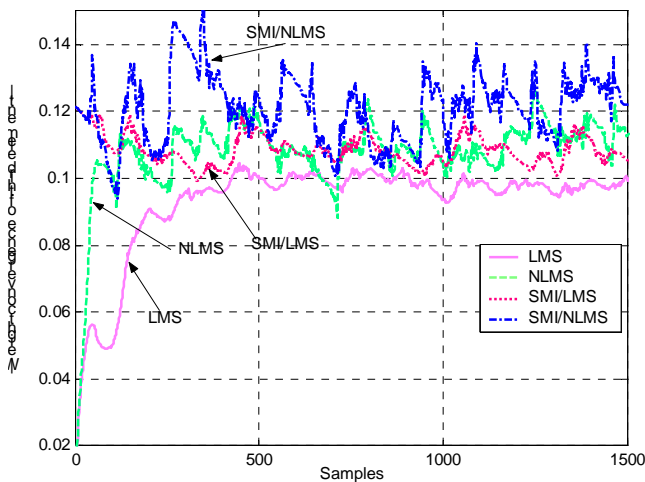


Figure 7. A weight convergence vs. the number of samples, for the proposed algorithms (2nd scenario).

4 Conclusions

In this work, the SMI, LMS, N-LMS, hybrid LMS and hybrid N-LMS adaptive algorithms were investigated. Their ability to respond automatically to an unknown interference environment by steering nulls in the direction of interferences and main lobe

in the direction of interest, was presented. Simulation results were also provided in order to understand various aspects, such as convergence and stability, of these algorithms.

Two scenarios were developed. In the first, where noise was added after the signal impingement to the antenna, SMI was found to have the faster convergence with higher complexity. Between the N-LMS and LMS, it was found that the former has faster convergence, but lower MSE value. Based on SMI, N-LMS and LMS, two hybrid algorithms with the simplicity of LMS-family and the convergence speed of SMI were proposed. In the second scenario, where the white gaussian noise was added on the signal before impingement to the antenna array, even if all algorithms manage to converge, their mean square errors result in higher values than the values of the previous scenario.

Acknowledgments

This work was supported by the Greek Ministry of National Education and Religious Affairs and the European Union under the EΠΕΑΕΚ II projects: “Archimedes – Support of Research Groups in TEI of Crete – Smart antenna study & design using techniques of computational electromagnetics and pilot development & operation of a digital audio broadcasting station at Chania (SMART-DAB)” and “Reformation of the Electronics Dept’s syllabus”.

References

- [1] B. Widrow and S.D. Stearns, *Adaptive Signal Processing*, Prentice Hall, 1985.
- [2] S. Haykin, *Introduction to Adaptive Filters*, Macmillan Publishing Company, 1985.
- [3] R.T Compton, *Adaptive Antennas: Concepts and Applications*, Prentice Hall, 1988.
- [4] S. Haykin, *Adaptive Filter Theory*, Prentice Hall, 1991.
- [5] B. Widrow and E. Walach, *Adaptive Inverse Control*, Prentice Hall, 1996.
- [6] W. Murray, *Numerical Methods for Unconstrained Optimization*, Academic Press, 1972.
- [7] I.S. Reed, J.D. Mallett and L.E. Brennan, “Rapid convergence rate in adaptive arrays”, *IEEE Trans. Aerosp. Electron. Syst.*, vol. AES-10, pp.853-863, Nov. 1974.
- [8] D.T.M. Slock, “On the convergence behavior of the LMS and the normalized LMS algorithms”, *IEEE Trans. Signal Process.*, vol. 41, pp. 2811-2825, 1993.

References

- [1] S. Sampei: “*Applications of Digital Wireless Technologies to Global Wireless Communications*,” Prentice Hall, Upper Saddle River, New Jersey, 1997.
- [2] R. Prasad: “*CDMA for Wireless Personal Communications*,” Artech House, Boston, 1996.
- [3] L.C. Godara, “Applications of Antenna Arrays to Mobile Communication, Part I: Performance, Improvement, Feasibility and Systems Considerations” *Proceedings of the IEEE*, Vol. 85, No. 7, Jul. 1997, pp. 1029-1060.
- [4] Warren L. Stutzman, Gary A. Thiele “*Antenna Theory and Design*”, John Wiley & Sons Inc. New York, 1981.
- [5] J. S. Blogh and L. Hanzo, “*Third Generation Systems and Intelligent Wireless Networking: Smart Antennas and Adaptive Modulation*” John Wiley & Sons Inc. New York, 2002.
- [6] John Litva and Titus Kwok-Yeung Lo. “*Digital Beamforming in Wireless Communications*”, Artech House, Boston, 1996.
- [7] Okamoto, Garret T. “*Smart Antenna Systems and Wireless Lans*”, New York Kluwer Academic Publishers, 2002.
- [8] Jack H. Winters. “*Smart Antennas for Wireless Systems*”, IEEE Personal Communications, February 1998
- [9] S.U. Pillai, “*Array signal processing*”, Springer - Verlag, New York, 1989
- [10] B. D. Van Veen and K.M. Buckley, ‘Beamforming: A versatile approach to spatial filtering.’ *IEEE ASP Magazine* pp.4-24, April 1988
- [11] Simon Haykin, “*Adaptive Filter theory*”, Prentice hall, Englewood Cliffs, New Jersey, 1991
- [12] Allan V. Oppenheim, Ronald W. Schaffer, “*Discrete-time signal processing*” Prentice Hall, Englewood cliffs, New Jersey, 1988

- [13] B. Widrow, P. E. Mante, L. J. Griffiths, and B. B. Goode, "Adaptive antenna systems", *Proceedings of IEEE*, vol. 55, pp. 2143-2159, December 1967.
- [14] R. A. Monzingo and T. W. Miller, "*Introduction to Adaptive Arrays*", John Wiley & Sons, 1980.
- [15] B. Widrow and S. D. Stearns, "*Adaptive Signal Processing*", Prentice Hall, 1985.
- [16] T. S. Rappaport, "*Wireless Communications: Principles and Practice*", Prentice Hall, Upper Saddle River, New Jersey, 1996.
- [17] J. E. Hudson, "*Adaptive Array Principle*", Peter Peregrinus Ltd., 1981.
- [18] H. Harada, R. Prasad, "*Simulation and software radio for mobile communications*", Artech House, 2002
- [19] J.C. Liberti, Jr. & T.S. Rappaport "Smart Antennas for Wireless Communications: IS-95 & Third Generation CDMA Applications", Prentice Hall, 1999
- [20] Chum Loo, Norman Second, "Computer model for fading channel with application to digital transmission", *IEEE Trans. Vehicular technology*, pp. 700-707, 1991
- [21] T. S. Rappaport, J. H. Reed and B. D. Woerner. "Position Location Using Wireless Communication on Highways of the Future", *IEEE Communications Magazine*, pp. 33-41, October 1996.
- [22] M. Hellebrandt, R. Mathar, M. Sheibenbogen, "Estimating Position and Velocity of Mobiles in a Cellular Radio Network", *IEEE Trans. on Vehicular Technology*, Vol. 46, No. 1, pp. 65-71, February 1997.
- [23] M. Hellebrandt, R. Mathar, "Location tracking of Mobiles in a Cellular Radio Networks", *IEEE Trans. on Vehicular Technology*, Vol. 48, No. 5, pp. 1558-1562, February 1999.

- [24] M. Hata. "Empirical Formula for Propagation Loss in Land Mobile Radio Services", *IEEE Trans. on Vehicular Technology*, Vol. 29, No. 3, pp. 317-325, August 1980.
- [25] R. Owen, L. Lopes, "Experimental analysis of the use of angle of arrival at an adaptive antenna array for location estimation", *IEEE International Symposium on Personal, Indoor and Mobile Radio Communications, PIMRC*, Vol. 2, pp. 607-611, 1998.
- [26] S. Fisher, H. Koorapaty, E. Larsson, A. Kangas. "System performance evaluation of mobile positioning methods", Vehicular Technology Conference, 1999 IEEE 49th, Vol. 3, pp. 1962-1966, 1999.
- [27] S. Fisher, H. Grubeck, A. Kangas, H. Koorapaty, E. Larsson, P. Lundqvist. "Time of arrival estimation of narrowband TDMA signals for mobile positioning", Personal, Indoor and Mobile Communications, *The N-nth IEEE International Symposium on:*, Vol. 1, pp. 451-455, 1998.
- [28] GL Stuber, "*Mobile wireless communications*", Kluwer, Dordrecht, 1996
- [29] Marquardt, D., "*An Algorithm for Least Squares Estimation of Nonlinear Parameters*," *SIAM J. Appl. Math.* Vol. 11, pp. 431-441, 1963.
- [30] Hagan, M.T., M. Menhaj, "Training feedforward networks with the Marquardt algorithm", *IEEE Transactions on Neural Networks*, vol.5, no. 6, pp. 989-993, 1994
- [31] Battiti R., "First and second order methods for learning: between steepest descent and Newton's method", *Neural computation*, vol. 4, no. 2, pp.141-166, 1992
- [32] M. Mouly M.B. Pautet "*The GSM system for mobile communications*". Printed by themselves
- [33] G. V. Tsoulos, "Smart antennas for mobile communication systems", *Electronics and Communication Engineering Journal*, vol. 11, no. 2, pp. 84-94, April 1999.

- [34] D. Papadimitriou, I.O. Vardiambasis “Hybrid Algorithms for Adaptive Array Systems”, *Proceeding of the 4th WSEAS Int. Conf. on TELECOMUNICATIONS & INFORMATICS, Prague, CZ, pp.176-181, March 13-15, 2005*
- [35] Simon Haykin, Ed., “*Advances in Spectrum analysis and Array Processing*”, vol.3, Prentice Hall, Englewood Cliffs, N. Jersey, 1995.
- [36] X. Wang, P.R.P. Hoole, E.Gunawan, “An electromagnetic-time delay method for determining the positions and velocities of mobile stations in a GSM network”, *Progress in Electromagnetic research, PIER 23, pp. 165-186, 1999*
- [37] Hoole, P.R.P., “*Smart Antenna and Signal Processing for Communications, Biomedical and RADAR Systems*”, WIT Press, 2000